Clean Hydrogen Partnership

Co-funded by the European Union

HyUSPRe

Hydrogen **U**nderground **S**torage in **P**orous **Re**servoirs

Equipment requirements and capital as well as operating costs for the hydrogen scenarios

Prepared by: Jacopo de Maigret, FBK
Diego Viesi, FBK

.

Please cite this report as: de Maigret, J., Viesi, D., 2023: Report on equipment requirements and capital as well as operating costs for the hydrogen scenarios, H2020 HyUSPRe project report. 106 pp incl. appendices.

This report represents HyUSPRe project deliverable number D7.1

The HyUSPRe consortium

Funded by

Acknowledgement

This project has received funding from the Fuel Cells and Hydrogen 2 Joint Undertaking (now Clean Hydrogen Partnership) under grant agreement No 101006632. This Joint Undertaking receives support from the European Union's Horizon 2020 research and innovation programme, Hydrogen Europe and Hydrogen Europe Research.

Disclaimer

This document reflects the views of the author(s) and does not necessarily reflect the views or policy of the European Commission. Whilst efforts have been made to ensure the accuracy and completeness of this document, the HyUSPRe consortium shall not be liable for any errors or omissions, however caused.

Executive summary

One of the tasks in Work Package 7 of the HyUSPRe project involves spatio-temporal optimization modeling of a green hydrogen supply chain linking production and demand centers within the European energy system (Task 7.1). The aim is that of generating and assessing future scenarios which see hydrogen contributing to the European energy system. In particular, it is of interest to assess the role played by large-scale, seasonal, hydrogen storage in perspective of an energy system with as strongly growing share of non-dispatchable, intermittent renewable power supply.

To do so in a reliable manner, the model requires a strong basis of input parameters along with their future forecasts. Firstly, solar and wind resource potentials for the production of green hydrogen as well as hydrogen demand scenarios were assessed and presented in Deliverable D1.2 of Work Package 1 (Groß *et al.*, 2022). The second necessary step is that of characterizing the green hydrogen supply chain in terms of techno-economic parameters of its constituent elements. This is the content of Task 7.2 of Work Package 7. In particular the aim is that of creating a literature-backed dataset of techno-economic parameters to serve as input to the modeling activities of Task 7.1.

To achieve this result, a large number of sources was screened and relevant data points were collected. Most technologies of the hydrogen supply chain benefit from extensive literature coverage, leading to plenty of values per single parameter. In these cases, a statistical approach was taken, which consisted in calculating the 1st and 3rd quartiles of each set. Together with the average of the set, the two quartiles allowed to provide a range of values for each techno-economic parameter. This document reports the summarized findings the bibliographical research along with descriptions of the single elements of supply chain. The main output of Task 7.2, other than this report, is a summary dataset which is presented in the appendix of this document. Such a dataset is not only based on scientific literature and recognized reports, but has also benefitted from the review of scientific and industrial partners of the HyUSPRe project.

About HyUSPRe

Hydrogen **U**nderground **S**torage in **P**orous **Re**servoirs

The HyUSPRe project researches the feasibility and potential of implementing large-scale underground geological storage for renewable hydrogen in Europe. This includes the identification of suitable porous reservoirs for hydrogen storage, and technical and economic assessments of the feasibility of implementing large-scale storage in these reservoirs to support the European energy transition to net zero emissions by 2050. The project will address specific technical issues and risks regarding storage in porous reservoirs and conduct an economic analysis to facilitate the decision-making process regarding the development of a portfolio of potential field pilots. A techno-economic assessment, accompanied by environmental, social, and regulatory perspectives on implementation will allow for the development of a roadmap for widespread hydrogen storage by 2050, indicating the role of large-scale hydrogen storage in achieving a zero-emissions energy system in the EU by 2050.

This project has two specific objectives. Objective 1 concerns the assessment of the technical feasibility, associated risks, and the potential of large-scale underground hydrogen storage in porous reservoirs for Europe. HyUSPRe will establish the important geochemical, microbiological, flow, and transport processes in porous reservoirs in the presence of hydrogen via a combination of laboratory-scale experiments and integrated modelling; and establish more accurate cost estimates to identify the potential business case for hydrogen storage in porous reservoirs. Suitable storage sites will be identified, and their hydrogen storage potential will be assessed. Objective 2 concerns the development of a roadmap for the deployment of geological hydrogen storage up to 2050. The proximity of storage sites to large renewable energy infrastructure and the amount of renewable energy that can be buffered versus time varying demands will be evaluated. This will form a basis for developing future scenario roadmaps and preparing for demonstrations.

Document information, revision history, approval status

Document information

Title:	Equipment requirements and capital as well as operating costs for the hydrogen scenarios
Lead beneficiary:	FBK
Contributing beneficiaries:	FZJ, TNO, EIL
Due date:	M17 [2023.02.28]
Dissemination level:	Public
Published where:	HyUSPRe website
Recommended citation:	de Maigret, J., Viesi, D., 2023: Equipment requirements and capital as well as operating costs for the hydrogen scenarios, H2020 HyUSPRe project report. 106 pp incl. appendices.

Revision history

Version	Name	Delivery date	Summary of changes
V01	J. de Maigret	2023.03.29	Feedback and comments from partners considered.
V02	J. de Maigret	2023.04.10	Final comments implementation.
V03	H. Cremer	2023.04.14	Final layouted version.

Approval status

Role	Name	Delivery date
Deliverable responsible:	J. de Maigret	2023.04.10
Task leader:	J. de Maigret	
WP leader:	T. Groß	2023.04.11
HyUSPRe lead scientist	R. Groenenberg	2023.04.11
HyUSPRe consortium manager:	H. Cremer	2023.04.14

Abbreviations

AB ... *1,2-Dihydro-1,2-Azaborine*
ABEX ... *Abandonment Expenditure*
ASU ... *Air Separation Unit*
BECCSU ... *Biomass Energy with Carbon Capture, Storage and Utilization*
BF ... *Blast Furnace*
BOF ... *Basic Oxygen Furnace*
BTX ... *Benzene-Toluene-Xylene*
CAPEX ... *Capital Expenditure*
CCGT ... *Combined Cycle Gas Turbine*
CCS ... *Carbon Capture and Storage*
CCUS ... *Carbon Capture, Usage and Storage*
CHP ... *Combined Heat and Power*
CO ... *Carbon monoxide*
DAC ... *Direct Air Capture*
DBT ... *Dibenzyltoluene*
DME ... *Dimethyl Ether*
DN ... *Diametre Nominal*
DRI ... *Direct Reduced Iron*
EAF ... *Electric Arc Furnace*
EUR ... *Euro (2022)*
FA ... *Formic Acid*
FC ... *Fuel Cell*
FCEV ... *Fuel Cell Electric Vehicle*
FT ... *Fischer-Tropsch*
GHG ... *Greenhouse Gas*
GJ ... *Gigajoule*
GW ... *Gigawatt*
GWH ... *Gigawatt Hours*
HB ... *Haber-Bosch*
HHV ... *Higher Heating Value*
HVC ... *High-Value Chemicals*
ICE ... *Internal Combustion Engine*
LCOE ... *Levelized Cost Of Electricity*
LHV ... *Lower Heating Value*
LOHC ... *Liquid Organic Hydrogen Carrier*
MET ... *Methanol*
MEUR ... *Million Euros (2022)*
MTA ... *Methanol To Aromatics*
MTG ... *Methanol To Gasoline*
MTO ... *Methanol To Olefins*
NAP ... *Naphthalene*
NEC ... *N-Ethylcarbazole*
OCGT ... *Open Circuit Gas Turbine*
OPEX ... *Operational Expenditure*
PAX ... *Passengers*
PEM ... *Proton-Exchange Membrane*
PEMFC ... *Proton-Exchange Membrane Fuel Cell*
PET ... *Polyethylene Terephthalate*
PSH ... *Pumped Storage Hydropower*
PV ... *Photovoltaic*
RES ... *Renewable Energy Sources*
RWGS ... *Reverse Water-Gas Shift*
SMR ... *Steam Methane Reforming*
SOFC ... *Solid Oxide Fuel Cell*
TOL ... *Toluene*
TRL ... *Technology Readiness Level*
VOM ... *Variable Operation and Maintenance (cost)*
WEL ... *Water Electrolyzer*

List of Figures

Table of Contents

1 Introduction

There is an increasing interest in hydrogen's role in the European striving for a zero-emission energy system by 2050. Hydrogen is an energy vector that can potentially decarbonize multiple sectors (industry, heat, mobility). Therefore, efforts towards a reliable and economically feasible supply are gaining momentum. In this regard, it has been the focus of studies to define and assess the so-called green hydrogen supply chain. Such an entity comprehends all elements that ensure hydrogen to be produced, transported, stored and utilized.

In compliance with the EU zero-emission goals, the production of hydrogen must rely on renewable energy sources, discarding conventional – carbon dioxide emitting - hydrogen production via the reforming of natural gas. Renewable power generation (solar photovoltaic, wind, hydropower, biomass) is therefore to be coupled with water electrolyzers to produce green hydrogen. Green hydrogen production sites, however, might not find themselves near hydrogen consumption centers, mostly due to the renewable resource geographical constraints. For this reason, it is of interest to assess different hydrogen transport methods that allow to link production to consumption. However, due to the properties of hydrogen gas, mostly low volumetric energy density, it is recognized that it is necessary to convert hydrogen into other forms or compounds to transport it effectively, to then be re-converted before final use. The green hydrogen supply chain also requires storage options to act as buffers not only between production and consumption, but also throughout the conversion and transport infrastructure. Such storage options are available for both hydrogen gas and its derivatives and are characterized by short- to long-term storage cycles (intraday and intramonthly).

Hydrogen has however also been noted to serve a function of balancing energy demand and supply. By absorbing the excess renewable energy produced in favorable resource conditions, electrolyzers allow to avoid power curtailment by producing storable hydrogen for later use. Particularly, it is of interest to investigate the economic feasibility of this use of hydrogen in long-term balancing of the power grid. To achieve this, large-scale hydrogen storage is necessary and suitable options are identified in underground storage in porous reservoirs and salt caverns, which allow for seasonal storage cycles.

The following report aims at defining the green hydrogen value chain in terms of techno-economic characteristics of its constituent elements, which are illustrated in Figure 1. Through a review of relevant literature, data was gathered and summarized for hydrogen production (renewable energy generation and water electrolysis), hydrogen conversion (transformation of hydrogen gas into its derivatives), hydrogen transport and storage (of both hydrogen and its derivatives), derivative reconversion (from derivatives to hydrogen gas) and hydrogen final use (in the heat, power, industrial and mobility sectors). The main output of this work is a robust dataset proposing techno-economic parameters characterized by a range of values (optimistic and pessimistic scenarios) and future forecast trends. This dataset will serve as input to a spatio-temporal optimization model, developed within the HyUSPRe project, with the aim of evaluating the role played by large-scale underground hydrogen storage within the envisioned European zero-emission energy system.

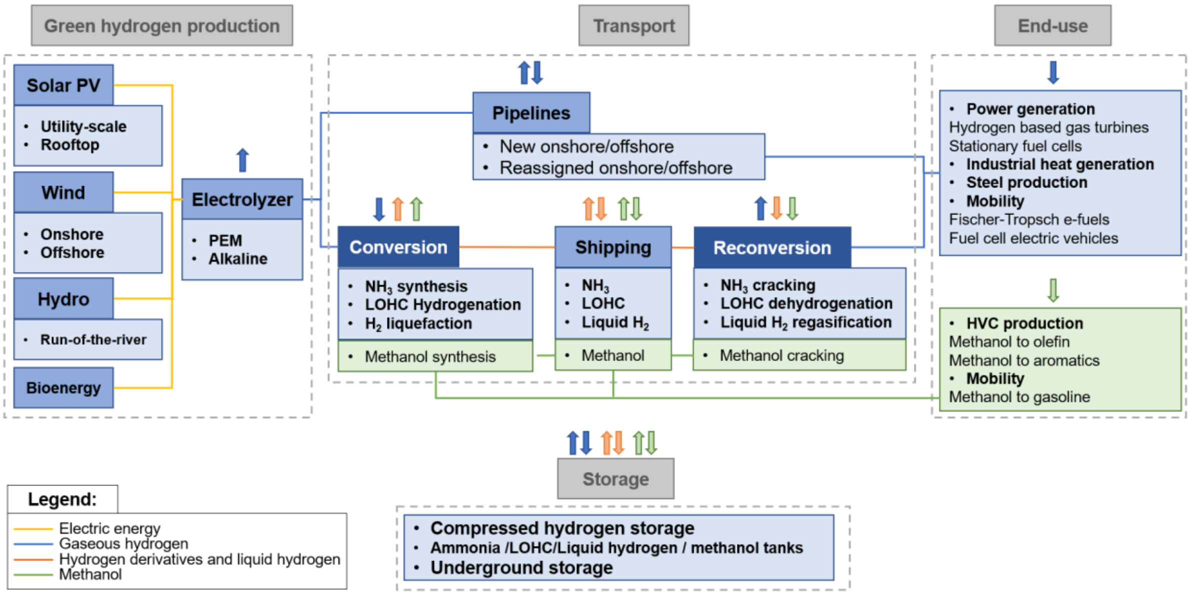

Figure 1. Schematic representation of the green hydrogen value chain assessed in this study.

The report can be divided into five major parts: green hydrogen production, hydrogen conversion and reconversion, transport of hydrogen and (selected) derivatives, storage of hydrogen and (selected) derivatives and hydrogen final use. First, in Chapter 3, green hydrogen production regards renewable power production from solar PV, wind, hydropower and biomass to be coupled with electrolyzers (proton exchange membrane or alkaline). In Chapter 4, the conversion and reconversion processes of hydrogen into and from its derivatives and liquefied form are assessed. The hydrogen derivatives included in the study are ammonia, liquid organic hydrogen carriers (LOHC), and methanol. In Chapter 5, the transport of hydrogen is discussed. The distinction is made between pipelines and ships. In the first case pipelines carrying gaseous hydrogen are further differentiated between onshore and offshore (both new and repurposed), whereas shipping regards ammonia, LOHC (including methanol), and liquid hydrogen derivatives.

In Chapter 6 storage technologies are presented for gaseous hydrogen and hydrogen derivatives. Special focus is put on large-scale underground hydrogen storage in salt caverns and porous reservoirs. The two typologies of underground storage are illustrated in terms of site description and preparation, equipment and necessary components, and key techno-economic parameters. Storage technologies are also assessed for compressed hydrogen, ammonia, LOHC, methanol and liquid hydrogen.

Lastly, in Chapter 7, multiple hydrogen final-use technologies are presented and discussed along with their characterizing techno-economic parameters. Here, three subcategories can be identified. Namely power generation (hydrogen-based turbines and stationary fuel cells), hydrogen use in industry (het generation, steel production [direct reduced iron, or DRI], and high-value chemical production), and hydrogen use in mobility (synthetic fuels for internal combustion engine vehicles and direct use of hydrogen in fuel cell electric vehicles.)

2 Methodology

This study reports the results of an extensive bibliographical research of techno-economic parameters with the aim of creating a solid dataset to be used for scenario definition. The research strives to be as comprehensive as possible and therefore includes many relevant references. This approach may lead to having a broad range of values for a specific parameter. To extrapolate summarized values from such ranges, a quartile analysis was implemented. Given a set of values found in different literature sources relative to a techno-economic parameter, the 1st and 3rd quartiles were calculated. Such values were then set to represent the upper and lower boundary of the presented data, identifying optimistic and pessimistic scenarios. Such an analysis is not affected by the so-called outliers, which are data points with exceptionally high or low value (relative to the rest of the values of the dataset), which might affect overall average values. By definition, the quartiles of a dataset divide the set into four subsets each containing 25% of the data points. Therefore, in the following analysis, the upper and lower boundaries enclose 50% of the literature sourced values. Lastly, the average of the set was calculated to determine the average scenario.

This approach was used throughout the data collection of this assessment whenever high volumes of data points were available. Some elements of the green hydrogen supply chain are extensively covered by literature whereas other do not benefit from such strong bibliographical support. In this latter case, the values presented in this study refer directly back to literature values, as it was not possible to apply the abovementioned statistical approach. The largest available datasets, which are also most complete in terms future trends, regard hydrogen production, comprising renewable energy generation (solar PV, wind, hydropower and biomass) and water electrolysis (alkaline and proton exchange membrane). Following, in terms of available data, are the conversion/reconversion technologies (ammonia, LOHC, liquefied hydrogen, methanol), transport technologies (pipelines and shipping), and hydrogen mobility (fuel cell electric vehicles). For other end uses such as hydrogen use in steel production/industrial heat generation and hydrogen use in gas turbines, literature is scarcer. Lastly, it is necessary to add that future forecasts are not always available in literature. Therefore, trend estimations were performed under technology specific assumptions which are reported in the according sections.

3 Green hydrogen production

By definition, green hydrogen implies the use of renewable electricity to power a water electrolyzer. The following subsections assess the techno-economic parameters of renewable power generation and electrolyzer technologies which are the very beginning of a green hydrogen supply chain.

3.1 Renewable electricity generation

The renewable energy sources considered in this assessment for the sustainable power generation are wind, solar, hydro and biomass. In the case of wind power, the distinction is made between onshore and offshore, while for PV between utility-scale (or field mounted) and rooftop mounted. Regarding hydropower, this study covers run-of-the-river systems as this configuration is most likely to be the one of choice in case of capacity expansion. Lastly, biomass generated power is assessed based on the different nature of the conversion technology (gasified/digested biomass CHP, conventional steam cycle).

These technologies find themselves at the very beginning of the hydrogen supply chain. It is of interest to assess their techno-economic parameters as they determine the cost of the electricity fed into the electrolyzers and therefore of the production of green hydrogen. The analysis reports the forecasts of the values of the parameters through to 2050, with a ten-year granularity (2020-2030-2040-2050). For each time horizon, a range of values was provided to cover optimistic to pessimistic scenarios. The values of the parameters reported here are the result of a statistical analysis of values found during an extensive bibliographical review of mostly scientific journal papers and reports.

3.1.1 Solar PV

The cost of renewable power generation has fallen greatly in the past decade. In particular, solar PV is good example of this, as economies of scale, learn-by-doing and manufacturing improvements have enabled significant total installed cost reduction. According to IRENA (2022b), the global installed capacity of utility-scale PV plants – which are defined as PV systems with peak power greater than 10 MWe (Jäger-Waldau, 2019) and represent the majority of the global PV deployment (IEA, 2019c) – has increased from 40 to 710 GW between 2010 and 2020. Such a large-scale production and deployment ensured a total installed cost reduction of 81% (global weighted average) in the same time period, mostly attributable to a solar module cost reduction of 93%. Alongside cost reduction, solar PV benefitted also from an increase in module efficiency (+24% between 2010 and 2020 [IRENA, 2022b]). A tangible effect of higher module efficiency lies in a lower land occupation for a given peak capacity. This was noted in the study of Bolinger and Bolinger (2022), in which they report that fixed-axis (i.e. not sun tracking) utility-scale PV plants have witnessed an increase of areal energy density of 52% between 2011 and 2019.

According to multiple literature sources, trends of installed costs are expected to follow their decreasing trajectory throughout the next decades. DNV GL (2019a) state that the overall installed capacity of solar PV (both utility-scale and rooftop) will increase thirty-fold between 2020 and 2050, with around 70% of the capacity represented by utility-scale. Brändle, Schönfisch and Schulte (2021) propose that the cost reduction will follow a learning rate of 30%, meaning that for every doubling of cumulative installed capacity the specific price of production will decrease by 30%. This reduction also affects the total installed cost of rooftop PV, which also presents a significant deployment potential, with up to 570 GWe potentially installable in Europe by 2030 (Bošnjaković, Čikić and Zlatunić, 2021). However, rooftop generation operates differently from utility-scale generation in that it represents a distributed generation system, as opposed to a centralized one. In this regard, there is a trade-off between the higher investment cost for rooftop PV, primarily due to the smaller scale (IRENA, 2022d), and the lower grid requirements and low usage of land area of rooftop PV (Gomez-Exposito, Arcos-Vargas and Gutierrez-Garcia, 2020)(Duman and Güler, 2020).

The present section aims to provide a comprehensive analysis of the available data regarding the techno-economic parameters of solar PV generation. For both utility-scale and rooftop PV many data points are available regarding total installed cost and their future forecasts. For this reason, the statistical approach illustrated in Chapter 2 is applied to generate the CAPEX curves in **Figure 2**. This route was only followed for the CAPEX of the technology since it is characterized by a significantly wide range of values depending on the sources. On the other hand, different sources seem to be more in agreement with one another regarding values of fixed operation and maintenance and lifetime, which are reported in the Appendix of this document in Chapter 10.1.

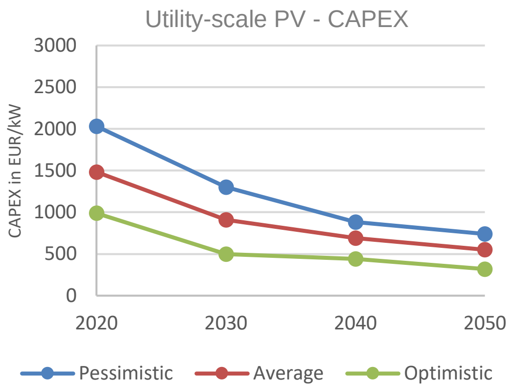

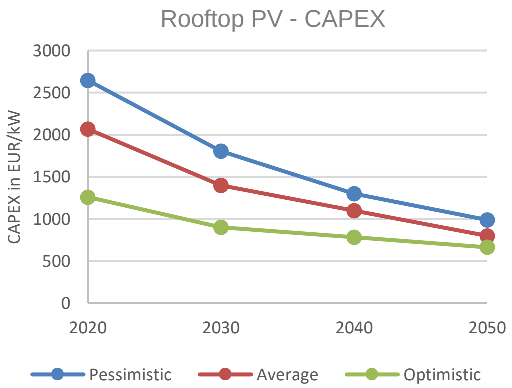

Figure 2. Utility-scale PV (left) and rooftop PV (right) CAPEX expected trends. The values represented summarize the values of the following references: Utility-scale (IRENA, 2019) (Brändle, Schönfisch and Schulte, 2021) (Janssen *et al.*, 2022)(Xiao *et al.*, 2021) (IRENA, 2022d) (Gernaat *et al.*, 2020)(Jäger-Waldau, 2019). Rooftop PV (Datta, Kalam and Shi, 2020)(Gernaat *et al.*, 2020)(Barbose and Satchwell, 2020)(Mokhtara *et al.*, 2021)(Bošnjaković, Čikić and Zlatunić, 2021) (Jäger-Waldau, 2019).

3.1.2 Wind power

In a similar way to solar PV, onshore and offshore wind power generation has undergone significant cost reduction and performance increase in the past decade (2010 to 2020), confirming their role as competitive cost energy generators (DNV GL, 2019a). In the case of onshore wind power, the cumulative installed capacity has increased four times in this time span, which enabled a 32% decrease in total installed cost through the same mechanisms of economies of scale, learn-by-doing and manufacturing improvements. Moreover, technology improvements brought to larger rotor diameters and increase in hub heights. This lead to a counter intuitive effect of a global average increase in capacity factors from 27% to 36% despite the expansion of wind farms into lower quality resource areas (IRENA, 2022d). Offshore wind power generation also benefitted from the scale up of the cumulative deployment, which increased more than ten-fold between 2010 and 2020. Offshore wind farms are on average shifting towards deeper waters and further from shore driven by geopolitical constraints and resource quality pursuit. These two elements increase the construction cost as deeper waters require more expensive foundations and a higher distance from shore determines more expensive power connections and more complex logistics. However, the cost reduction in turbine and tower cost ensure a total installed cost reduction of offshore wind comparable to that presented by onshore wind (IRENA, 2022d)(Xiao *et al.*, 2021). The access to a better quality resource, along with the abovementioned technological improvements, also determined an increase in the global average capacity factor of offshore wind, reaching 44% within the EU (IRENA, 2022d).

In a similar manner to solar PV, the capacity deployment trends are also forecasted to increase in the upcoming decades. According to the forecasts by DNV GL (2019a), cumulative onshore wind capacity will be six times that of 2017, while offshore will undergo a much steeper increase with a 80-fold increase. Brändle, Schönfisch and Schulte (2021) propose that the cost reduction will follow a learning rate of 18% and 16% in the case of onshore and offshore wind, respectively.

Following the same rationale adopted for the techno-economic assessment of solar PV, the statistical approach presented in Chapter 2 is adopted to extrapolate values of CAPEX (relative to total installed cost) and their future forecasts from a number of sources. The trends are reported in Figure 3. This route was only followed for the CAPEX of the technology since it is characterized by a significantly wide range of values depending on the sources. On the other hand, different sources seem to be more in agreement with one another regarding values of fixed operation and maintenance and lifetime, which are reported in the Appendix of this document in Chapter 10.1.

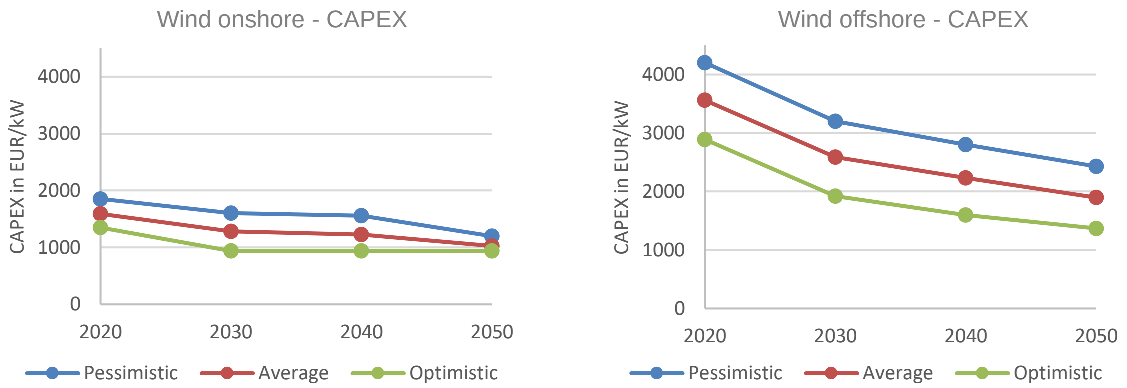

Figure 3. Onshore (left) and offshore (right) wind CAPEX expected trends. The values represented summarize the content of the following references: (IRENA, 2019)(IEA, 2019c)(Pregger *et al.*, 2019)(DNV GL, 2019a)(Brändle, Schönfisch and Schulte, 2021) (Janssen *et al.*, 2022) (Xiao *et al.*, 2021)(IRENA, 2022b)(IRENA, 2022d).

3.1.3 Run-of-the-river hydropower

Hydropower is the most largely deployed renewable energy generation technology and therefore represents the prominent source of renewable power. In 2020 it was accounted that hydropower plants contributed one sixth of global power generation (IRENA, 2022c). The first installations date back to over a century ago and new projects are still in pipeline today. Hydropower also represents the cheapest among the generation technologies despite being capital intensive (IRENA, 2023).

Hydropower plants can be grouped into three categories based on the principle of operation: impoundment/reservoirs hydropower plants, pumped storage hydropower (PSH) plants and run-of-the-river (RoR) hydropower plants. Common to all three categories is the exploitation of the water's gravitational potential energy to move a hydro turbine to generate power. Impoundment plants make use of large dams to create reservoirs where water is stored to be subsequently processed by the turbine to generate power prior to being discharged downstream. Differently, the configuration of PSH plants allows for further impoundment of the discharged water downstream the turbine. The water can then be pumped back into the upstream reservoir under specific grid conditions such as low energy cost or surplus generation from renewable generation. Thanks to this characteristic, PSH currently plays the role of the largest power storage system at disposal of the energy grid. Lastly, RoR hydro power plants require a very small dam or no dam at all in order to divert a portion of the flow of a river towards a penstock and then to the turbine, prior to re-joining the river it was originally withdrawn from. RoR hydropower plants are less impactful from social and ecological point of view as well requiring less capital-intensive construction works. A distinctive characteristic of hydropower plants is the quick response time to generation requirements, due to their rapid ramp-up and ramp-down capabilities. This feature allows to contribute greatly to grid stability (even more so in the case of PSH), conferring to this generation technology an important role in balancing the grid ever more populated with intermittent, distributed renewable energy sources (IRENA, 2022c) (IRENA, 2023) (IRENA, 2012).

According to IRENA (2023), at a global level, there are currently 1,230 GW of deployed conventional (reservoir and RoR) hydropower plants and 130 GW of PSH. The forecasted increase between 2022 and 2037 is expected by +515 GW for conventional and +136 for PSH, for the most part located in Asia. At a European level, most of the hydropower potential is exploited and feasible expansion is likely to occur through RoR hydropower plants with low heads (European Commission, 2014). For this reason, this assessment focuses on this typology of hydropower plant. In general, costs are specific to the single case and plant specifications. Reported in Figure 4 are the results of the statistic approach presented in Chapter 2, applied to the CAPEX of RoR plants (and their forecasts) found in literature. Similarly to solar PV and wind power generation, the statistical analysis was only applied to the values of CAPEX, seen as the different sources are in agreement with one another regarding values of fixed operation and maintenance and lifetime, which are reported in the Appendix of this document in Chapter 10.1.

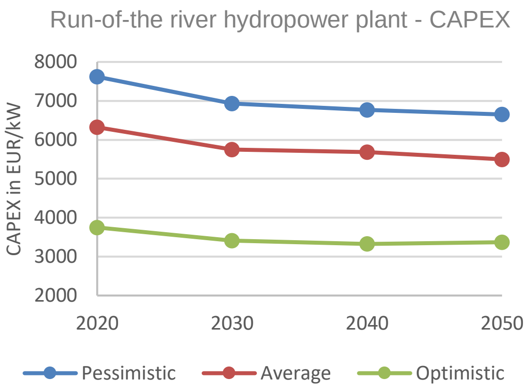

Figure 4. Run-of-the-river hydropower CAPEX. The values represented summarize the content of the following references:(DOE, 2016)(NREL, 2021)(Statista, 2022c)(European Commission, 2014)(Tsiropoulos, Tarvydas and Zucker, 2018).

3.1.4 Biomass generated power

The conversion of biomass to heat and power is a well-known process which relies on technologies similar to those employed for conventional fossil fuels. Biomass conversion to power may mainly follow three different paths: direct combustion, conversion to methane through anaerobic digestion prior to combustion, and conversion to syngas (a mixture of carbon monoxide and hydrogen) prior to combustion. In the case of direct combustion, solid biomass is firstly broken down to the necessary size (wood chips, pellets, dust) to then undergo combustion in a furnace in which a boiler produces high temperature steam which in turn drives a conventional steam turbine. In the case of anaerobic digestion, biomass is placed in oxygen-free digestors (tanks) in which bacterial activity breaks down the biomass to produce methane gas. The methane gas can then be utilized as fuel in conventional furnaces to generate steam or in gas turbines. Lastly, the gasification of biomass produces syngas from biomass placed in low-oxygen environment reactors under high temperatures. The syngas can then be utilized as fuel in conventional furnaces to generate steam or in gas turbines. Differently from solar PV and wind, biomass benefits from a certain degree of dispatchability of the resource. The feedstock may be sourced as residue of agricultural/forestry activities or may also be cultivated as dedicated energy crop (IRENA, 2022c). In Figure 5, the results of the statistical analysis illustrated in Chapter 2 applied to the CAPEX of biomass power generation plants, is reported. The analysis includes all the above-mentioned biomass conversion technologies. The higher values represent biomass gasification plants and municipal biomass waste incinerator plants (direct combustion) in which higher investments are necessary for the gasification section and exhaust treatments sections, respectively (De Vita *et al.*, 2018). Values of fixed/variable operation and maintenance costs and lifetime, are reported in the Appendix of this document in Chapter 10.1.

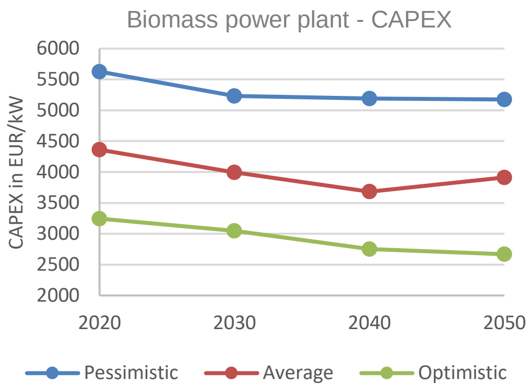

Figure 5. Biomass generated power CAPEX. The values represented summarize the content of the following references: (Grosse *et al.*, 2017) (De Vita *et al.*, 2018) (IEA, 2010).

3.2 Water electrolysis

For the production of green hydrogen, the power produced from renewable sources is fed to an electrolyzer. Such devices are able to split water (H_2O) into its constituents when an electric potential is applied, thanks to the presence of an electrolyte. The nature of the electrolyte determines different type of electrolyzers with different techno-economic parameters. At the moment, the most established types of electrolyzers are the proton exchange membrane water electrolyzer (PEM-WEL) and the alkaline water electrolyzer (A-WEL).

In terms of investment costs, A-WELs are generally cheaper than PEM-WELs because of their slightly higher maturity and lack of expensive electrode catalysts. However, PEM-WELs outperform A-WELs under certain types of operating conditions. For example, PEM-WELs are able to quickly ramp up (or down) their operating point as a function of the electricity input, other than being able to fully cover the operating range (0-100%). For this reason, PEM-WELs are deemed as more suitable to follow the intermittent nature of renewable power generated from wind or solar. However, A-WELs development in the years to come will likely allow to close the performance gap between the technologies (Hydrogen Europe, 2020).

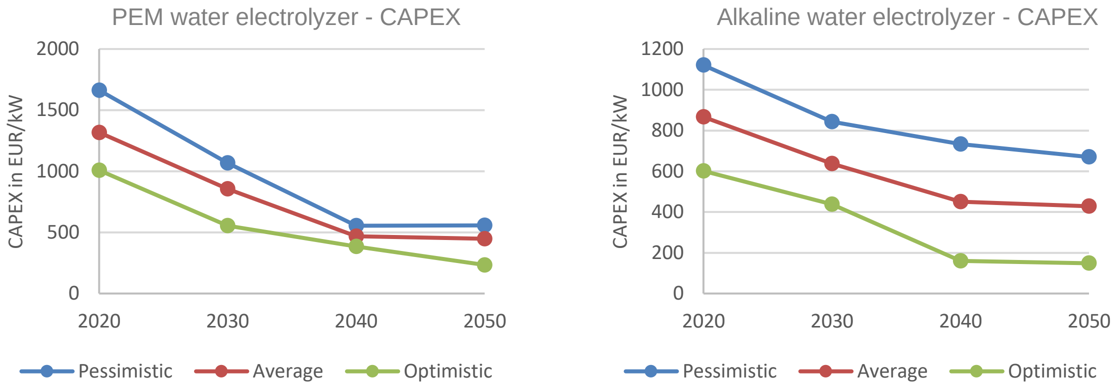

Figure 6. PEM-WEL (left) and A-WEL (right) CAPEX. The values represented summarize the values the following references: (Brändle, Schönfisch and Schulte, 2021) (IEA, 2019b) (Böhm, Goers and Zauner, 2019)(Hydrogen Europe, 2020)(Glenk and Reichelstein, 2019)(Smolinka *et al.*, 2018)(Bertuccioli *et al.*, 2014)(Holst *et al.*, 2021)(Böhm *et al.*, 2020) (Janssen *et al.*, 2022)(Vartiainen *et al.*, 2021) (IRENA, 2020) (Zauner *et al.*, 2022).

The cost per kilogram of the produced green hydrogen by an electrolyzer is mostly attributable in equal amounts to the electrolyzer CAPEX (reported in Figure 6 as a summary of literature values processed via the Chapter 2 methodology) and the cost of the electricity (levelized cost of electricity, LCOE) fed into the electrolyzer. Therefore, a fundamental technical parameter needed for the assessment of the cost of hydrogen production is electrolyzer efficiency, the calculation of which is reported in Figure 7. The value of efficiency describes the amount of electric energy needed to produce one kilogram of hydrogen. If this value is compared with the energy contained in one kg of hydrogen, the efficiency can be expressed as a percentage of either the higher or lower heating value of hydrogen. Differently from fuel cells, electrolyzer electric efficiency is calculated with respect to the higher heating value (HHV) (Figure 8). The reason for this convention is that all the energetic content of the hydrogen gas being produced by the electrolyzer is assumed to be available. For fuel cells, it is assumed on the other hand that the difference between the lower heating value (LHV) and the HHV (the latent heat of water vaporization) does not contribute to the electric production. Therefore, electric efficiency of fuel cells is calculated considering the LHV as the energetic input to the system.

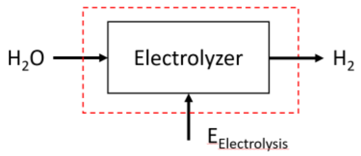

$$\eta = \frac{HHV_{H2}\left[\frac{kWh}{kg_{H2}}\right]}{E_{Electrolysis}\left[\frac{kWh_{el}}{kg_{H2}}\right]}$$

Figure 7. Electrolyzer boundaries (left) for efficiency calculation (right).

Differently from the well-established sustainable power generation technologies reported in Chapter 3.1, electrolyzers are still a developing technology. This implies that the increase of capacity deployment will not only enable learn-by-doing and learn-by-researching effects on the costs of this technology, but also on the efficiency. According to literature-based forecasts, the electric energy needed to produce one kilogram of hydrogen will decrease by 10-17% for PEM-WELs and 9-10% for A-WELs between today and 2050. PEM-WELs will pass from consuming 55-52 kWh/kg_{H2} to 49-45 kWh/kg_{H2}, while A-WELs will decrease from 53-49 kWh/kg_{H2} to 49-45 kWh/kg_{H2}.

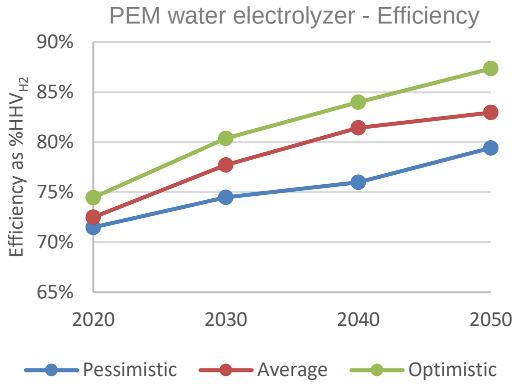

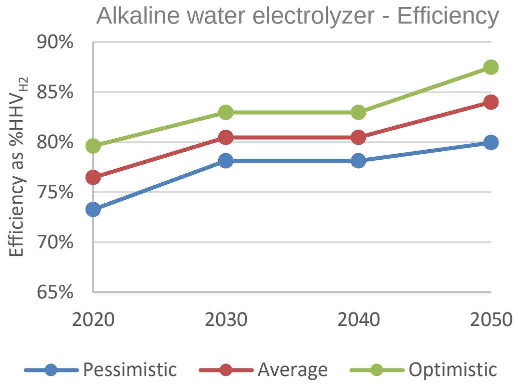

Figure 8. PEM-WEL (left) and A-WEL (right) efficiency. The values represented summarize the values the following references: (Brändle, Schönfisch and Schulte, 2021) (IEA, 2019b) (Hydrogen Europe, 2020) (Smolinka *et al.*, 2018) (Bertuccioli *et al.*, 2014) (Holst *et al.*, 2021) (Janssen *et al.*, 2022) (Vartiainen *et al.*, 2021) (IRENA, 2020).

Yet another difference with the sustainable power generation technologies of section 3.1 lies in the variable operation and maintenance costs (VOM). VOM costs are attributable to the stack component of the electrolyzer having a different useful life compared to the electrolyzer system. The more hydrogen is produced the more often the stack needs replacement due to its degradation. The stack life is usually provided in hours and its duration is also affected by the technological development forecasted for the next decades. PEM-WEL stack life is forecasted to improve from 30-90k hours today to 100-150k hours in 2050, with a similar improvement for A-WELs from 60-90k hours today to 100-150k hours in 2050 (IEA, 2019b). Bearing in mind that the CAPEX of the stack represents around 50% of the total CAPEX for the electrolyzer system (IRENA, 2020), it is possible to determine the necessary stack replacement costs as a function of the operating hours of the system. Regarding electrolyzers coupled with renewable energy sources, it was estimated that the VOM costs associated with stack replacement decrease from 0.158-0.045 EUR/kWh$_{H2}$ to 0.024-0.005 EUR/kWh$_{H2}$ between now and 2050 for PEM-WELs, and from 0.063-0.020 EUR/kWh$_{H2}$ to 0.019-0.005 EUR/kWh$_{H2}$ for A-WELs.

4 Hydrogen conversion and reconversion

The hydrogen supply chain sees hydrogen transport linking supply and demand. The different typologies of hydrogen transport determine a cost increment per kilogram of hydrogen to be added to the cost of production. Intuitively, hydrogen can be compressed and injected into pipelines or tanks which transport hydrogen to its destination. However, based on the distance and capacity of the hydrogen flow, other means of transportation might be more optimal, i.e. the incremental cost of transportation per kilogram of hydrogen may be lower. These other means of transportation see the hydrogen being converted into other compounds or forms, presenting an increased density of hydrogen per unit volume. After being transported to destination, the hydrogen bearing compound must be reconverted into gaseous hydrogen. Both the conversion and the reconversion steps require energy (electrical and/or thermal) which determine the process efficiency.

The conversions considered in this techno-economic assessment are hydrogen to ammonia, liquid organic hydrogen carriers (LOHC), liquid hydrogen and methanol. In all cases conversion and reconversion are assessed in terms of plant costs and efficiencies. It is important to bear in mind however, that while LOHC and liquid hydrogen are always reconverted back into hydrogen gas, ammonia and methanol have a market demand as compounds.

4.1 Ammonia

The main advantage of ammonia for hydrogen transport is not only the increase of hydrogen density per unit volume but also the maturity of the transport of this carrier. Ammonia is already a globally traded commodity and benefits from an established supply chain infrastructure mostly due to its use as industrial feedstock. Its use can potentially be extended to fuel maritime navigation or stationary power generation with the appropriate internal combustion engine or fuel cell design.

4.1.1 Synthesis

Ammonia synthesis is the process through which nitrogen from the surrounding air is combined with hydrogen. In the great majority of cases the process used is the Haber-Bosch (HB) process, in which the standard components are the air separation unit (ASU) and the synthesis reactor. The first component allows to separate nitrogen from the surrounding air and can either be a cryogenic ASU or a pressure swing absorption ASU. Hydrogen may be produced via reforming of natural gas or gasified coal/natural gas, or electrolysis and is mixed with the nitrogen flow to generate the so-called forming gas. The forming gas is then fed into the synthesis reactor where high temperatures and pressures (in presence of a catalyst) ensure the reaction. The chemical reaction taking place is:

$$N_2 + 3H_2 \leftrightarrow 2NH_3$$

By considering the molar mass of the reactants and products (28 g/mol for N_2, 2 g/mol for H_2 and 17 g/mol for NH_3), the resulting mass ratio between hydrogen input and ammonia output is 3/17. Meaning that for every kilogram of ammonia produced, at least ~0.176 (3/17) kilograms of hydrogen are necessary. In this assessment, the input hydrogen is assumed to be completely converted into ammonia.

The system boundaries for the evaluation of the efficiency of the HB process are reported in Figure 9 along with the expression of the efficiency.

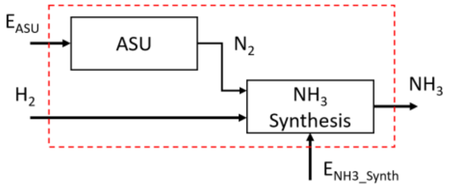

$$\eta = \frac{5.17\left[\frac{kWh}{kg_{NH3}}\right]}{33.3\left[\frac{kWh}{kg_{H2}}\right]\frac{3}{17}\left[\frac{kg_{H2}}{kg_{NH3}}\right] + \left(E_{ASU} + E_{NH3\ Synth}\right)\left[\frac{kWh}{kg_{NH3}}\right]}$$

Figure 9. Ammonia synthesis (Haber-Bosch) boundaries (left) for efficiency calculation (right)

The efficiency accounts for the output product to be one kilogram of ammonia corresponding to the inputs of hydrogen and energy to ensure the production of that kilogram of ammonia. The energy is required to ensure reaction temperatures of around 500°C and pressures of 200-400 bar (IRENA, 2022a).The ASU energy consumption makes up for between 13% (Morgan, 2013)(Proton Ventures, 2017) and 30% (IEA, 2019a) of the over-all ammonia production process, depending on the nature of the ASU technology and plant size. The overall energy consumption of the HB process ranges between 0.4 and 1.1 kWh/kg$_{NH3}$, determining hydrogen to ammonia conversion efficiencies of 74% and 83%, respectively.

Regarding costs of ammonia synthesis plants, the specific investment cost or CAPEX decreases with the increase of plant capacity varying between EUR 584-930 per kW of input hydrogen (EUR 664-1,057 per kW of produced ammonia) in the case of a throughput of 1,000 ton$_{NH3}$/day, and between EUR 376-709/kW$_{H2}$ (EUR 427-805/kW$_{NH3}$) in the case of 3,000 ton$_{NH3}$/day (ISPT, 2017)(Tremel *et al.*, 2015)(Bartels, 2008). The upper and lower boundaries for each capacity represent optimistic and pessimistic scenarios of the assessment. Although ammonia synthesis is a mature process and plant design is well-known, a new and innovative modular design approach in underway, which has CAPEX reduction potential of up to 25% (IRENA, 2022a). For this reason, this assessment considers ammonia synthesis CAPEX decreasing through to 2050. Figure 10 depicts the CAPEX values of ammonia synthesis plants by summarizing literature values through the statistical approach described in Chapter 2. Values of fixed/variable operation and maintenance costs and lifetime are reported in the Appendix of this document in Chapter 10.1.

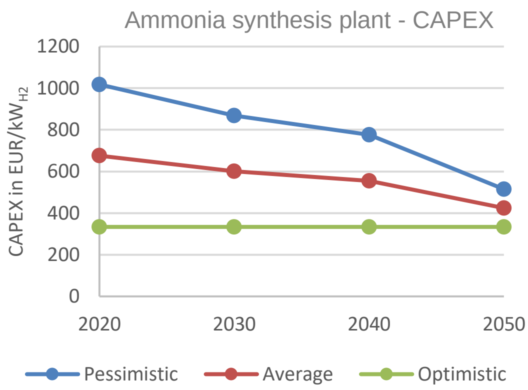

Figure 10. Ammonia synthesis CAPEX. The values represented summarize the values of the following references: (IEA, 2019a)(Sadler *et al.*, 2018)(Vos, Douma and Van den Noort, 2020) (Ikäheimo *et al.*, 2018)(Cesaro *et al.*, 2021)(Bartels, 2008)(Tremel *et al.*, 2015)(Ishimoto *et al.*, 2020)(Morgan, 2013)(Sekkesaeter, 2019)(Hank *et al.*, 2020)(Guidehouse, 2021a)(IRENA, 2022a).

4.1.2 Cracking

Through cracking, ammonia is broken down into its constituents under high temperatures (about 1,000°C without catalyst or 500°C with catalyst) and low pressures of about 20-40 bar (opposite to synthesis conditions). Regarding the efficiency of the process, the boundaries for its calculation are reported in Figure 11.

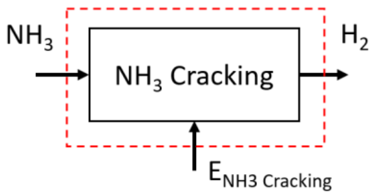

$$\eta = \frac{33.3\left[\frac{kWh}{kg_{H2}}\right]}{33.3\left[\frac{kWh}{kg_{H2}}\right] + E_{NH3\ Cracking}\left[\frac{kWh}{kg_{H2}}\right]}$$

Figure 11. Ammonia cracking boundaries (left) for efficiency calculation (right).

The process mostly uses thermal energy (given the high temperatures required) and to retrieve 1 kg of hydrogen the energy needed is between 4.43 and 7.63 kWh/kg$_{H2}$, yielding efficiencies of 88.3% to 81.4% with respect to the lower heating value of hydrogen.

Similar to ammonia synthesis, specific investment costs (CAPEX) of cracking plants also strongly depend on plant size. CAPEX values vary between EUR 277 and 1,000 for capacities of roughly 500 ton$_{H2}$/day, and between EUR 184 and 501 /kW$_{H2}$ for capacities of roughly 2,500 ton$_{H2}$/day. Ammonia cracking for hydrogen production/recovery is not an established and mature process. Therefore, CAPEX reduction is likely to occur if this technology's capacity deployment increases (Figure 12). Values of fixed/variable operation and maintenance costs and lifetime are reported in the Appendix of this document in Chapter 10.1.

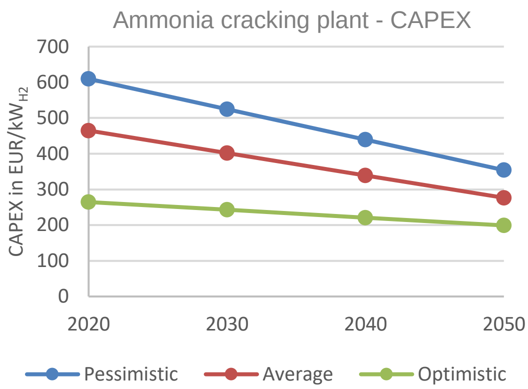

Figure 12. Ammonia cracking plant CAPEX. The values represented summarize the values of the following references: (IEA, 2019a)(Sadler *et al.*, 2018)(Vos, Douma and Van den Noort, 2020)(Ishimoto *et al.*, 2020)(ISPT, 2017) (Sekkesaeter, 2019)(de Vries, 2019) (Cesaro *et al.*, 2021) (Guidehouse, 2021a) (Lanphen, 2019) (IRENA, 2022a).

4.2 Liquid organic hydrogen carriers (LOHC)

LOHC are organic chemical compounds which can be loaded with hydrogen (hydrogenation) to be transported to destination where the hydrogen is then unloaded (dehydrogenation). The dehydrogenated carrier is then transported back to the point of supply to undergo hydrogenation again, starting another cycle. There are a variety of organic chemical compounds suitable to be used as hydrogen carriers. The common characteristic is the presence of a carbon-carbon bond that gives way to hydrogen-carbon bonds during hydrogenation (IRENA, 2022a). The differences between the various LOHC lies in their cost, energy need for hydrogenation/dehydrogenation, hydrogen capacity per kilogram and ease of handling.

The assessed LOHC are:

- Naphthalene (NAP)
- Toluene (TOL)
- Dibenzyltoluene (DBT)
- N-Ethylcarbazole (NEC)
- 1,2-Dihydro-1,2-Azaborine (AB)
- Methanol (MET)
- Formic acid (FA)

Niermann *et al.* (2019) report that cost per kilogram of the abovementioned carriers vary between EUR 0.60/kg and EUR 0.8/kg for NAP and TOL respectively, EUR 4/kg for DBT, and up to EUR 40/kg and EUR 100/kg for NEC and AB, respectively. MET and FA, the only two non-aromatic organic compounds, are both synthesized from carbon dioxide (CO_2), and differently from the rest of the LOHC, it is likely not economically feasible to recycle CO_2 after dehydrogenation. Instead, it can be locally sourced at the time of need, with the price determined by the CO_2 production technology.

Another parameter that describes LOHC is the hydrogen carrying capacity. This value is given in weight percentage and varies between 4%wt and 7%wt for most of the cited carriers with the exception of methanol. Methanol has a much higher hydrogen density with over 12.5 kg_{H2}/kg_{MeOH}. These values represent a drawback for this technology as the volume of carrier needed to satisfy hydrogen demands will determine high initial investment costs. The costs will not only regard the carrier itself but also the transport infrastructure, be it ships, trains or trucks.

On the other hand, LOHC have the advantage of the relative ease of transport. This is due to the derivation of most of the mentioned carriers from the well-established petrochemical sector. In this regard, LOHC also benefit from their stability at standard conditions, absence of boil-off rates (unlike liquified hydrogen) and with the exception of formic acid, non-toxicity.

4.2.1 Hydrogenation

The hydrogenation of an LOHC is an exothermic process which requires high pressures (10-50bar) and generates temperatures of 50-250°C (Niermann *et al.*, 2019). Energy consumption is due to the compressors needed to reach hydrogenation pressures. The boundaries of the hydrogenation plant are reported in Figure 13.

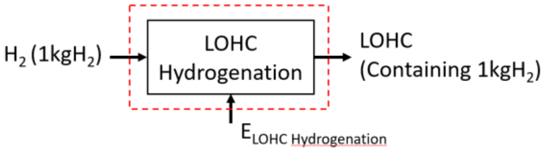

$$\eta = \frac{33.3 \left[\frac{kWh}{kg_{H2}}\right]}{33.3 \left[\frac{kWh}{kg_{H2}}\right] + E_{LOHC\ Hydrogentaion} \left[\frac{kWh}{kg_{H2}}\right]}$$

Figure 13. LOHC hydrogenation boundaries (left) for efficiency calculation (right).

The required pressure for hydrogenation is dependent on the specific carrier and it dictates the energy consumption of the process. The electrical energy required per kilogram of hydrogen loaded into the carrier varies between 0.37-1.8 kWh/kg_{H2} for all of the aromatics discussed. The lower end of the range of energy consumption is characteristic of high-pressure electrolysis (PEM-WEL) production, where the compression needs are minimal or even not required. The corresponding efficiencies to vary between 99% and 95% with respect to the lower heating value of hydrogen. Lastly, it is important to note that given the exothermic nature of LOHC hydrogenation excess heat is generated with temperatures ranging between 50 to

250°C. This heat may find use in other processes such as power generation or satisfying other heating needs.

The CAPEX of hydrogenation plants is directly dependent on plant capacity and the productivity of the specific LOHC. Productivity expresses the yield of hydrogenated LOHC per unit length and unit time. Higher values of productivity ensure lower plant CAPEX, because of the smaller physical size of the plant to produce one kilogram of hydrogenated LOHC. As example of capacity dependency, there is a 20% CAPEX decrease between 100 ton_{H2}/day and a 1,000 ton_{H2}/day DBT hydrogenation facility, passing from EUR 97/kW_{H2} to EUR 77/kW_{H2} (Stöckl, Schill and Zerrahn, 2021). Moreover, given the low commercial availability of these technologies, an increase in deployment can leverage learn-by-doing and learn-by-researching effects to ensure a decrease in CAPEX in the upcoming years. The graph in Figure 14 proposes a range for hydrogenation plant CAPEX condensing the different types of LOHC (applying the methodology of Chapter 2) with the exception of formic acid. The low productivity of this carrier causes its CAPEX to be an outlier when compared to other LOHCs.

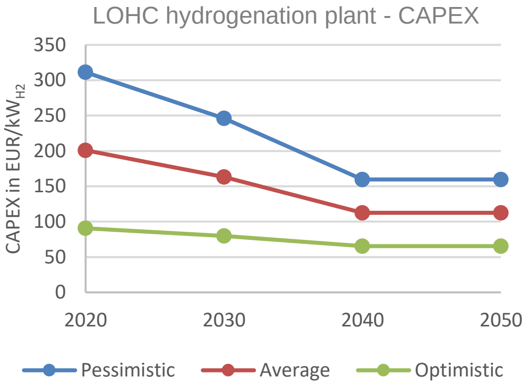

Figure 14. LOHC hydrogenation plant CAPEX. The values represented summarize the values the following references: (Reuß *et al.*, 2017)(IEA, 2019a)(Niermann *et al.*, 2019) (Vos, Douma and Van den Noort, 2020) (Teichmann, Arlt and Wasserscheid, 2012) (Sekkesaeter, 2019) (Hank *et al.*, 2020)(Raab, Maier and Dietrich, 2021)(Guidehouse, 2021a)(IRENA, 2022a).

4.2.2 Dehydrogenation

After the LOHC has been hydrogenated and transported to its destination via ship, train, truck it needs to undergo a reverse process that extracts the hydrogen from the carrier molecules. This hydrogen unloading process is called dehydrogenation and is exactly the inverse reaction to hydrogeneration. The process is endothermic, meaning it requires heat for the reaction to occur, and the quantity of heat is the same that was released during the exothermic hydrogenation step. In addition, oppositely to hydrogenation, dehydrogenation is a low-pressure process occurring at atmospheric pressure.

The energy needs of the dehydrogenation step is embodied in the thermal energy required to reach the reaction temperatures. These temperatures vary between 60 and 420°C for formic acid and methanol respectively, 80°C for 1,2-Dihydro-1,2-Azaborine, and between 270 and 320°C for the rest of the aromatic carriers (Niermann *et al.*, 2019). The energy required to reach these temperatures allows to define the efficiency of the process. The boundaries for the calculation of the efficiencies are reported in Figure 15.

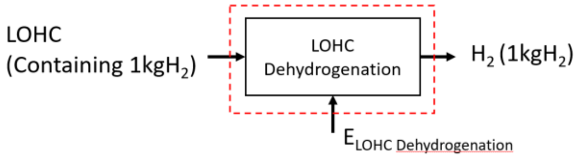

$$\eta = \frac{33.3\left[\frac{kWh}{kg_{H2}}\right]}{33.3\left[\frac{kWh}{kg_{H2}}\right] + E_{LOHC\ Dehydrogenation}\left[\frac{kWh}{kg_{H2}}\right]}$$

Figure 15. LOHC dehydrogenation boundaries (left) for efficiency calculation (right).

By considering the aromatics as the reference carrier, the dehydrogenation energy requirement reported in literature vary widely, presenting values between 9.3 and 17 kWh_{th}/kg_{H2} (Guidehouse, 2021a)(IEA, 2019a), yielding efficiencies of 78% and 66%, respectively with respect to the LHV of hydrogen. The energy consumption range considered in this assessment, also supported by further literature, was decided upon being 10.2 and 12.2 kWh_{th}/kg_{H2} for today's values, which can potentially be improved by acquiring experience in this still developing sector to 10 and 11 kWh_{th}/kg_{H2} in 2050.

Dehydrogenation plant CAPEX, similarly to hydrogenation, is both dependent on plant size and LOHC productivity. Toluene dehydrogenation plants present CAPEX values between EUR 80 and 564/kW_{H2} (Sekkesaeter, 2019)(Raab, Maier and Dietrich, 2021), while between EUR 155 and 973/kW_{H2} for Dibenzyltoluene (Vos, Douma and Van den Noort, 2020)(Runge *et al.*, 2019). The graph in Figure 16 condenses literature-based CAPEX values for LOHC dehydrogenation plants (applying the methodology of Chapter 2). The values regard the aromatic compounds and exclude formic acid due to its high capex (caused by its low productivity) and methanol, which will be assessed separately.

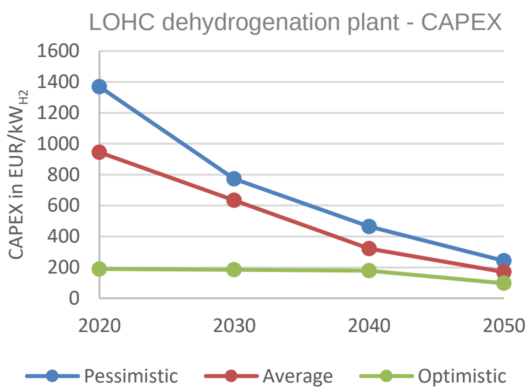

Figure 16. LOHC dehydrogenation plant CAPEX. The values represented summarize the values the following references: (Reuß *et al.*, 2017)(IEA, 2019a)(Niermann *et al.*, 2019) (Vos, Douma and Van den Noort, 2020)(Runge *et al.*, 2019)(Sekkesaeter, 2019)(Hank *et al.*, 2020)(Raab, Maier and Dietrich, 2021)(Guidehouse, 2021a)(Lanphen, 2019)(IRENA, 2022a).

4.3 Liquefied hydrogen

In a different approach when compared to ammonia and LOHC, liquefying hydrogen increases the hydrogen content per unit volume without bonding the hydrogen to a carrier, reaching energy densities of 2.4 $kWh/liter_{LH2}$ against 1.3 kWh/liter of compressed hydrogen at 700 bar (and 25°C) (Reuß *et al.*, 2017). Liquefied hydrogen (LH2) is used today for rocket propulsion and other niche applications and is far from developed to the scale of global hydrogen trade volumes. Investment costs and energy requirements of the LH2 supply chain are almost completely embodied in the liquefaction and storage for transport steps. In the first case, large amounts of energy are needed to reach liquefaction temperature (-260°C), and in the second case, special insulated vessels are required as well as energy is needed to maintain low temperatures. Moreover, during storage for transport additional losses occur due to the boil-off of part of the hydrogen.

4.3.1 Liquefaction

There are multiple processes to achieve hydrogen liquefaction which in general have three phases: compression, cooling and expansion. Gaseous hydrogen is compressed and the excess heat removed through a heat exchanger to reach ambient temperature (300 K). The compressed hydrogen is then cooled by other cold streams through additional heat exchangers, to below its inversion temperature (80 K). The cold streams can be liquid nitrogen (Joule-Thomson process [DOE, 2019]), helium (H2-He cascade system) or hydrogen itself (Claude process and Linde-Hampson process, [Abdi, Chiu and Martin, 2019]). Lastly, the cooled hydrogen stream is then expanded via throttling valve to reach its final temperature of 20 K and partially liquefy.

Hydrogen liquefaction is an energy intensive process when compared to ammonia synthesis or LOHC hydrogenation. This is due mainly to compressors and the production of cooling streams such as nitrogen in the Joule-Thompson process. The overall energy need for the liquefaction of one kilogram of hydrogen ranges between 6.67 kWh/kg$_{H2}$ (Linde, 2019) and 10 kWh/kg$_{H2}$ (Berstad, Skaugen and Wilhelmsen, 2021). However, despite the maturity of this technology there is a lack of large-scale plants. Similarly to the effect of economies of scale on investment costs, the scale of the plants also influences their specific energy consumption. Between a 10 ton$_{H2}$/day and a 100 ton$_{H2}$/day facility the energy consumption per kilogram of liquefied hydrogen decrease from 12.5 to 9.3 kWh/kg$_{H2}$ (-25.6%), and from 9.3 to 8.69 kWh/kg$_{H2}$ (-6.5%) between a 100 ton$_{H2}$/day and a 200 facility ton$_{H2}$/day (DOE, 2019). Taking this effect into consideration, the energy consumptions assessed in this report are considered to decrease through to the year 2050 to a range of 5.5 and 6.1 kWh/kg$_{H2}$. The efficiencies are calculated using the boundaries of the liquefaction process depicted in Figure 17.

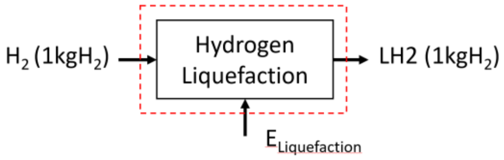

$$\eta = \frac{33.3\left[\frac{kWh}{kg_{H2}}\right]}{33.3\left[\frac{kWh}{kg_{H2}}\right] + E_{Liquefaction}\left[\frac{kWh}{kg_{H2}}\right]}$$

Figure 17. Hydrogen liquefaction boundaries (left) for efficiency calculation (right).

The efficiencies yielded with the abovementioned energy consumptions range between 77% and 83% with today's values and between 86% and 84% with future decreased values. The efficiency was calculated considering the LHV of hydrogen.

Regarding investment costs, liquefaction present higher CAPEX values compared to ammonia synthesis and LOHC hydrogenation. However, liquefaction plants are also susceptible to economies of scale which ensure lower CAPEX values for higher capacities. The values of the CAPEX decrease from EUR 1,766-3,100/kW$_{H2}$ to EUR 1,280-1,439/kW$_{H2}$ and finally to EUR 969-1,142/kW$_{H2}$ for 10, 50 and 200 ton$_{H2}$/day plant capacities (D'Amore-Domenech, Leo and Pollet, 2021;
Stöckl, Schill and Zerrahn, 2021). As for cost reduction potential over time, liquefaction still has room for the development of large-scale plants, which can enable learn-by-doing effects to decrease the CAPEX, as illustrated in Figure 18 (which condenses literature found values through the methodology of Chapter 2).

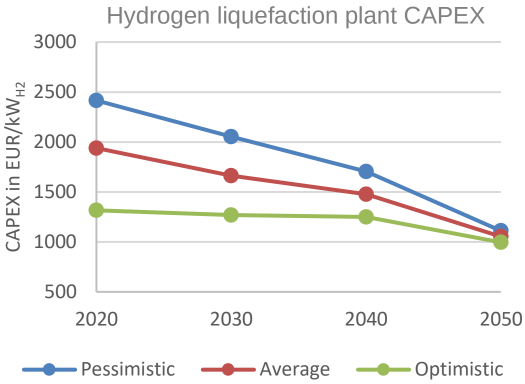

Figure 18. Hydrogen liquefaction plant CAPEX. The values represented summarize the values the following references: (Reuß *et al.*, 2017)(DOE, 2019)(IEA, 2019a)(Sadler *et al.*, 2018) (Stolzenburg and Mubbala, 2013)(Vos, Douma and Van den Noort, 2020)(Teichmann, Arlt and Wasserscheid, 2012)(D'Amore-Domenech, Leo and Pollet, 2021)(Stöckl, Schill and Zerrahn, 2021)(IEA, 2015)(Sekkesaeter, 2019) (Hank *et al.*, 2020)(Raab, Maier and Dietrich, 2021)(Guidehouse, 2021a) (Brändle, Schönfisch and Schulte, 2021)(Brändle, Schönfisch and Schulte, 2020)(IRENA, 2022a).

4.3.2 Regasification

After the liquid hydrogen is transported via ships or trucks to its destination it undergoes regasification to be converted into gaseous form. When compared to the liquefaction and transport steps, regasification is both less costly and less energy intensive. The thermal energy needed for regasification can be provided by the environment and the only additional energy required are for pumping the liquid hydrogen. Moreover, another advantage of the regasification step is the significantly lower energy needed to reach high pressures. It takes less than a third of the energy to pump liquid hydrogen from 3 to 700 bar than it would take to compress gaseous hydrogen to obtain the same pressure ratio (1.2 kWh/kg$_{H2}$ versus 4 kWh/kg$_{H2}$) (IRENA, 2022a). The efficiencies are calculated using the boundaries of the regasification process reported in Figure 19.

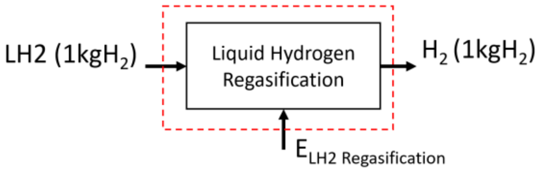

$$\eta = \frac{33.3\left[\frac{kWh}{kg_{H2}}\right]}{33.3\left[\frac{kWh}{kg_{H2}}\right] + E_{LH2\ Regasification}\left[\frac{kWh}{kg_{H2}}\right]}$$

Figure 19. Hydrogen regasification boundaries (left) for efficiency calculation (right).

The energy consumption per kilogram of regasified hydrogen varies between 0.075 kWh/kg$_{H2}$ (Vos, Douma and Van den Noort, 2020; Sekkesaeter, 2019; Guidehouse, 2021) and 0.6 kWh/kg$_{H2}$ (Reuß *et al.*, 2017; Lanphen, 2019). The non-maturity of regasification tehnology may guarantee some room for improvement if this path is adopted thgouh to 2050, potentially decreasing the upper limit from 0.6 to 0.4 kWh/kg$_{H2}$ (IRENA, 2022a). Efficiencies calculated with respect to the LHV of hydrogen range between 98% and 99%.

Investment costs for regasification plants represent only a fraction of those of liquefaction and transport. With values ranging between EUR 73 (Raab, Maier and Dietrich, 2021; Element Energy, 2018)) and 315/kW$_{H2}$ (Vos, Douma and Van den Noort, 2020) which could decrease to between EUR 60 and 190/kW$_{H2}$ in 2050 if the cost reduction potential is exploited (IRENA, 2022a), as reported in Figure 20.

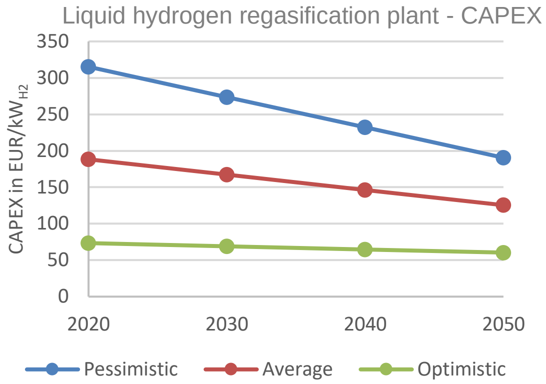

Figure 20. Liquid hydrogen regasification plant CAPEX. The values represented summarize the values the following references: (IEA, 2019a)(Sadler *et al.*, 2018) (Vos, Douma and Van den Noort, 2020)(Element Energy, 2018)(Sekkesaeter, 2019) (Raab, Maier and Dietrich, 2021)(Guidehouse, 2021a)(Lanphen, 2019) (IRENA, 2022a).

4.4 Methanol

Methanol is a well-known product which is currently largely traded and consumed worldwide. It is the feedstock of many chemical plants that convert it into a variety of products such as formaldehyde, acetic acids, plastics, aromatics (methanol-to-aromatics, MTA), olefins (methanol-to-olefins, MTO), gasoline (methanol-to-gasoline, MTG), and dimethyl ether (DME). Moreover, methanol synthesis could also be seen as the hydrogenation of an organic carrier (CO_2) and thus be considered as an LOHC. It was decided however to discuss methanol in its own section due to its wide variety of uses (not only as a hydrogen carrier). Like ammonia, methanol benefits from its status as established traded good and can exploit the existing trading infrastructure and production facilities' maturity.

Methanol is synthesized from syngas which is a mixture of carbon monoxide and hydrogen. The origin of syngas can be renewable or non-renewable (fossil), which determined the carbon intensity of the produced methanol. The Methanol Institute identifies green, blue, grey and brown methanol. Green indicates methanol produced from completely renewable syngas. Such syngas originates from CO_2 either obtained through biomass gasification, direct air capture (DAC), or biomass energy carbon capture and storage and utilization (BECCSU), while the hydrogen component of syngas is produced through electrolysis powered from renewable electricity (green hydrogen). Blue methanol is synthesized from syngas which can originate either from green hydrogen and non-renewable CO_2 from carbon capture and utilization and storage (CCUS), or blue hydrogen in combination with renewable or non-renewable CO2 (where blue hydrogen is hydrogen produced with steam methane reforming [SMR] of natural gas equipped with CCS). Lastly, grey and brown methanol are produced with syngas originated from reformed natural gas or gasified coal, respectively (IRENA and Methanol Institute, 2021).

4.4.1 Synthesis

Methanol synthesis is the process through which syngas (a mixture of carbon monoxide [CO] and hydrogen [H_2]) is combined to produce methanol (CH_3OH, also denoted as MeOH).

$$CO + 2H_2 \leftrightarrow CH_3OH$$

As already discussed, syngas can be produced through biomass gasification, natural gas reforming or coal gasification. In these three cases, the gasification/reforming process directly produces the mixture of CO and H_2 to be fed to the MeOH synthesis reactor. On the other hand, when the raw materials are carbon dioxide and hydrogen, an intermediate reverse water gas shift (RWGS) step is needed, which is an endothermic reaction which requires input thermal energy:

$$CO_2 + H_2 \leftrightarrow CO + H_2O$$

The overall reaction for the CO_2 and H_2 to MeOH process is:

$$CO_2 + 3H_2 \leftrightarrow CH_3OH + H_2O$$

By considering the molar mass of the reactants and products (44 g/mol for CO_2, 2 g/mol for H_2, 32 g/mol for CH_3OH and 18 g/mol for H_2O), the resulting mass ratio between the input hydrogen and the output methanol is 3/16. Meaning that for every kilogram of methanol produced, at least 3/16 kilograms of hydrogen are necessary. In this assessment, the input hydrogen is assumed to be completely converted into methanol.

This study focuses on the CO_2 and H_2 as inputs pathways (disregarding gasification/reforming of natural gas, biomass and gas) seen as the assessment regards the green hydrogen supply chain. The system boundaries for the evaluation of the efficiency of the MeOH synthesis from CO_2 and H_2 process are reported along with the expression of the efficiency in Figure 21. The MeOH synthesis box includes the RWGS step.

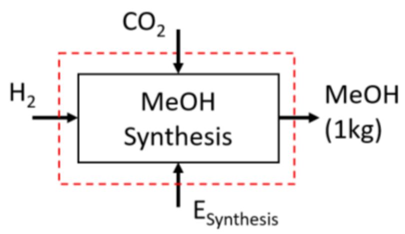

$$\eta = \frac{5.54 \left[\frac{kWh}{kg_{MeOH}}\right]}{33.3 \left[\frac{kWh}{kg_{H2}}\right] \frac{3}{16} \left[\frac{kg_{H2}}{kg_{MeOH}}\right] + E_{MeOH\,Synth} \left[\frac{kWh}{kg_{MeOH}}\right]}$$

Figure 21. Methanol synthesis boundaries (left) for efficiency calculation (right).

The energy needed for RWGS and MeOH synthesis varies according to literature between 0.15 kWh/kg_{MeOH} (Hank *et al.*, 2020; Michailos *et al.*, 2018) and 0.56 kWh/kg_{MeOH} (Zang, Sun, A. Elgowainy, *et al.*, 2021), effectively yielding efficiencies of 86.6% and 81.4% with respect to the LHV of MeOH and H_2, respectively.

Like the other conversion processes, investment costs of MeOH synthesis plants dependent on capacity. For a 300 ton_{MeOH}/day production capacity the total investment was found to be of around 71 MEUR (Szima and Cormos, 2018), which in terms of input hydrogen results in a CAPEX of EUR 910/kW_{H2}. For greater capacities of 866 and 872 ton_{MeOH}/day of methanol production the total investment were found to amount to 67 and 86 MEUR, or EUR 298 and 381/kW_{H2} (Runge *et al.*, 2019; Hank *et al.*, 2020).

The RWGS and MeOH synthesis processes are well established and thus will not present decreasing trends in terms of energy consumption or costs between today and 2050. However, the CO_2 and H_2 feedstock for the MeOH production has great cost reduction potential. The cost of green hydrogen, as already discussed, reflects the cost of LCOE and electrolyzer CAPEX and is therefore going to follow their decreasing trends. On the other hand, the cost of CO_2 production by capture might also see a decrease in time with technology development, especially in the case of DAC. For the purpose of this study, the CO_2 consumption is considered as a variable operation and maintenance cost (VOM), and allows to account for optimistic and pessimistic scenarios based on the origin of the CO_2, as well as their evolution in time.

The captured CO_2 with the most competitive costs is of renewable nature. Anaerobic digestion for the production of biogas and bioethanol production processes have CO_2 as a by-product. The first sees exhaust streams with 35-45% CO2 concentrations (Olsson *et al.*, 2020), the latter reaches concentrations of nearly 100% (Global CCS Institute, 2017; Leeson *et al.*, 2017). The cost per ton of captured CO_2in the two cases is of EUR 30/tonCO_2 for anaerobic digestion exhaust stream CO_2 capture and EUR 13-22/ton_{CO2} for bioethanol production (IRENA and Methanol Institute, 2021). The second pathway of CO_2 supply is CCS applied to fossil fuel generated exhausts (coal and natural gas power plants) or non-renewable process emissions (iron/steel and cement production). The higher cost of captured CO2 is mainly due to the lower concentrations of it in the exhaust streams, which ranges between 12-14% and 3-5%, for coal and natural gas power plants respectively, and between 20-30% and 15-30% for iron/steel and cement production, respectively. The resulting costs of CO_2 captured from such exhaust streams results to be in the range of EUR 38-136/ton_{CO2} today and between EUR 22 and 112/ton_{CO2} (IRENA and Methanol Institute, 2021). Lastly, the highest cost of captured CO2 is attributable to direct air capture or DAC. Due to its low concentration, which is the CO_2 atmospheric concertation of 400 part per million (0.04%), costs rise up to EUR 327-654/ton_{CO2}. However, this technology is still in its early days and development and deployment may contribute to the fall of these high prices in the range of EUR 54-163/ton_{CO2} (IRENA and Methanol Institute, 2021; Fasihi, Efimova and Breyer, 2019).

Relating back to the dependency of the cost of methanol production on the cost of the input CO_2, the cost contribution of CO_2 to the final cost of produced methanol was estimated for CO_2 originated from biogas/bioethanol, CCS from fossil fuel power plants, and DAC. The values are in the range respectively of EUR 40, 109 and 493/ton_{MeOH} with today technology costs, and EUR 40, 77 and 231/ton_{MeOH} for technologies characteristics in 2050 (accounting for improvements in DAC and fossil CCS). Lastly, the cost of methanol also depends on the cost of the input hydrogen. On this regard, IRENA and the Methanol instituted provide a map that illustrates the dependency of the cost of methanol on the different combinations of CO_2 and H_2 costs (Figure 22).

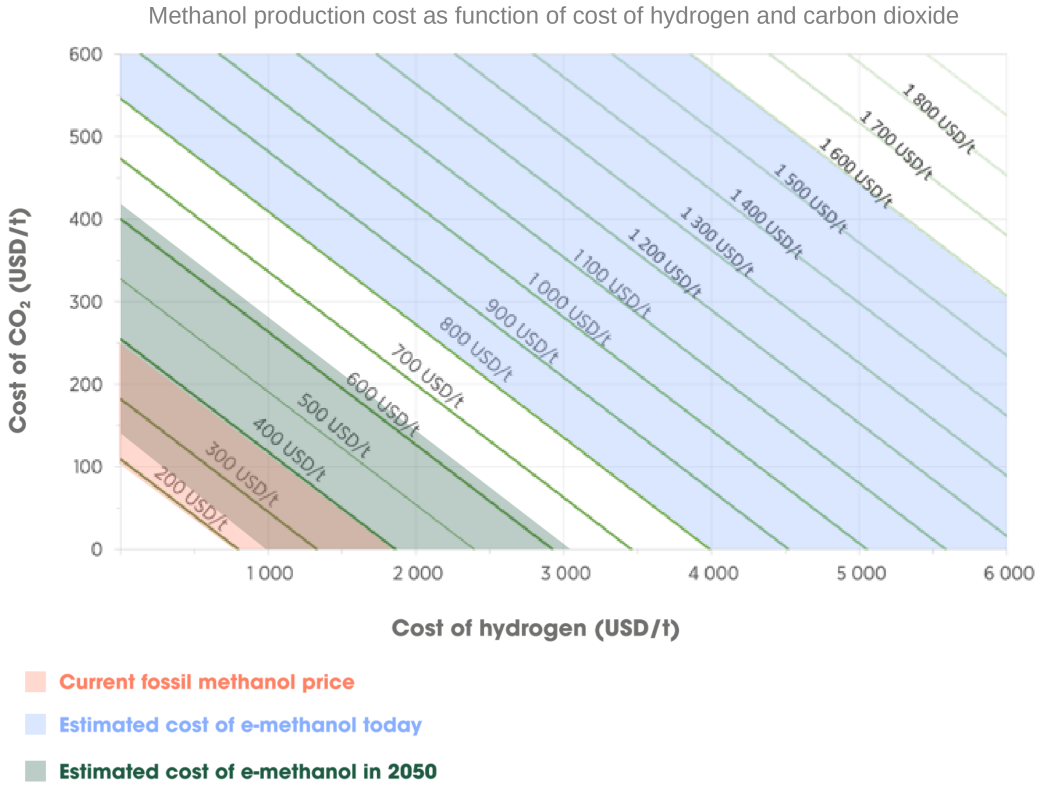

Figure 22. Cost range of methanol synthesized from hydrogen and carbon dioxide, as a function of their different combinations of costs (IRENA and Methanol Institute, 2021).

4.4.2 Cracking

Methanol is mainly traded to be used as feedstock for the production of other chemicals such as formaldehyde, acetic acids, plastics, aromatics (methanol-to-aromatics, MTA), olefins (methanol-to-olefins, MTO), gasoline (methanol-to-gasoline, MTG), and dimethyl ether (DME). However, there is also the possibility for methanol to have the function of hydrogen carrier. Methanol can be seen as the hydrogenated form of CO_2, and for this reason its dehydrogenation will be assessed in this section.

The system boundaries used for the calculation of the efficiency of methanol dehydrogenation are the same as those used in the dehydrogenation of other LOHC. In a similar manner to the other LOHC dehydrogenation processes, the overall energy requirements (mainly due to the thermal energy requirements) are higher in comparison to hydrogenation. According to JRC (2022), for every kilogram of methanol, the system requires 1.706 kWh/kg_{MeOH} (1.613 thermal and 0.094 electrical), which yields an efficiency of ~80% with respect to the LHV of hydrogen output and MeOH input.

The investment costs vary with plant size, passing from EUR 197/kW_{H2} of a plant with an overall cost of 126.7 MEUR (2467 ton_{MeOH}/day input) to EUR 375/kW_{H2} of a plant with an overall cost of 34.4 MEUR (353 tonMeOH/day input) (JRC, 2022).

5 Transport of hydrogen and its derivatives

In order to link hydrogen from the production/conversion sites to demand/reconversion sites, hydrogen may be transported in different ways. In this assessment, compressed gaseous hydrogen is transported via pipelines while hydrogen in its converted forms is assumed to be transported in bulk by ship. In the case of hydrogen pipelines, the assessment regards both new and repurposed pipelines, for onshore and offshore hydrogen transport. In the case of ships, the study regards bulk carriers of ammonia, LOHC (methanol is included here) and liquid hydrogen.

5.1 Onshore and offshore pipelines

Compressed hydrogen pipelines are an already existing means of transportation in contexts where pure hydrogen is transported by producers to large users such as refineries or chemical plants. This technology is therefore known and established and might be attractive to enable hydrogen trade between regions. The main characteristic of such pipelines is the grade of steel used for their production, which has to be resistant to the phenomenon known as hydrogen embrittlement. Hydrogen embrittlement occurs when hydrogen diffuses in the steel lattice, due to the small relative size of the hydrogen molecule. This cause the loss of ductility of the steel and the degradation of already existent defects in the lattice itself.

In this assessment, a distinction is firstly made between onshore and offshore pipelines for hydrogen transport, followed by a distinction between new and repurposed pipelines. The latter represents the process through which natural gas pipelines could be reassigned to transport pure hydrogen. Blending of hydrogen in natural gas is not considered for various disadvantages which characterize this path. The techno economic parameters which characterize hydrogen pipelines are the pressurization requirements and costs. In the first case, both initial pressurization and repressurization needs along the pipeline have to be accounted for. On the other hand, the costs are mostly associated with the initial investment and the electrical energy needed to maintain the operating pressure.

The specific investment cost of new hydrogen is provided in literature as a function of pipe diameter per unit length. However, this value is itself dependent on operating pressure due to the fact that higher pressures in pipelines require thicker pipeline walls. For 50cm pipeline diameter, the cost per km varies between MEUR 0.728/km (Reuß, 2019) and MEUR 1.668/km (Guidehouse, 2021a), while for a 100cm pipe diameter the cost was found to be between MEUR 1.62/km (Reuß, 2019) and MEUR 4.2/km (Baufumé *et al.*, 2013).

The reassignment of natural gas grid pipelines for the use as pure hydrogen pipelines can ensure a significant cost reduction on the investment. The additional costs are attributable to the possible need of pipeline conversion to be hydrogen ready. For example, the pipeline might need dedicated lining to avoid the abovementioned hydrogen embrittlement phenomenon, or new fitting and gaskets might be needed at joints due to hydrogen being more prone to leak (another consequence of the small relative size of the molecule). The specific costs associated with repurposing of the pipelines varies between MEUR 0.24/km and MEUR 0.6/km for a 50 cm pipe diameter and between MEUR 0.36/km and MEUR 0.72/km (Guidehouse, 2021b).

Regarding offshore pipelines cost assessment, the procedure adopted was that of implementing literature backed coefficient to be multiplied to the CAPEX values of onshore pipelines. The coefficients were found to be between 1.3 and 2.3 according to the Hydrogen Council, (2021) and between 1.6 and 2.14 according to data gathered by Statista, (2021). Through this methodology, the values of CAPEX for new onshore varies between MEUR 1.33 and 3.05/km for 50 cm diameter pipes and between MEUR 2.96 and 7.68/km for 100 cm diameter pipes. This pathway was also adopted for offshore repurposed pipelines, the CAPEX of which was multiplied by the average coefficient to obtain values of MEUR 0.44 and 1.10/km for 50 cm diameter pipelines and MEUR 0.66 and 1.32/km for 100 cm diameter pipelines.

5.2 Shipping

The shipping transport option was considered for hydrogen carriers: ammonia, LOHC (which also includes methanol), and liquid hydrogen. In the first two cases, the technologies are both well-established due to the large traded volumes of ammonia and some LOHC (toluene or methanol). The shipping of liquefied hydrogen on the other hand is not deployed on a large scale today and further development may occur. All shipping vessels were assumed to use maritime fuel oil (bunker fuel) as prime mover.

5.2.1 Ammonia

Bulk ammonia ships and loading and unloading terminals (with ammonia storage capabilities) are technologies in use today. The capacity of the ships varies between 3,410 and 109,248 ton_{NH3}/ship (Sekkesaeter, 2019), which corresponds to a hydrogen capacity of 601.7 and 19,256.5 ton_{H2}/ship. The specific investment cost was found to vary slightly with ship capacity. Ships with 110,000 ton_{NH3} load capacity present costs between EUR 1,047/ton_{NH3} (Sekkesaeter, 2019) and EUR 1,695/ton_{NH3} (Al-Breiki and Bicer, 2020), yielding overall investment costs of MEUR 114.3 and MEUR 185.2, respectively.
Ships with a smaller capacity of 57,970 ton_{NH3} (Ishimoto *et al.*, 2020) and 52,000 ton_{NH3} (Sadler *et al.*, 2018) have slightly higher values calculated to be EUR 2,198/ton_{NH3} and EUR 1,115/ton_{NH3}, respectively. Effectively yielding overall investment costs of MEUR 127.4 and MEUR 58, respectively.
These values, along with other found in literature, were translated in terms of hydrogen carrying capacity of the ship. It was therefore established that CAPEX values vary between EUR 0.34 and EUR 0.19 for every kWh of hydrogen transported by the ship.

Lastly, cryogenically stored ammonia (which is characteristic of large-scale shipping) does suffer from the boil-off phenomenon. However, this boil-ff stream can be re-liquefied and pumped back into the storage vessel on board the ship with little energy penalty (JRC, 2022). Therefore, other than the energy needs to propel the ship, no additional losses are to be accounted for.

5.2.2 LOHC

Similar considerations as for the ammonia ships can be done for LOHC shipping and port terminals. As stated in Chapter 4.2, most of the promising LOHC are aromatics (toluene) or methanol, which are already traded via bulk shipping and stored in port terminals destined to the chemical and petrochemical industry.

Regarding investment costs, LOHC shipping also manifests a decreasing trend in specific CAPEX with the increase of ship capacity, which can range between 5,220 and 167,040 ton_{LOHC}. The CAPEX varies between EUR 259.3/ton_{LOHC} (toluene/dibenzyltoluene) (Sekkesaeter, 2019) and EUR 860/ton_{LOHC} (toluene) (Guidehouse, 2021a), for capacities of 167,040 and 138,720 tons of LOHC, respectively. For smaller capacity ships the CAPEX were found to be EUR 583/ton_{LOHC} (dibenzyltoluene) (Hank *et al.*, 2020) and EUR 1,141.6/ton_{LOHC} (generic LOHC) (Teichmann, Arlt and Wasserscheid, 2012), for capacities of 73,080 ton_{LOHC} and 45,000 ton_{LOHC}, respectively.

To assess CAPEX values in terms of transported hydrogen, an average hydrogen density per kilogram of LOHC was assumed to be 5%wt. Moreover, additional references were also considered to provide a possible range of CAPEX values of LOHC ships. The values range between EUR 0.39 and 0.65 for every kWh_{H2} of ship capacity. An advantage of this means of hydrogen transport is the absence of boil-off phenomenon. Therefore, other that the energy required to propel the ship, no additional losses are witnessed.

5.2.3 Liquefied hydrogen

Differently from the two previous cases of ammonia and LOHC shipping, liquid hydrogen shipping is still far commercial maturity, with only a few pilot projects. Investment costs are going to be higher due to the technological requirements needed to maintain the hydrogen in its liquid form (mainly insulated tanks). By comparing various literature resources no direct correlation was found between ship capacity and specific cost (CAPEX). The range of cost per kWh of transported hydrogen was determined through a statistical analysis of the values found in literature and was set between EUR 1.05/kWh_{H2} and EUR 3.92/kWh_{H2}, which translates into EUR 34 965/ton_{H2} and EUR 130 536/ton_{H2}. With an average carrying capacity of around 110,000 ton_{H2}/ship, the investment required would be between MEUR 14,359 and MEUR 3,846. Moreover, according to IRENA (2022) and JRC (2022), the future forecasts of such high CAPEX values are not likely to decrease. The range reported by the two studies lies between EUR 1.05/kWh_{H2} and EUR 1.5/kWh_{H2}.

In addition, the transported liquid hydrogen undergoes the boil-off phenomenon. Due to the non-ideality of the storage vessel insulation some of the liquid hydrogen will want to evaporate, and in order to avoid dangerous high pressures, it is vented/burned and therefore lost. The rate at which this phenomenon happens is in the order of 0.1%/day to 0.4%/day (Vos, Douma and Van den Noort, 2020).

6 Storage of hydrogen and its derivatives

The storage of hydrogen (and its derivatives) plays a crucial role all along the green hydrogen supply chain. It is used for hydrogen transportation, it serves as temporary stock at shipment terminals, but most importantly it could serve as a buffer between supply and consumption whenever there is a mismatch between the two. In the following subsections, different storage technologies are assessed and presented. Special focus is put on large-scale hydrogen underground storage, which could potentially make up for the major issue of the spatio-temporal mismatch of renewable power generation and electricity demand across Europe.

6.1 Storage vessels for hydrogen and its derivatives

This section is dedicated to small- and medium- the storage technologies for hydrogen gas and its derivatives such as ammonia, LOHCs and liquid hydrogen.

6.1.1 Compressed hydrogen

Above-ground pressurized hydrogen storage

A well-known system to store hydrogen in compressed form has two fundamental elements: a compressor and a vessel. However, this assessment regards the techno-economic data of the vessel alone. Compressed hydrogen vessels are capable of storing hydrogen in a pressure range of up to 1000 bar, however achieving such pressures entails high operating costs. Moreover, scaling up the capacity of the vessel also increases the initial investment due special material needed for its manufacturing. Metallic and polymer materials are suitable for intermediate pressures while new and innovative composite materials allow to reach storage pressures of up to 1000 bar (DNV GL, 2019b). In order for such systems to be economically attractive (i.e. to provide a competitive levelized cost of storage) it is advised to design small to medium sized storage capacities (~500kg$_{H2}$ at 200bar) with charge/discharge cycles lasting hours up to months (ENTEC, 2022) (DNV GL, 2019b). Potential applications could be encountered in industrial sites or hydrogen refueling stations in the form of stationary tube racks or transportable tube trailers. Element Energy (2018) asses the use of distributed compressed hydrogen vessels as a balancing element in a hydrogen transmission network, allowing to absorb and release hydrogen following low and high demand. Two storage vessels are discussed. First large vertical tanks operating at transmission network pressure (50-80 bar) that require no (additional) compression. These may hold up to 405kg$_{H2}$ each and are envisioned to be installed in groups of ten. Their specific cost amounts to EUR 483/kg$_{H2}$. High pressure storage vessels (430bar) assembled in batteries of steel tubes would require compression from transmission pressure levels. Compression needs and more resistant vessels would require higher investment cost of EUR 2,318-3,119/kg$_{H2}$. Considered the pressure range at which the different vessels operate, the overall installed cost proposed by this assessment ranges between EUR 421 and 1,940/kg$_{H2}$.

Pipe systems

Pipe system storage of compressed hydrogen sees gas stored in an underground, localized, and interconnected pipe system. An advantage of pipe storage over above-ground storage is that is has no (or negligible) footprint, which could enable the utilization of the ground for other purposes (e.g. agriculture). A few meters below the surface hydrogen pipelines, with a diameters of 1.4m (DN 1400) are welded together in parallel to form a single storage unit of up to 6,300m^3 of free volume (which corresponds to a cumulative length of the pipe system storage of 4km) (Welder *et al.*, 2018). Smaller interconnector pipes are used to better distribute the pressure and temperature gradients. However, floating bearings are needed to accommodate any thermal dilation of the piping during injection and withdrawal phases. The whole system is slightly inclined to ensure that any accumulation of water can be gathered and bled with a valve. Such technology is used for short term hydrogen storage to satisfy peak demand, as the capacity is not comparable to natural underground formations for seasonal storage. The investment costs mostly regard the procurement of the pipelines/compressor and the site excavation, with additional costs in the installation of the pipelines (welding) and the re-earthing of the site. Surface components are comprised of compression and metering system, while no treatment unit is needed because the quality of the withdrawn hydrogen is delivery ready (HyUnder, 2013). The operating pressure range is suggested by Welder *et al.* (2018) to be between 7 and 100 bar, potentially accumulating 1.5 GWh of hydrogen, with injection rates of 63 MW (which ensures the complete emptying of the storage in 24 hours). Differently from underground storage in geological formations, the minimum pressure value is not set to guarantee thermal/structural stability of the storage, but rather to maintain reasonable operating conditions of the compressor for delivery into the transmission network (HyUnder, 2013). Considering the abovementioned factor, this assessment proposes a CAPEX for this storage technology to vary between EUR 9.14 and 10.5/kWh$_{H2}$ (or EUR 304-350/kg$_{H2}$), a fixed OPEX of around 19% of the CAPEX per year and a lifespan of 30 year (Welder *et al.*, 2018)(HyUnder, 2013).

Line packing
Line packing is a practice widely used in the natural gas transmission/distribution networks (Element Energy, 2018). The principle is that of exploiting the existing pipeline infrastructure for storage of the gas. By widening the operational pressure range of the pipelines (a.k.a. working pressure range), it is possible to inject and withdraw (and therefore store) a larger quantity of gas within a section of the network. This technique could be transferable to hydrogen transmission/distribution networks (hydrogen backbone), and could be able to accommodate hourly supply and demand fluctuations (Guidehouse, 2021c) (ENTEC, 2022) (Wijk and Wouters, 2021) (Agora Energiewende, 2021). Hydrogen gas line packing could be thought of as a type of distributed storage, and encouraged near demand centers (Element Energy, 2018). According to ENTEC (2022), a 24 inch pipe with a length of 100km could store up to 43 tons$_{H2}$ if the pressure is increased from 50 bar to 60 bar.

6.1.2 Ammonia tanks

With regard to hydrogen transport in its converted form of ammonia, there is the necessity to store this medium in import/export shipping terminals. The characterizing techno-economic parameters of stationary ammonia tanks are then also applicable to the vessels used for transportation. Ammonia tanks benefit from the maturity of the technology conferred by the extensive trade this carrier has witnessed in the past decades. As mentioned in Chapter 4.1, it is of interest of assessing ammonia as a hydrogen carrier because of it high energy density of 124 kg$_{H2}$/m$^3_{NH3}$ (ENTEC, 2022) in its liquid form, which is 1.7 times the amount of hydrogen present in one cubic meter of liquefied hydrogen (IRENA, 2022a). Ammonia is stored in its liquid form and to achieve this, two paths can be pursued. The first path sees the compression of the ammonia to 8bar while the second sees the ammonia refrigerated to -33°C (and can be maintained at atmospheric pressure) (ENTEC, 2022) (IRENA, 2022a)(Guidehouse, 2021a). The use of either one or the other storage method depends on the capacity of the vessel. Compression is more economically sensible for small- (<270ton$_{NH3}$) and intermediate-scale (450-2,700ton$_{NH3}$) storage. Refrigerated tanks are, on the other hand, suitable for large-scale storage (4,500-55,000ton$_{NH3}$) (ENTEC, 2022). The reason of this capacity-based differentiation is due to the fact that the cost increase of steel tanks for pressurized ammonia for greater capacity increases the cost of storage to the point where it is not feasible anymore. The greater capacity refrigerated tanks avoid the use of thick, costly, steel by employing either one or two layers of, relatively cheaper, insulation (ENTEC, 2022) (IRENA, 2022a). According to JRC (2022), in the case of large-scale refrigerated tanks, between 41 and 45 tons of ammonia could be stored per ton of steel used. In this regard, ENTEC (2022) also reports that the specific cost per unit of ammonia stored also reflect the effect of the economies of scale (with a scaling factor of around 0.7). It was estimated that the specific cost of a 55 $kton_{NH3}$ storage is EUR 1,164/ton_{NH3} (EUR 6,500/ton_{H2}, EUR 0.20/kWh_{H2}). Lastly, it is necessary to note that the refrigerated vessel has the additional characteristic of presenting a boil-off rate of 0.04%/day (IRENA, 2022a) (ENTEC, 2022)(JRC, 2022). However, the boil-ff is a smaller concern compared to that encountered in liquefied hydrogen tanks (Guidehouse, 2021a) and it could even be possible to re-liquefy the ammonia boil-off stream through a compression refrigeration cycle and pumped back to storage (JRC, 2022).

6.1.3 LOHC and methanol tanks

In a similar way to ammonia, LOCHs and methanol benefit from a well-established industry developed in the past decades. In this regard, both carriers present conventional oil product behavior (IRENA, 2022a), such as being in liquid form in atmospheric conditions and other properties like flammability. Therefore, conventional liquid fuel tanks may also be used for LOHC/methanol storage (Niermann *et al.*, 2019) (Raab, Maier and Dietrich, 2021), which additionally benefit from the little to no geographical constraints on their placement and medium-scale storage capabilities (ENTEC, 2022). According to Reuß *et al.* (2017), an LOHC infrastructure could also be built utilizing the existing – capillary - oil infrastructure. In the carriers stay hydrogenated for a long period of time without great costs and the only losses witnessed are due to some side reactions that cause 3% loss per year (and a complete lack of boil-off losses) (IRENA, 2022a). Characteristic costs of LOHC and methanol storage tanks are found to be EUR ~7/kg_{H2} (EUR 0.21/kWh_{H2}) and EUR 3.8/kg_{H2} (EUR 0.11/kWh_{H2}). Such costs are lower compared to other hydrogen derivatives storage tanks despite the low percentage of hydrogen contained in such carriers (4-7%wt for LOHC, and 12.5%wt for methanol) (IRENA, 2022a).

6.1.4 Liquefied hydrogen tanks

Storage vessels suitable for hosting liquefied hydrogen at temperatures of -253°C and atmospheric pressures (DNV GL, 2019b) are also a well-known technology, also due to their deployment in the aerospace industries for many decades. NASA already owns large-scale spherical storages of liquefied hydrogen with capacities of 3,200 m^3 and 4,700 m^3 (227 and 334 tons of hydrogen, respectively), and Kawasaki Heavy Industries has a 10,000m^3 vessel planned (IRENA, 2022a). An advantage of liquid hydrogen storage is the high volumetric energy density, which is four times that of gaseous hydrogen at 200bar (ENTEC, 2022). A major issue of storing hydrogen in its liquefied form is the inevitable losses due to boil-off. It is necessary to dispose of the evaporated quantity of hydrogen since the constant volume of the vessel leads to potentially dangerous overpressures (maximum allowed pressure 1.2MPa) (JRC, 2022). These losses occur despite the high insulation of the tanks and amount to between 0.05% and 2.5% per day. As mentioned for ammonia, the boil-off stream could potentially be re-liquefied and pumped back to the storage but presents a high energy expenditure (IRENA, 2022a). In order to minimize the boil-off losses highly insulated vessels are designed. The majority of such vessels are double-hulled allowing for a vacuum pumped gap packed with additional insulating material (IRENA, 2022a) (JRC, 2022). Another technique in limiting the boil-off losses lies in the spherical shape that liquid hydrogen vessels have. Thanks to the geometrical properties of the sphere, the exposed surface to volume ratio is minimized along with the overall heat absorption. However, this particular shape presents manufacturing challenges and therefore has higher costs (IRENA, 2022a). A cheaper but slightly less effective alternative is represented by cylindrical vessels. Costs of liquefied hydrogen vessels are determined by the material necessary and manufacturing techniques and range between EUR 2.7/kWh_{H2} and EUR 5.2/kWh_{H2} (DNV GL, 2019b; Guidehouse, 2021a; ENTEC, 2022; JRC, 2022).

6.2 Underground storage

The assessment of large-scale hydrogen storage is of particular interest because it could potentially enable storage of energy for periods of months to seasons. Therefore, large-scale hydrogen storage could play an important enabling role in reducing the curtailment of renewable energy produced by solar and wind. Electrolyzers could absorb the surplus energy resulting from the mismatch between low power demand and high RES supply that would otherwise be curtailed to produce green hydrogen which, once compressed, can be stored for later use when demand exceeds supply (BNEF, 2020). Seasonal storage of energy in the form of hydrogen requires very large storage capacities (hundreds of millions to billions of Sm^3) and for this reason, its implementation cannot realistically be envisioned in a conventional storage vessel (be it a pressurized tank, ammonia, LOHC, LH2 tanks) as this would require too much aboveground space, meet with unacceptable health, safety and environmental risks, and be too expensive. The means by which large-scale hydrogen storage is possible is by exploiting particular – favorable – conditions in the subsurface. There are four main typologies of geological storage reservoirs that allow for such great volumes of gas to be stored safely: hydrocarbon reservoirs, aquifers, salt caverns, and lined rock caverns (Lord, Kobos and Borns, 2014). In the following sections, an assessment of large-scale hydrogen storage is conducted for depleted hydrocarbon reservoirs in porous rock formations and for (salt) caverns formed in salt deposits.

6.2.1 Salt caverns

Salt caverns are man-made cavities in underground salt deposits. Salt deposits may exist either in the form of bedded salts or salt domes. Bedded salts are commonly laterally continuous, and their internal composition is “predictable”, however their thickness can be a limiting factor for cavern development. Salt domes are laterally not continuous, and their internal composition is not “predictable”, but they are not height-limiting for cavern development, i.e., higher caverns can be created. It has been proven that salt is effectively impermeable, i.e., it does not allow fluids to flow through it. As such, salt caverns can be seen as perfect storage containers for long-term storage of gases and liquids. In a single salt cavern, made by solution mining of salt, a volume of one hundred million Sm^3 of gas can typically be stored, while in porous reservoirs, the main focus of this project, volumes of gas of 0.5 to 5 billion Sm^3 can be stored. Salt cavern storage is proven technology for natural gas and has great potential for the storage of green hydrogen (Caglayan *et al.*, 2020). Following are some examples where salt caverns for hydrogen storage are operational:

- Teesside, UK (active since 1959 storing 95%)[1]
- Spindletop, US (95% hydrogen storage, remaining content not documented)
- Clemens Dome, US (95% hydrogen storage)[1]
- Moss Bluff, US (95% hydrogen storage)[1]

Salt cavern leaching operation

The procedure through which such cavities are created in the salt deposit is known as leaching. Having ensured that the depth and thickness of a salt deposit are suitable to host a salt cavern a borehole is drilled to the depth of the bottom of the envisioned salt cavern. At intervals during the drilling operation, a casing (concentric metal pipe) is inserted into the hole, and cement is placed around it, to avoid the open hole from collapsing. After the drilling operation is completed, a (temporary) leaching completion is installed. Two concentric pipes are run down

[1] The remaining content of the operating salt cavern storage sites of Teesside (UK), Clemens Dome (US) and Moss Bluff (US) is reported in literature to be 3-4% CO_2 (Muhammed *et al.*, 2022).

the borehole (Figure 23, left), of which the inner tube (inner leaching string) has a diameter that is smaller than the outer tube (outer leaching string), allowing for a gap, called “annulus”. Similarly, the diameter of the outer tube is smaller than that of the casing, leaving a second annulus. This annulus allows for the introduction of a so-called “blanket fluid” (nitrogen or oil are commonly used for this) that shields the roof of the cavern from being leached to make sure that the cavern develops according to design specifications. Leaching starts at the deepest point of what will become the cavern, where fresh (or very low salinity) water is pumped into the deposit via the inner tubing and brine (water with dissolved salt) is extracted through the annular space between the inner and the outer tubing. This configuration is known as direct leaching. Alternatively, in reverse leaching fresh water is injected into the deposit through the annular space between the inner and the outer tubing and the brine is extracted through the inner tubing. The choice between direct and reverse leaching allows for either growing the cavern from the bottom (direct) vs. at the top (reverse), thereby effectively making it possible to “steer” the development of the cavern to meet the design specifications. Throughout the leaching operation insoluble material (claystone, shale, anhydrite etc.) is released from the salt that sinks to the bottom of the cave, forming the so-called “sump”.

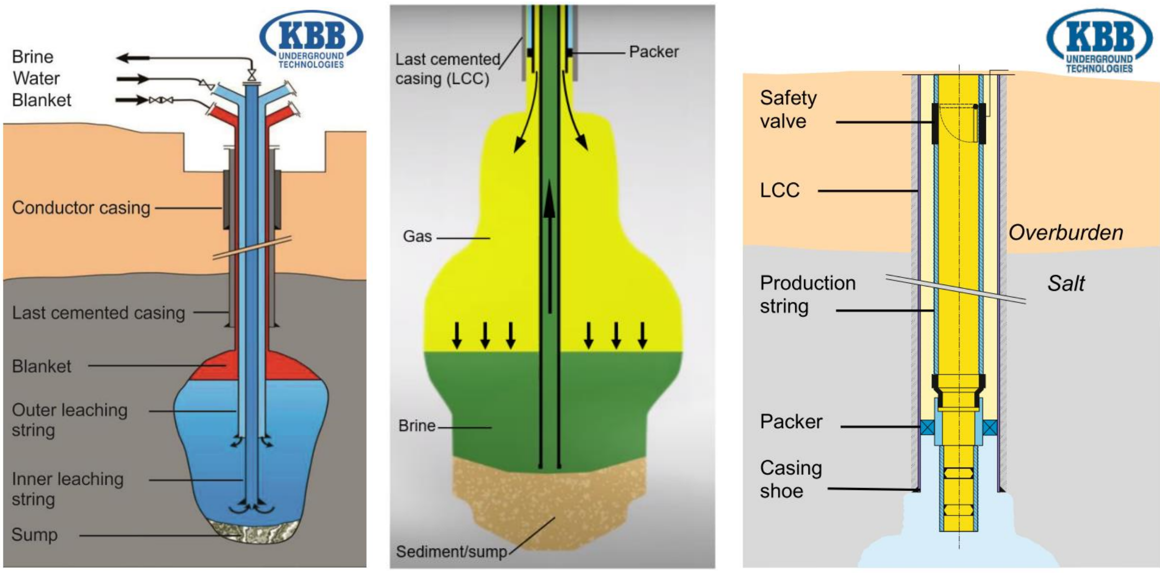

Figure 23. (Left) Example of reverse leaching operation. (Center) Cavern conversion operation. (Right) Converted cavern ready for operation of gas storage (HyUnder, 2013).

Once the leaching operation is concluded (i.e. the cavern has developed according to design specifications in terms of volume and geometry) the cavern must be converted to a gas storage cavern. To this end, a gastight completion is installed, i.e., the leaching wellhead is replaced by a gastight (hydrogen-compliant) wellhead, and the annular space between the casing and the outer tubing is closed off with a packer. The process of debrining and first gas fill is then executed, whereby gas (hydrogen in this case) is injected through the remaining open annular space between the outer and inner tubing, pushing the brine upward and out through the inner tubing. Once completed, the inner tubing (debrining string) is pulled, leaving a (gas) production tubing inside the casing with a closed-off annulus in-between that can be monitored for leakage. The cavern is now ready for gas storage.

Salt cavern gas storage components

A salt cavern storage facility consists of surface and subsurface components. In the previous section, the subsurface components were already reviewed, in particular the cavern (storage reservoir) and the well (incl. the wellhead, although at the surface) (Figure 23 [right]). The components at surface include the valve system at the wellhead (also called “Christmas tree”), the compression train for gas injection into the cavern, and the gas conditioning system that cleans and dries the withdrawn gas prior to reinjection into the network. The compression system is composed of displacement compressors equipped with intercoolers to avoid gas temperatures to rise above temperature thresholds. Such thresholds are derived from geological constraints regarding thermal stability of the cavern walls (discussed further below). The injection pressure is usually set to the maximum operating pressure of the cavern, which is also constrained by the geology of the site and is discussed further below. The gas withdrawal system on the other hand, has the task of extracting the stored gas from the cavern in a controlled manner and conditioning it prior to delivery. In most cases, the storage pressure is higher than the delivery pressure and therefore, only a pressure reducer is needed to achieve delivery pressure (otherwise a booster compressor would be required). The gas conditioning unit is composed firstly of a drying unit and, primarily in case of storage in a depleted gas reservoir, a treatment unit for impurities removal. As mentioned, purification is more commonly required in pore storages that store in depleted hydrocarbon fields as the presence of small amounts of acid gases and light hydrocarbons in the residual gas is probable. It is important to note that both the injection and withdrawal process use energy. During injection, energy is needed to run the compressors (and to a lesser extent, the intercooler fans), while for gas withdrawal (not considering a booster compressor) energy is required for the regeneration of the adsorption unit in the drying process. These values where found in literature to range between 0.026 and 0.089 $kWh/kWh_{Stored\ H2}$ for injection and between 0.005 and 0.009 $kWh/kWh_{Stored\ H2}$ for withdrawal (Tarkowski, 2019; Hystories, 2022; JRC, 2022).

Salt cavern techno-economic parameters

For the utilization of a salt cavern for gas storage, it is relevant to assess the quantity of gas that can be stored and the rate at which the gas be injected or withdrawn. The quantity of gas that can be stored is determined by the minimum and maximum operating pressure of the cavern, and the geometric volume of the cavern. The value of maximum operation pressure must be chosen so to not jeopardize the geomechanical stability of the cavern. Salt caverns can be operated in 'wet' mode or 'dry' mode. Wet mode indicates operation in which gas pressure is kept constant by changing the volume of brine in the cavern, and is uncommon. On the other hand, in 'dry' mode operation, which is much more common, the gas pressure changes (between a max. and min. pressure) as the gas is injected and withdrawn. The maximum allowable pressure in the cavern is limited by the maximum pressure gradient, and calculated at the depth of the last cemented casing shoe (which is considered to be the weakest point; Hystories, 2021). For example, considering a depth of the last cemented casing shoe of 1,000 m and assuming a maximum allowable pressure gradient of 0.18 bar/m (≈80% of the lithostatic gradient) the determined maximum operating pressure is ≈180 bar. Similarly, there is also a minimum operating pressure to limit the amount of cavern convergence (and subsidence) and ensure the geomechanical stability of the cavern. The minimum pressure is calculated with an assumed minimum pressure gradient, e.g., 0.06 bar/m and evaluated at 2/3 of the cavern height, which would result in a minimum pressure of 60 bar (Hystories, 2021). In a similar way, a minimum and maximum temperature are also determined for the specific cavern site. The operational pressure range as defined by the maximum and minimum pressures, together with the geometric volume of the cavern, determines the working gas volume, and also to large extent the injection and withdrawal rates.

It is important to note that the cavern will not be emptied completely during its storage operational lifetime since a minimum pressure must be maintained at all times (see above). The volume of gas that must always be present in the cavern is called **cushion gas**. The difference between the volume of cushion gas (at minimum operating conditions) and the volume present at maximum operation conditions is called **working gas**, which is the volume of gas that can actually be stored (cycled). Under the abovementioned pressure conditions, the cushion gas represents between 20% and 45% of the total gas (Hystories, 2021; Hanson *et al.*, 2022). In the view of storing hydrogen gas, considering cavern volumes of 200-600 thousand m^3 and the minimum and maximum operating pressures, salt caverns could hold between 16.7 and 47.0 MSm^3 of hydrogen working gas per cavern (standard cubic meter refers to the volume occupied by a gas at 15°C and 1 atm. in the case of hydrogen). Corresponding to ~1,500 and ~4,000 tons of hydrogen (1 Sm_3 contains 0.085 kg_{H2}). which in return correspond to 47 to 133 GWh_{H2}.

Another relevant parameter that characterizes salt caverns for gas storage is the rate at which the gas can be injected and withdrawn. These values depend on certain thresholds defined by the necessity of guaranteeing structural stability of the caverns. order to maintain a suitable level of heat transfer between the gas and salt cavern walls to guarantee thermal stability, a maximum pressure decrease of 10 bar/day should be ensured (Hystories, 2021). Another phenomenon that must be avoided is erosion-induced corrosion, which occurs at the wellhead (withdrawal) and cavern entrance (injection) when too high fluid velocities are reached (Groenenberg *et al.*, 2020) (Element Energy, 2018). Taking into account such constraints the injection and withdrawal rates of hydrogen to and from salt caverns are determined to lie between 1.5 and 4.4 MSm^3/day per cavern (or 4.3 and 12.5 GWh/day), corresponding to the 200 and 600 thousand m^3 cavern volume described above, respectively. Such values are also in line with (HyUnder, 2013; Lord, Kobos and Borns, 2014; Welder *et al.*, 2018).

Salt cavern storage sites are commonly composed of multiple caverns in close proximity to each other. The caverns are appropriately spaced to ensure stability, avoid interaction, and minimize surface subsidence. In the Hystories project (2021), notional cavern storage sites with 5 and 12 caverns were defined corresponding to the 600 thousand and 200 thousand m^3 cavern volumes respectively. All caverns of a site are envisioned to work in parallel and be operated under the same pressure regime, hence both the working gas volumes (as well as the cushion gas volumes) and the injection/withdrawal rates are added together to define storage site characteristic storage capacities of ~17 and ~21 ktons of hydrogen, and achievable rates of injection and withdrawal of between ~51 and ~63 GWh/day.

The economic characterization of hydrogen storage in salt caverns presented in this assessment distinguishes between surface and subsurface components. For the surface components the investments costs are normalized with respect to injection/withdrawal rates of hydrogen. For the subsurface components, the normalization regards the hydrogen contained in the working gas of the salt cavern. Surface components include compression system (injection), the hydrogen conditioning system (withdrawal), the piping, the balance of plant as well as the planning and installation costs. The subsurface elements of cost include drilling, leaching operation, cavern conversion and first gas fill. According to literature, the values of CAPEX with respect to surface components range between EUR 183/kW_{H2} and EUR 327/kW_{H2} (hydrogen transiting the facilities) (Lord, Kobos and Borns, 2014; Michalski *et al.*, 2017; Hystories, 2022). On the other hand, the CAPEX related to the subsurface facilities and operations ranges between EUR 0.25/kWh_{H2} and EUR 0.49/kWh_{H2} (hydrogen stored as working gas). According to literature leakages may occur leading to self-discharge losses between 0% (Davies *et al.*, 2020; Hystories, 2021) of up to 1% per year (Lord, Kobos and Borns, 2014).

The technical lifetime of a salt cavern storage site is limited by the lifespan of the surface facilities, the wells, and by cavern convergence. The lifetime of a salt cavern storage facility was set to be 30 years (Lord, Kobos and Borns, 2014; Welder *et al.*, 2018; Agora Energiewende, 2021). The subsurface components, which consist of the salt cavern and well(s), tend to be more durable. At the end of the lifespan of a salt cavern storage facility, special care must be taken in order to safely decommission the facility and abandon the salt caverns and wells. The economic effort to do so is embodied in the abandonment expenses (or ABEX), which in this assessment is also differentiated between the expense related to surface and subsurface facilities. Regarding the subsurface portion of the plant, water or brine is pumped back in the cavern. This to both retrieve the remaining gas (cushion gas) and to ensure that no more salt is being dissolved from the cavern wall (once the solution is fully saturated). The wellhead remains accessible for periodic inspections until the solution inside the cavern is fully saturated and the cavern walls are thermally stabilized. Subsequently, the well is plugged for permanent abandonment and the wellhead is removed for the soil to be restored. The ABEX is reported by Hystories (2022) to be around 20% of the CAPEX, for both surface and subsurface facilities.

It is also of relevance to assess the potential of repurposing already existing salt caverns (currently used for the storage of natural gas) to be hydrogen ready. The main advantage of this route is, intuitively, the avoidance of the initial expenses necessary to create the cavern. Drilling and leaching operations as well as all the equipment and indirect costs could be therefore saved. Additional costs could be incurred due to the upgrading of components to be able to handle hydrogen (different steel grades) and the proper disposal of old equipment as well as additional purging processes to prevent hydrogen contamination (Agora Energiewende, 2021).

6.2.2 Pore storage

The two main differences between pore storages and salt caverns are, firstly, that salt caverns are man-made cavities while porous reservoirs are naturally occurring in the subsurface. The second difference lies in the structure of the subsurface storage element. Salt caverns are essentially large voids of space, whereas porous reservoirs are rock formations with high enough and interconnected (to ensure gas permeability) porosity. As already mentioned, such formations are naturally occurring and are host to hydrocarbons (hydrocarbon reservoirs) and/or water (aquifers). The reservoirs' tightness to the fluid they are bearing is proven simply by the occurrence of the fluid, that has been contained in the reservoir for many years prior to their discovery. The porous reservoirs' tightness is guaranteed by the presence of a sealing caprock which prevents the hydrocarbons or water to diffuse towards the surface, and lateral sealing which allows to contain the hydrocarbon or water in a confined in space (Figure 24).

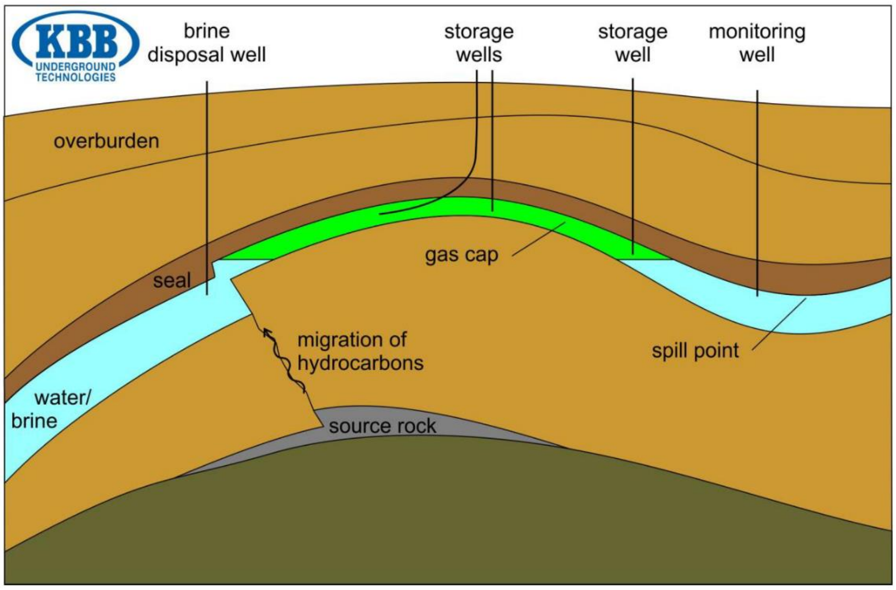

Figure 24. Cross-section of a generic hydrocarbon deposit depicting the cap-rock and the lateral seal (Groenenberg *et al.*, 2020).

Oil and natural gas fields have been the subject of assessment for many decades due to the interest in the exploitation of their hydrocarbon content. The concept of gas storage in such reservoirs is based on the utilization of the fields once the hydrocarbon extraction is considered completed. The scope of this assessment only regards gas storage in depleted gas fields. Gas storage in depleted oil reservoirs has been trialed in a few cases and resulted in production and treatment issues, and will therefore be excluded (HyUnder, 2013). Differently from gas fields, aquifers can potentially be used as gas storage systems without the need of depletion of the reservoir. However, it is necessary to assess and ensure that the porous formation, originally hosting water, is suitable for gas storage. In both cases it is of paramount importance to assess and verify that the storage of high-pressure gas does not affect the geology/lithology surrounding the reservoir, which could potentially jeopardize its tightness to the gas.

The majority of porous reservoirs that are in use for gas storage today lie at depths between 500-2,500 m (with some reservoirs at depths of up to 3,500m, in particular in the North Sea region), have relatively high porosities of 10-30%, and widely ranging permeabilities of 20-2,000 mD[2] (Cavanagh *et al.*, 2022b). These elements are verified through geological characterization of a site, an activity well-known from decades of exploration in the oil and gas industry. Depleted natural gas fields have been successfully converted into natural gas storage and are the most prominent typology of large-scale storage. The main reason of this is the advantage presented by prior knowledge about the reservoir, and the re-use of existing infrastructure (production wells, some surface components) (Hanson *et al.*, 2022). However, in order to convert the production site to a gas storage site, additional production (and monitoring) wells may have to be drilled. The number of storage wells required typically depends on the intended function(s) of the storage facility, i.e., short(er) term storage cycles (storage for days to weeks) with usually higher rates of injection and withdrawal requiring more wells vs. long(ter)-term storage cycles (intra-to-interseasonal and/or strategic storage) requiring lower rates of injection and withdrawal.

Aquifers may also be used for the storage of gas given that the abovementioned requirements of cap-rock and trapping elements presence are satisfied. When storing gas in an aquifer, the gas simply displaces the water in the porous structure. This leads to a dynamic boundary between the two phases which continuously shifts in space during injection and withdrawal operations (Yousefi, 2021). Unlike depleted gas fields, virgin aquifers need significant field development work to be used as gas storage. Since there is no well infrastructure in place in such undeveloped aquifers, all surface and subsurface infrastructure would need to be put in place (Guidehouse, 2021c). Moreover, aquifers also lack the geological surveys which depleted gas fields underwent during the exploration phase, which also contribute to a higher investment cost (Thiyagarajan *et al.*, 2022). For these reasons, aquifers tend to be the last option for gas storage where depleted reservoirs or salt caverns are not available (Lord, Kobos and Borns, 2014).The following assessment therefore focuses only on the characterizing techno-economic parameters of depleted gas fields.

Pore storage components

Similarly to large-scale storage in salt caverns, the components of a storage facility in a depleted gas field can be grouped in surface and subsurface components. The subsurface category includes all parts of the well from the wellhead downwards and the reservoir, while the surface facilities include all components between the wellhead and the delivery point. Cemented boreholes reach depths of ~1,000 to ~3,500 m (HyUnder, 2013), remnant of the natural gas extraction operations. At the level of the reservoir, the cemented outer casing has a perforated interval that allows for gas to flow from the well into the reservoir during injection, and back out into the well during withdrawal (Figure 25). Inside the cemented casing is the

[2] mD unit of measure represents the millidarcy, where 1 Darcy ~ 10^{-12} m^2.

production tubing. As can be seen in Figure 25, the seal between the cemented casing and the production tubing is formed by a packer that is placed above the reservoir itself.

The surface components are basically equal to those discussed for salt caverns. The valve system at the well head (also called “Christmas tree”) regulates the flow to and from the reservoir, the compression system allows for injection, and the gas conditioning system ensures that the withdrawn gas has the required quality for re-injection into the network. Reciprocating compressors with intercooling stages allow for injection of gas at temperatures within safe ranges. At the time of withdrawal, gas delivery pressure is ensured by a pressure reducer. The gas undergoes conditioning (drying, separation, purification) which in the case of storage in depleted gas field is more critical when compared to storage in salt caverns. The interaction between the stored gas and the porous reservoirs may give way geochemical and biochemical reactions as well as mixing of the stored gas with residual natural gas present in the reservoir as well as residual moisture. The gas conditioning unit is composed firstly of a drying unit and, primarily in case of storage in a depleted gas reservoir, a treatment unit for impurities (acid gases such as H_2S, CO_2 and hydrocarbons such as CH_4, C_2H_6) removal. It is important to note that both injection and withdrawal systems use energy. During injection energy is needed to run the compressors (and to a lesser extent, the intercooler fans), while for gas withdrawal (not considering a booster compressor) energy is required to run the purification and dehydration units. These values where found in literature to be of 0.019 $kWh/kWh_{Stored\ H2}$ for injection and 0.045 $kWh/kWh_{Stored\ H2}$ for withdrawal (DNV GL, 2019b; Hystories, 2022).

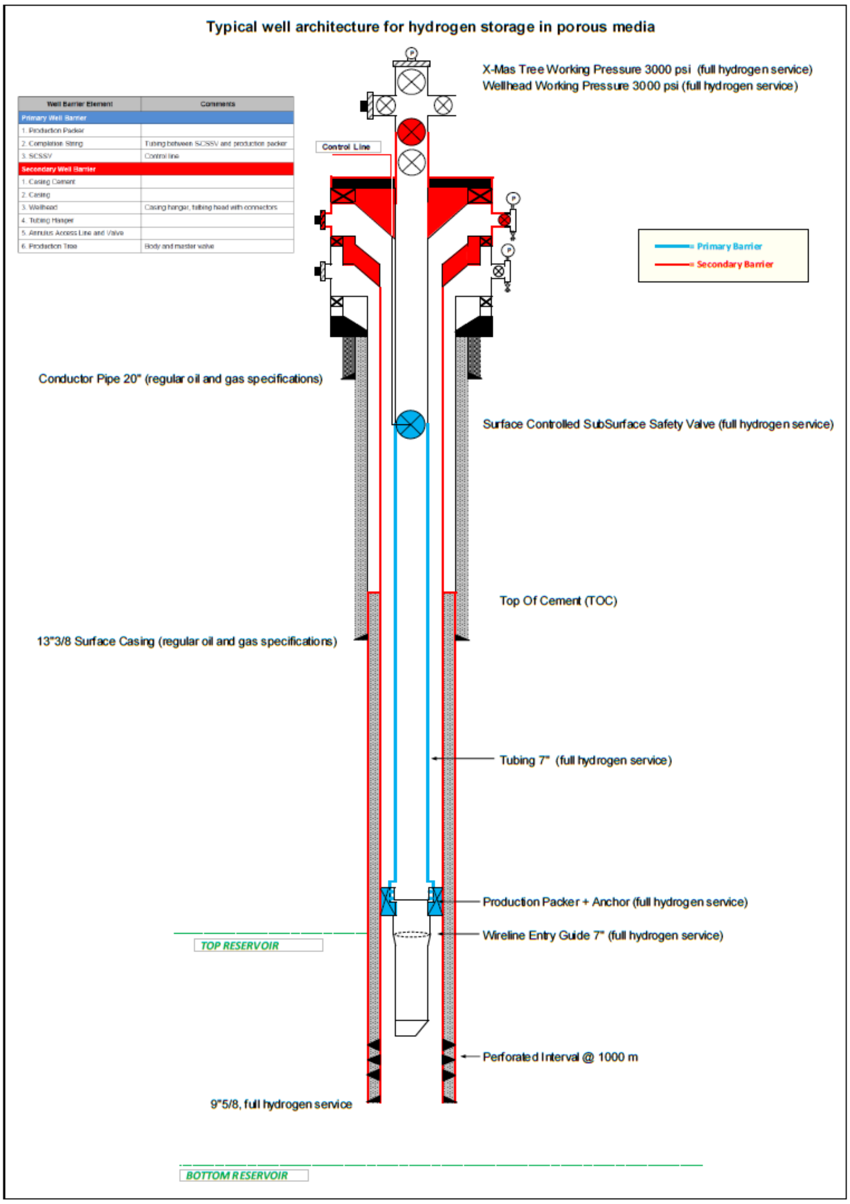

Figure 25. Schematic representation of the subsurface components (and valve system [Christmas tree]) of underground gas storage in porous media (Hystories, 2021).

Pore storage techno-economic parameters

The technical parameters of pore storages are constrained and defined by the reservoir characteristics, which vary from reservoir to reservoir, contrary to salt caverns, whose geometry and dimensions can be defined by necessity. Nonetheless, the concepts illustrated for salt caverns regarding operating pressures, volumes and flow rates are also applicable to porous reservoirs. As part of Work Package 1 of the HyUSPRe project the potential of hydrogen storage in porous reservoirs in Europe was assessed and reported in Deliverable 1.3 (Cavanagh *et al.*, 2022a). The work, based on among others Gas Infrastructure Europe's public database on storage sites (GIE, 2021), resulted in a longlist of 108 natural gas stores in porous reservoirs (84 in depleted gas fields, 24 in aquifers) in operation that could be converted to hydrogen stores. The underlying rationale to this approach is that the analyzed storage sites benefit from a proven history of natural gas storage and inclusion in the existing gas network which reflects the current demand and market. The overall capacity across Europe, in terms of existing natural gas storage in porous reservoirs, is 1,328 TWh. Summarizing the data of the single porous storage reservoirs (excluding the largest sites), it was determined that the average natural gas capacity of a porous reservoirs in Europe is 9 TWh (double that of salt caverns).

The work then proceeds to assess the conversion of the working gas capacity from natural gas to hydrogen. In this regard, two hydrogen working gas capacity estimation methods are proposed. The first, indicated through WGC-ED (working gas capacity-energy density), employs a static conversion based on the ratios of the physical properties of hydrogen and natural gas and of their energy densities. The second method (WGC-90), estimates the working gas capacity based on the ratio between hydrogen and natural gas deliverabilites over a withdrawal period of 90 days. The two pathways produce conversion factors of 0.25 and 0.5 respectively through which it is possible to derive the hydrogen capacity from the abovementioned natural gas capacities. The study also assesses the capacity attributable to 31 planned porous reservoir sites and 1 closed site. The resulting hydrogen capacities are summarized in Table 1.

Table 1. Total capacities of porous reservoirs in Europe by operational, planned and closed sites. Hydrogen capacities are determined from natural capacities through the energy density (WGC-ED) and rate-limited methods (WGC-90).

Capacity (TWh)	Conversion factor	108 Operational	31 Planned	1 Closed	Total
Natural gas	-	1328	136	30	**1494**
Hydrogen (WGC-ED)	0.25	332	34	7.5	**373**
Hydrogen (WGC-90)	0.5	664	68	15	**747**

The resulting capacities of 373 TWh and 747 TWh can be compared to the forecasted hydrogen storage demand in 2050 ranging between 500 and 1,000 TWh (considering a storage demand equal to 30% of overall demand, as is today with natural gas), highlighting how porous reservoir site may host large part of future stored hydrogen.

In their assessment, Hystories (2021) conducted a statistical analysis on a large number of underground natural gas storage facilities in porous media around the world and propose a characteristic value of capacity based on the most commonly encountered storage site. The resulting representative parameters regard minimum and maximum operating pressures of 60 and 120 bar respectively, which correspond to a working gas volume of 200 MSm^3 and a cushion gas volume of 135 MSm^3 (40% tail gas to total gas ratio). Such value corresponds to 568 GWh, or 17,000 ton, of stored hydrogen as working gas. The approach also assessed the withdrawal rate, that depends on the number of operating wells present on the site, which varies between 6 and 52 wells. The corresponding withdrawal rates are of 2 and 6 MSm^3/day (respectively 6 and 17 GWh/day). However, this value is site dependent and has been reported to reach 21.3 GWH/day (HyUnder, 2013), between ~60 and ~70 GWh/day (Amid, Mignard and Wilkinson, 2016) and up to ~120 GWh/day (HyUnder, 2013).

As was done for gas storage in salt caverns, the economic characterization of underground storage of hydrogen in depleted gas fields differentiates between surface and subsurface components. For the surface components the investment costs are normalized with respect to injection/withdrawal rates of hydrogen transiting between the wellhead and the network. For the subsurface components, the normalization regards the hydrogen contained in the working gas of the storage site. Surface components include compression system (injection), the hydrogen conditioning system (withdrawal), the piping, the balance of plant as well as the planning and installation costs. The subsurface elements of cost include the costs for re-use or P&A of existing wells, drilling of additional wells (if the number of wells inherited from the natural gas facility are not sufficient) and first gas fill. According to literature, the values of CAPEX with respect to surface components range between EUR 257/kW$_{H2}$ and EUR 430/kW$_{H2}$

(hydrogen transiting the facilities). On the other hand, the CAPEX related to the subsurface components and operations ranges between EUR 0.09/kWh$_{H2}$ and EUR 0.28/kWh$_{H2}$ (hydrogen stored as working gas) (HyUnder, 2013; Lord, Kobos and Borns, 2014; ENTEC, 2022; Hystories, 2022).

The energy required for the injection and withdrawal (discussed above) of hydrogen to and from the reservoir could be considered as losses. According to literature hydrogen loss could occur due to leakages and biological activity. According to (Amid, Mignard and Wilkinson, 2016) leakages could be responsible for the loss of 0.035% of the stored hydrogen over a year, while biological activity could potentially convert 3.7% of the hydrogen to methane and biomass of the lifespan of the reservoir. Geochemical reactions of hydrogen within the porous media may cause the formation of H_2S, the dissolution of hydrogen in water to produce acidic solutions (which may undermine components' functioning), and methanation of CO_2 and CO. Biochemical reactions on the other hand, are enabled by microorganisms that thrive in reservoir pressures and temperatures. As already mentioned, the presence of such organisms is limited by high salinity and is therefore more likely to occur in porous reservoirs than salt caverns. Such organisms may consume hydrogen and generate methane, acetic acid, CO_2, H_2S and also reduce iron (Yousefi, 2021). All these are elements that constitute losses, i.e., that part of the injected hydrogen is not recoverable.

The technical lifetime of a depleted gas field storage site is mostly limited by the surface facilities, and amounts to around 30 years (Lord, Kobos and Borns, 2014; Hystories, 2022). The subsurface components, which consist of mostly the wells, tend to be more durable provided they are properly built, maintained and monitored. At the end of the lifespan of the storage, special care must be taken in order to safely shut down the facility. The economic effort to do so is embodied in the abandonment expenses (or ABEX). The ABEX is reported by Hystories (2022) to be around 20% of the CAPEX, for both surface and subsurface facilities.

7 Hydrogen final use

In the following section, the techno-economic parameters of demand-characterizing hydrogen technologies are summarized. The final use of hydrogen spans across multiple sectors as it theoretically can satisfy demands of electricity, heat, H2-as-feedstock and mobility.

7.1 Power generation

The techno-economic assessment of power generation from hydrogen is a crucial element in the evaluation of the long-term energy storage potential of this energy vector. Costs and performance of hydrogen power generation technologies contribute to determining the feasibility of energy storage through hydrogen.

7.1.1 Hydrogen fired gas turbines

Gas turbines are well-known in power production usually utilizing natural gas as fuel. However, blending of hydrogen gas and methane is common in certain applications. For example, refineries employ gas turbines with specific designs that allows them to be fired by by-product gas streams with high hydrogen contents (for example from catalytic cracking units with 15-20%vol hydrogen [Mukherjee and Singh, 2021]). Building onto this knowledge, many manufacturers are now looking to produce turbines able to run high hydrogen content gas streams if not solely on hydrogen gas (Ansaldo Energia, Baker Hughes, General Electric). The challenges faced by research and development are due both to hydrogen gas handling and the nature of hydrogen combustion. In the first case, the gas handling systems require materials that are not prone to degradation in the presence of hydrogen and must be leak resistant. In the second case, hydrogen differs from natural gas when combusting as hydrogen is more reactive, which may cause phenomena known as autoignition (when the mixture ignites in the premixing chamber as opposed to the combustion chamber) and flashback (when the flame speed is higher that the stream injection velocity so that the flame front travel back into the burner tube). Lastly, higher flame temperatures also cause higher NOx emissions, therefore extra design steps must be undertaken in order to either decrease the flame temperature or abate the NOx in the flue gas streams (ETN Global, 2020).

Tecno-economic data is presented for both open circuit gas turbines (OCGT) and combined cycle gas turbines (CCGT) designed to run on 100% hydrogen gas. The first typology is characterized by a power-producing gas turbine discharging its flue gases into atmosphere and therefore not utilizing their heat content for further power production. The second typology on the other hand utilizes a heat recovery steam generator to exploit the heat content of the flue gases for further power generation in a secondary steam power plant. According to Öberg, Odenberger and Johnsson (2022), investment costs for a new 100% H2 OCGT vary between EUR 536/kW_{el} and EUR 583/kW_{el} while for a new 100% H2 CCGT vary between EUR 1,072/kW_{el} and EUR 1,165/kW_{el}. The efficiencies of the two typologies are between 27% and 32% (considering the electrical output) for the OCGT and 58% and 62% (considering the electrical output and the thermal recovery) for the CCGT (DNV GL, 2019b). Regarding non-fuel variable costs, these vary between EUR 0.002/kWh_{el} and EUR 0.015/kWh_{el} for the OCGT and between EUR 0.001/kWh_{el} and EUR 0.006/kWh_{el} (Grosse *et al.*, 2017; Oh, Lee and Lee, 2021).

7.1.2 Stationary Fuel Cells

Fuel cells allow to convert hydrogen gas to electric energy through an electrochemical reaction (inverse reaction to electrolysis). There are a variety of typologies of fuel cells differing on the nature of the materials (electrodes, membranes), operating temperatures and difference in

gases accepted. Regarding this last point, it is necessary to note that some fuel cells are able to process not only pure hydrogen, but also other hydrogen-bearing gases which, through high temperatures, are cracked/reformed to isolate the hydrogen gas prior to the power generating electrochemical reaction.
Considering the different typologies of fuel cells (alkaline fuel cells, phosphoric acid fuel cell, molten carbonate fuel cell, proton exchange membrane fuel cell, and solid oxide fuel cell), those deemed as suitable for stationary power generation are mainly proton exchange membrane fuel cells (PEMFC) and solid oxide fuel cells (SOFC). PEM fuel cells benefit from the maturity of the technology, low maintenance costs (due to the solid electrolyte), high efficiencies and low temperatures. However, lower temperatures (80-200°C) also require a better performing, and thus more expensive, catalyst. For this reason, the more innovative SOFC are also assessed, which with their high operating temperatures (700-800°C) require less performing catalyst for the electrochemical reaction (Cigolotti and Genovese, 2021).

According to data gathered by Cigolotti and Genovese (2021) and the forecasts presented by Hydrogen Europe (2020), PEMFC specific investment costs decrease from between EUR 2,858/kW$_{el}$ and EUR 5,255/kW$_{el}$ in 2020 to EUR 1,000/kW$_{el}$ and EUR 3,000/kW$_{el}$ in 2030. Further forecasts were determined within this study assuming that cost reduction phenomena occurring in PEM electrolyzers would also impact cost reduction in PEMFC. By applying this rationale, specific investment costs were determined to fall to a range of EUR 722/kW$_{el}$ and EUR 195/kW$_{el}$ in 2050. Regarding the electrical efficiencies of PEMFC systems, value increase from between 35 and 42% (with respect to the LHV of hydrogen) to 53 and 58%LHV. With a similar reasoning to the one adopted for the specific investment, the efficiency improvements may ensure values of between 56 and 65%LHV$_{H2}$ in 2050. CAPEX and efficiency values of PEMFC are reported in Figure 26 and Figure 27, respectively.

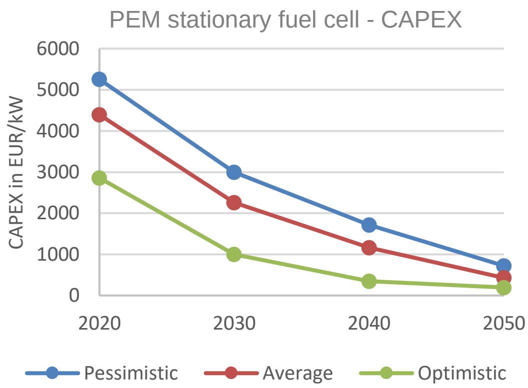

Figure 26. Proton exchange membrane fuel cell (PEMFC) CAPEX. The values represented summarize the values the following references: (Hydrogen Europe, 2020)(Battelle Memorial Institute, 2016)(Marocco *et al.*, 2021) (Cigolotti and Genovese, 2021).

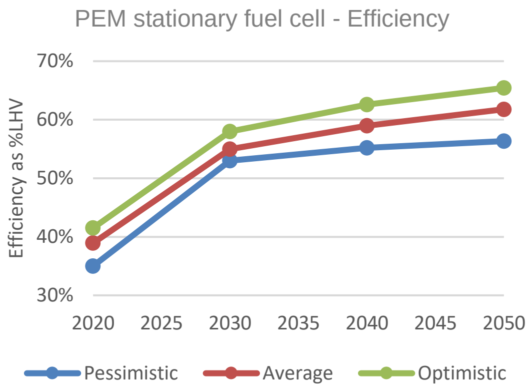

Figure 27. Proton exchange membrane fuel cell (PEMFC) efficiency with respect to the LHV of hydrogen. The values represented summarize the values the following references: (Hydrogen Europe, 2020) (Cigolotti and Genovese, 2021).

Regarding SOFC, The specific investment costs found in literature are in general higher than those of PEMFC, with 2020 values varying between EUR 4,224/kW_{el} and EUR 11,100/kW_{el} (Cigolotti and Genovese, 2021; Safari and Ali, 2020; Al-Khori, Bicer and Koç, 2021), but are forecasted to decrease, as reported by Hydrogen Europe (2020), to between EUR 2,220/kW_{el} and EUR 3,885/kW_{el} by 2030. As for the efficiencies, the values vary between 35 and 55%LHV_{CH4} in 2020 and 55 to 65%LHV_{CH4} in 2030. The values are provided as a percentage of the LHV of methane because the necessary reforming to obtain hydrogen occurs within the fuel cell due to the high temperatures.

7.2 Industrial heat generation

Another application of hydrogen gas is its use as fuel for heat generation in industry. Industrial heat demand accounts for one-fifth of global energy consumption and since its mostly satisfied with fossil fuels, it is responsible for 12% of global CO_2 emissions (DENA, 2019). This shows the potential substitution of fossil fuels for heat generation in industry with green hydrogen could have significant impact in emissions abatement. On this matter, Element Energy (2019), conducted a study on quantifying challenges and efforts of the conversion of industrial heat generation equipment from natural gas fired to hydrogen fired. The study finds that most of industrial equipment can be retrofitted to become hydrogen fired. However, the different combustion characteristics of hydrogen (heat transfer characteristics, high concentrations of NOx and moisture in the flue gases) might in some cases interfere with the final product quality, especially for direct fired heaters. For example, glass furnaces and kilns are sensitive to the moisture content in flue gases as well as the radiant heat transfer to product. On the other hand, indirect fired equipment, such as water boilers, are less susceptible to changes is combustion characteristics. For this reason, this assessment regards industrial water boilers.

The procedure followed to determine the investment costs of the retrofitted water boilers sees the marking up with values suggested by Element Energy (2019) specific investment cost of traditional natural gas fired boilers presented by Grosse *et al.* (2017). The results obtained this way for tank type boilers are between EUR 263/kW_{th} and EUR 385/kW_{th} for 1 MW_{th} capacity, EUR 194/kW_{th} and EUR 229/kW_{th} for 10 MW_{th} capacity, and EUR 181/kW_{th} and EUR 205/kW_{th} for 20 MW_{th} capacity. For larger, water tube boilers, of over 20 MW_{th} the specific investment was assessed to be between EUR 169/kW_{th} and EUR 193/kW_{th}.

7.3 Steel production

Iron and steel production is the most energy intensive among the industries demanding about 7% of global energy demand and is responsible for 7-9% of global GHG emissions (Kim *et al.*, 2022). These emissions originate not only from the fossil fuels used to satisfy thermal energy requirements but also from the so-called process emissions of the chemical reaction occurring in the of the steel making processes. The majority of steel is produced through the blast furnace/basic oxygen furnace (BF/BOF) route. Here, iron ore (containing iron oxide) is reduced to iron in a blast furnace (BF) thanks to high temperatures of up to 2,000°C. Coke is added to the BF in order to supply both the necessary energy for the reduction reaction and the carbon which binds with the oxygen removed from the iron ore forming CO and CO_2 (Wang *et al.*, 2021). The product of the blast furnace is the so-called pig iron, which is a high carbon content metal (3.8-4.7% carbon). The pig iron is then sent to the basic oxygen furnace (BOF) in which a jet of pure oxygen burns some of the carbon in the pig iron generating CO and CO_2 gas, lowering the overall carbon content to about 0.3-0-9%, obtaining steel.

An alternative steel making route to the BF/BOF is the direct reduction of iron paired with an electric arc furnace route (DRI/EAF). The main difference between BF/BOF and DRI/EAF lies in the reduction of iron oxide into iron, which for DRI/EAF occurs at temperatures below the melting point of iron (800-1,200°C, ensured either by the combustion of natural gas or coal) in the presence of a reduction agent. The reduction agent can either be in gaseous or solid form, where in the first case it is constituted by hydrogen, carbon monoxide or a mixture of both (syngas) and in the second by elemental coal (International Iron Metallics Association, 2019). The product of the direct reduction is the so-called sponge iron and, depending on the reduction agent, either water or CO_2 byproduct. The sponge iron is then sent to an electric arc furnace, in which three electrodes generate current reaching melting temperatures allowing for elemental carbon to be added to increase the carbon content to obtain steel (Bellona, 2021).

The most common direct reduction route sees the reforming of natural gas to obtain the reducing gas, and in particular the process known as Circored utilizes pure hydrogen as the reduction agent (H/DRI/EAF). According to Otto *et al.* (2017), for every ton of Circored steel, 8.3 GJ (out of the 18 GJ per ton of steel of the overall process) of natural gas are needed only for the production of hydrogen via reforming, having considered a hydrogen need of about $58kg_{H2}/ton_{steel}$. The emissions associated with the 8.3 GJ of natural gas could potentially be avoided by producing hydrogen through electrolysis powered by renewables. This would result in CO_2 emissions reduction of 66%, decreasing from 1,206 kg_{CO2}/ton_{steel} of the grey hydrogen route to 409 kg_{CO2}/ton_{steel} (Otto *et al.*, 2017).

Investment costs not considering the water electrolyzers were extrapolated from IEA (2019a) and Vogl, Åhman and Nilsson (2018) and amount to between EUR 540 and 722 /ton_{steel}/year in 2030. This translates into EUR 2,151/kW_{H2} and EUR 4,054/kW_{H2}, having considered a hydrogen need of 58 kg_{H2}/ton_{steel}.

7.4 High-value chemicals production

High-value chemicals can be differentiated between light olefins and aromatics. Light olefins, namely ethylene (C_2H_4) and propylene (C_3H_6), are the most widely used base compounds used in the production of plastics (polyethylene and polypropylene). Aromatics, mainly benzene (C_6H_6), toluene (C_7H_8) and xylene (C_8H_{10}), which will be referred to as BTX, are compounds used in a wide range of applications. Benzene is the base compound of synthetic materials such as nylon, resins and polycarbonates as well as being gasoline additive with the function of increasing octane rating. Toluene is the base compound for polyurethane but is also used in the manufacturing of glues, paint/paint thinners and explosives. Xylene (and its isomers), has similar solvent properties to toluene and benzene but is also the base compound of polyethylene terephthalate (PET) (which is widely used in packaging) and polyester clothing.

It can therefore be deduced that HVCs play an important role in the chemical industry as they are the fundamental building blocks of widely used products. However, the main production route of HVCs is via the petrochemical industry, as they are mainly derived from naphtha through a process known as steam cracking which releases between 1.6 and 1.8 ton_{CO2} per ton of product (Groß *et al.*, 2022). It is therefore of interest assessing alternative, decarbonized pathways for the production of such fundamental products. An emerging HVC production process is the upgrading of the less valuable methanol to olefins or aromatics. The processes are known as methanol-to-olefins (MTO) and methanol-to-aromatics (MTA), and if the methanol is produced from renewable hydrogen and carbon dioxide (as reported in Chapter 4.4.1) the emissions associated with he produced HVC would be null.

The costs associated with an MTO plant are function of plant size, as usual with chemical plants. Figure 28 illustrates that specific investment costs decrease by over 50% when capacity is increased 3.2 times, passing from a EUR 458/kW_{MeOH} at 1,106$kton_{MeOH}$/year to an average of EUR 220/kW_{MeOH} 2,456$kton_{MeOH}$/year.

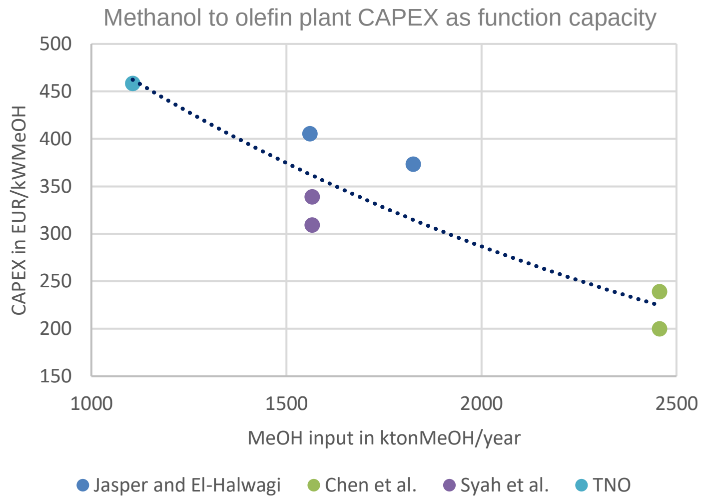

Figure 28. Methanol-to-olefin investment plant cost with respect to methanol input. Sources: (Jasper and El-Halwagi, 2015), (Chen *et al.*, 2022), (Syah *et al.*, 2021), (TNO, 2021).

The MTO reaction is enabled by reactor temperatures of over 500°C and pressures of 2.5 bar in the presence of catalysts (Zhao, Jiang and Wang, 2021)(Gogate, 2019). Therefore the energy consumption of the process will regard both thermal (steam) and electrical (compressors/pumps), with a ratio of thermal over electrical of about 3.4 (Xiang *et al.*, 2015)(Mai *et al.*, 2014). The efficiency of the process was determined considering the boundaries and formula reported in Figure 29:

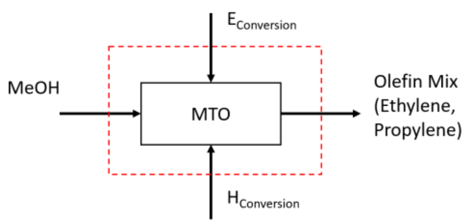

$$\eta = \frac{E_{Olefin\,Mix}\left[\frac{kWh}{kg_{OM}}\right]\frac{1}{2.57}\left[\frac{kg_{OM}}{kg_{MeOH}}\right]}{5.54\left[\frac{kWh}{kg_{MeOH}}\right]+\left(E_{Conversion}+H_{Conversion}\right)\left[\frac{kWh}{kg_{MeOH}}\right]}$$

Figure 29. Methanol-to-olefin production boundaries (left) for efficiency calculation (right).

Xiang *et al.* (2015) suggest that for every ton of olefin produced the steam consumption ($H_{Conversion}$) is of about 5.1 GJ while the electricity consumption ($E_{Conversion}$) is of 1.5 GJ. Moreover, the mass ratio between the input methanol and the output olefin mix is 2.57, which, together with the LHV of methanol and olefin mix allow to determine the efficiency of the process to be of between 70% and 80%.

It is also of interest to assess the produced olefin costs to put in perspective with the price of petrochemical olefins. In this regard Mai *et al.* (2014) performed a sensitivity analysis of the cost per ton of the produced olefin as a function of methanol prices. Their results show that olefin production cost varies linearly between EUR 578/ton_{Olefin}, corresponding to a cost of methanol of EUR 129/ton_{MeOH}, to EUR 2325/ton_{Olefin}, corresponding to a cost of methanol of EUR 779/ton_{MeOH}. With reference to Figure 22 in Chapter 4.4, extending the aforementioned relationship between methanol and olefin cost to fossil methanol and e-methanol it is possible to draw conclusions on the outlook for renewable olefins. Current fossil methanol prices range between EUR 200 and 400/ton_{MeOH}, which yields olefin production costs of between EUR 772 and 1,320/ton_{Olefin}. The current range of e-methanol prices lies between EUR 800 and 1,600/ton_{MeOH}, yielding olefin costs of EUR 2,386 and 4,537/ton_{Olefin}. These high prices could potentially decrease to EUR 1,041 and 1,848/ton_{Olefin}, when, by 2050, technology advancements in green hydrogen production and renewable CO_2, will allow to witness e-methanol prices reach the range of EUR 300 and 600/ton_{MeOH}. For comparison, the global price of fossil-based propylene and ethylene (obtained from steam cracking of naphtha) reached EUR 1,133/$ton_{Propylene}$ (Statista, 2022b) and EUR 1,233/$ton_{Ethylene}$ (Statista, 2022a). This could potentially mean that renewable olefins obtained via the MTO process could still manage to ensure some marginal profit in the upcoming years.

The production of aromatics from methanol, or MTA, has a lower technology readiness level compared to MTO (TRL of 6-7 vs 8-9) (Groß *et al.*, 2022). Moreover, the MTA process has lower reaction temperatures (370-540°C) and a different (more acidic) zeolite catalyst compared to the MTO process (Bazzanella, Ausfelder and DECHEMA, 2017).

The costs associated with an MTA plant were retrieved from Niziolek *et al.* (2016). Similarly to the MTO process, and other chemical industrial processes, the specific investment costs depend on the annual throughput of the plant, as reported in Figure 30:

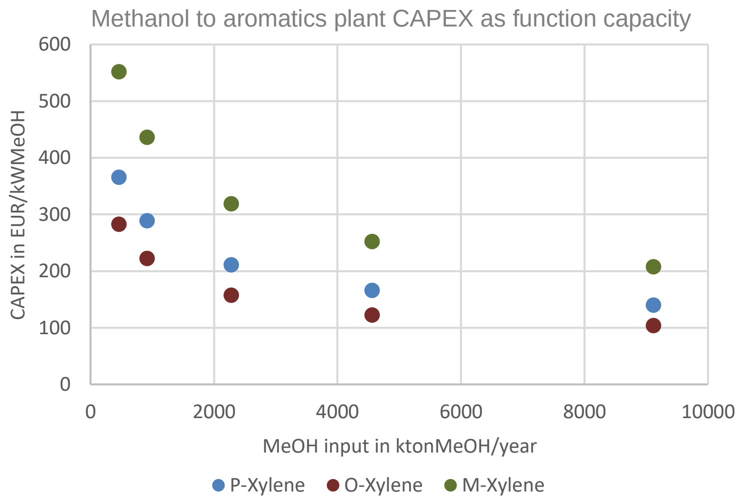

Figure 30. Methanol-to-aromatics investment plant cost with respect to methanol input. The three different cost levels represent three different cases Niziolek *et al.* (2016) analyzed to describe which isomer of xylene the plant was tuned to produce in addition to benzene and toluene).

As already stated, the MTA process requires lower temperatures (370-540°C) compared to MTO, but higher pressures reaching 20-25bar (Bazzanella, Ausfelder and DECHEMA, 2017). The thermal and electrical energy need are somewhat similar to the MTO process, with a thermal to electrical ratio of almost one: 2.1 GJ/ton$_{Xylene}$ of electricity and 2.15 GJ/ton$_{Xylene}$ of steam (Jiang *et al.*, 2020). However, the mass ratio between the input methanol and the output BTX was found to be much higher compared to the one of MTO (2.57), which values between 4.3 and 6, depending on the source. This aspect causes the values of efficiency of the process to be much lower if the only useful output of the system were considered to be benzene, toluene and xylene. The efficiency of the process was determined considering the boundaries and formula reported in Figure 31. The efficiency of the MTA process was found to range between 23% (Bazzanella, Ausfelder and DECHEMA, 2017) and 33% (Jiang *et al.*, 2020).

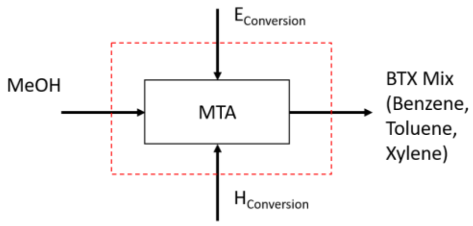

$$\eta = \frac{E_{BTX\ Mix}\left[\frac{kWh}{kg_{BTX}}\right]\frac{1}{5}\left[\frac{kg_{BTX}}{kg_{MeOH}}\right]}{5.54\left[\frac{kWh}{kg_{MeOH}}\right] + (E_{Conversion} + H_{Conversion})\left[\frac{kWh}{kg_{MeOH}}\right]}$$

Figure 31. Methanol-to-aromatics production boundaries (left) for efficiency calculation (right). The coefficient in the equation numerator was set as a midway point of 5 between the literature found value of the mass ratio between the input methanol and output BTX of 4.3 and 6.

Considerations regarding the production cost per metric ton of produced BTX as a function of methanol cost could be carried out due to the lack of literature data on this less mature process.

7.5 Mobility

Hydrogen could play a vital role also in decarbonizing all elements of the transport sector: road, maritime, aviation and rail. Hydrogen can be used for the production of synthetic fuels, or e-fuels, such as gasoline, kerosene and diesel, which could be directly used in the existing transport infrastructure. E-fuels would simply substitute conventional, fossil-based fuels in internal combustion engine (ICE) vehicles without the need of new powertrains. Hydrogen could otherwise be directly used as fuel in a fuel cell electric vehicle (FCEV), which would require the gradual substitution of ICE vehicles with FCEV ones.

7.5.1 Fischer-Tropsch e-fuels for internal combustion engines

The Fischer-Tropsch process, hereinafter FT, allows to obtain liquid hydrocarbons from syngas, which is a mixture of CO and H_2. The process is well established as it has been historically used to synthesize hydrocarbons from syngas obtained from coal gasification. The FT process however, could also be used to produce sustainable e-hydrocarbons from green hydrogen and renewable CO_2. However, an extra step is required to convert the H_2 and CO_2 in syngas, namely the water gas shift reaction (RWGS):

$$CO_2 + 3H_2 \leftrightarrow CO + 2H_2 + H_2O$$

The product of the FT process is a mix of hydrocarbons (sometimes denoted as e-crude) which is then fed into a fractionation column, as it is done in traditional refineries, to derive single e-fuels (e-kerosene, e-diesel). Prior to the fractionation column, a hydro-cracking unit allows for the conversion of unwanted waxes into hydrocarbons. The FT synthesis reaction is described by the following formula:

$$(2n+1)H_2 + nCO \leftrightarrow C_nH_{2n+2} + nH_2O$$

Zang, Sun, A. A. Elgowainy, *et al.* (2021) conducted a simulation study of such a system. They found that the energy needs of e-fuel production via the FT route are, for the most part, embodied in compression needs (CO_2 and H_2 streams are compressed to about 35 bar prior to the RWGS reactor), heating needs (600°C in the RWGS reactor). Without considering the energy need for H_2 production and CO_2 capture, the overall efficiency of the process is reported to be about 52%. Moreover, they also assessed the economics of the e-fuel plant and reported that the specific investment cost amounted to EUR 2,193/ton$_{Hydrocarbon}$/year (or EUR 908/kW$_{H2}$).

Regarding the cost of production of e-kerosene and e-diesel, its value is more sensitive to the variation of the price of H_2 than the price of CO_2. Increasing the cost of input hydrogen from EUR 2/kg$_{H2}$ to EUR 4/kg$_{H2}$ (fixing the cost of CO_2 to EUR 17.3/ton$_{CO2}$) causes the price of e-kerosene to rise from EUR 0.38/kWh$_{e\text{-}kero}$ to EUR 0.65/kWh$_{e\text{-}kero}$ and the price of e-diesel from EUR 0.62/kWh$_{e\text{-}diesel}$ to EUR 1.06/kWh$_{e\text{-}diesel}$ (+71% in both cases). On the other hand, increasing the price of CO_2 from EUR 17.3/ton$_{CO2}$ to EUR 34.6/ton$_{CO2}$ (fixing the cost of H_2 to EUR 2/ton$_{H2}$) causes the price of e-kerosene to rise from EUR 0.38/kWh$_{e\text{-}kero}$ to EUR 0.41/kWh$_{e\text{-}kero}$ and the price of e-diesel from EUR 0.62/kWh$_{e\text{-}diesel}$ to EUR 0.66/kWh$_{e\text{-}diesel}$ (+6% in both cases) (Zang, Sun, A. A. Elgowainy, *et al.*, 2021).

The forecasts of the cost of FT e-fuels, do show that there is cost reduction potential, both because the TRL of the process is 5-7 (Bazzanella, Ausfelder and DECHEMA, 2017) and because the cost of raw materials (hydrogen and carbon dioxide) are likely to decrease between now and 2050.

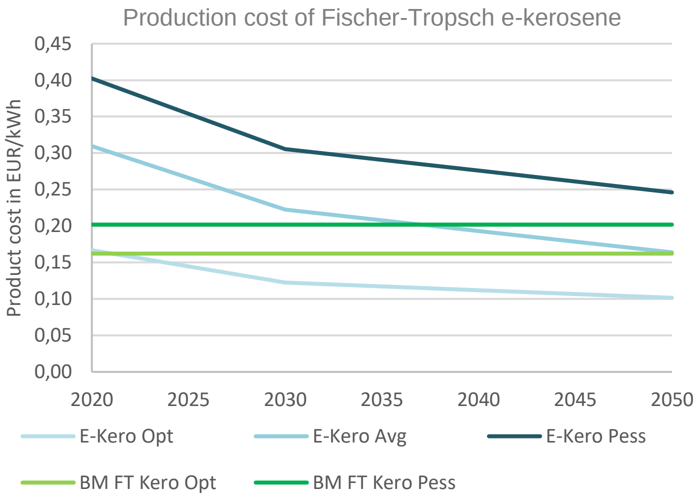

Figure 32. E-kerosene from FT process cost of production forecasts. Sources: E-Kerosene (Zang, Sun, A. A. Elgowainy, *et al.*, 2021)(Peters *et al.*, 2022)(Concawe, 2019)(ICCT, 2022a), Bio FT Kerosene (Swanson *et al.*, 2010).

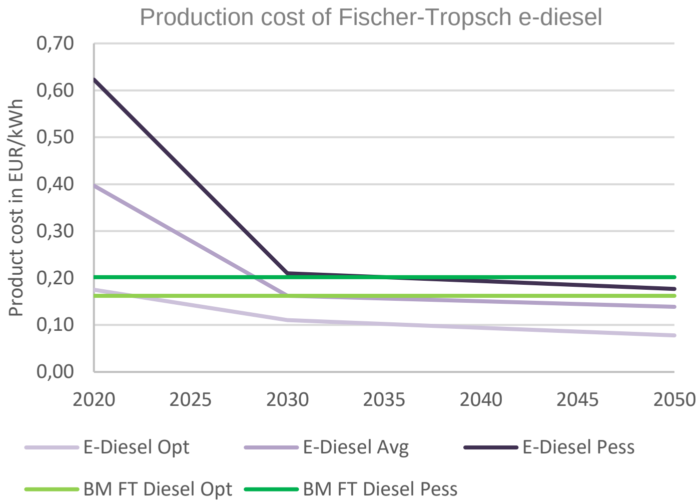

Figure 33. E-diesel from FT process cost of production forecasts. Sources: E-diesel (Zang, Sun, A. A. Elgowainy, *et al.*, 2021)(Peters *et al.*, 2022)(Ueckerdt *et al.*, 2021) (Concawe, 2019)(ICCT, 2022a), Bio FT Diesel (Swanson *et al.*, 2010).

Figure 32 and Figure 33 illustrate the decreasing trend of the production costs of e-kerosene and e-diesel, respectively. The cost of biogenic e-fuels is also reported superimposed as a useful term of comparison of a concurrent technology that could potentially find its role in decarbonizing the transportation sector. It can be seen how e-fuels and their biogenic counterpart become mutually competitive starting from 2030. As another term of comparison, it is useful to report that the current price of jet-A1 fuel (kerosene) and diesel are EUR 0.2/kWh$_{Kero}$ and EUR 0.086/kWh$_{Diesel}$.

7.5.2 Methanol-to-gasoline for internal combustion engines

The methanol-to-gasoline, or MTG, process consists in a similar route to MTO and MTA. Methanol (CH_3OH) is fed into a reactor where, in the presence of a catalyst and heated at 450°C and a pressure of 2bar, it is dehydrated (has its water removed) into dimethyl ether (DME, by the formula CH_3OCH_3). In the same reactor, the DME is then further dehydrated into light olefins:

$$2nCH_3OH \leftrightarrow nCH_3OCH_3 + nH_2O$$
$$nCH_3OCH_3 \leftrightarrow 2(CH_2)_n + nH_2O$$
$$2(CH_2)_n \leftrightarrow C_{2n}H_{4n}$$

The light olefins are converted into hydrocarbon through a process named oligomerization. A process carried out in a reactor at 200°C (exothermic reaction) and 40bar. The hydrocarbons undergo further treatments such as hydrogenation and isomerization in order to enhance the gasoline properties.

According to the results of a simulation described by Ruokonen *et al.* (2021), the production cost of gasoline produced through the MTG process was estimated to be EUR 3,716/ton$_{Gasoline}$ (EUR 0.33/kWh$_{Gasoline}$) with an input of renewable methanol price of EUR 1,050/ton$_{MeOH}$ (EUR 0.19/kWh$_{MeOH}$). Through this relationship it was possible to determine the MTG product cost trends reported in Figure 34. The optimistic and pessimistic scenarios were generated based on different methanol prices discussed in Chapter 7.4 when discussing their impact on the production cost of olefins and aromatics. Similarly, the decreasing trends in time reflect those of future renewable methanol prices. Finally, as a term of comparison, biomass based MTG gasoline prices are superimposed. Their initial lower values then become comparable to those of e-MTG gasoline due to the decreasing costs of green hydrogen and captured carbon dioxide that make up e-methanol.

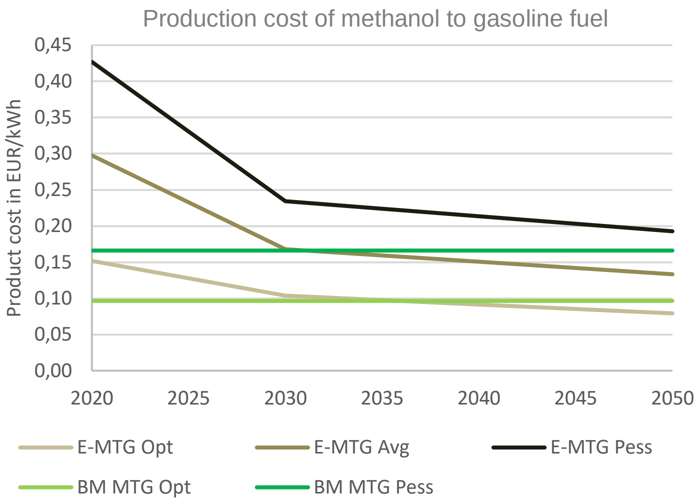

Figure 34. E-gasoline from MTG process cost of production forecasts. Sources: E-gasoline (Ruokonen *et al.*, 2021) and own assumptions, Bio MTG gasoline (Hennig and Haase, 2021),(PNNL, 2009), (NREL and PNNL, 2015).

7.5.3 E-fuel powered internal combustion engine vehicles

The main advantage of producing e-fuels is the ease of implementation within the current fleet of internal combustion engine (ICE) vehicles. The vast and capillary infrastructure in use today can accept and handle e-fuels without the need of any modifications. However, the cost per km travelled by the ICE vehicle is higher when burning e-fuels compared to fossil or biomass-based fuels. A literature-based research was conducted to determine the efficiency of the possible means of travel utilizing liquid fossil fuels: passenger cars, trucks, buses and airplanes. Passenger cars are assumed as gasoline-run, airplanes as kerosene-run, and truck/buses as diesel-run.

Efficiency data for passenger cars was obtained through the processing of multiple data points found in literature. The resulting values were set to a range between 0.60kWh$_{gasoline}$/km and 0.85 kWh$_{gasoline}$/km in 2020 (He *et al.*, 2021)(Viesi, Crema and Testi, 2017), and decreasing to between 0.5 kWh$_{gasoline}$/km and 0.71 kWh$_{gasoline}$/km by 2050 (Chen and Melaina, 2019)(Ruffini and Wei, 2018). Considering fossil-based gasoline (petrol) costs of EUR 0.225/kWh (EUR 2/lt), the resulting fuel-related cost of driving will result to be EUR 0.14/km and EUR 0.19/km in 2020 and EUR 0.11/km and EUR 0.16/km in 2050. On the other hand, considering the average cost of e-gasoline produced through the MTG route reported in Figure 34 equal to EUR 0.3/kWh in 2020 and EUR 0.13/kWh in 2050, the fuel related costs could potentially decrease from between EUR 0.25/km and EUR 0.18/km in 2020 and EUR 0.09/km and EUR 0.06/km in 2050 (Figure 35).

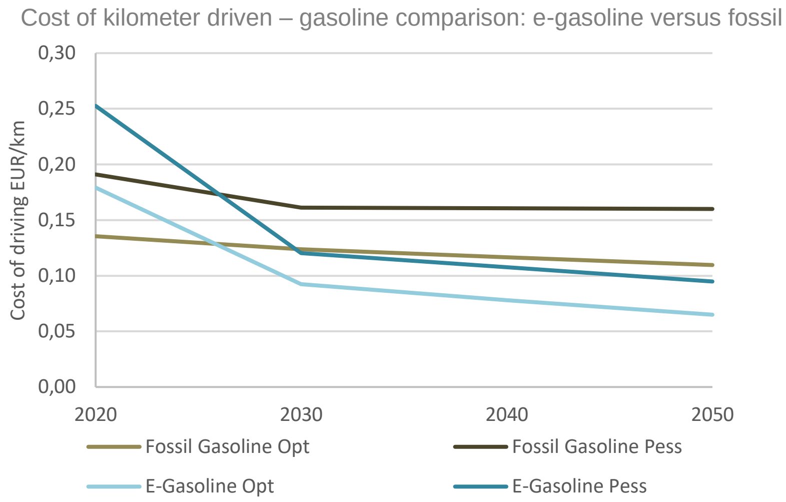

Figure 35. Comparison between the cost of km driven by an ICE car fueled by conventional fossil-based petrol and e-gasoline produced through the methanol-to-gasoline process.

In a similar way, long-haul trucks and buses can be fueled by e-diesel produced through the FT process illustrated in Chapter 7.5.1. The specific fuel consumption of ICE trucks is between 3.1kWh$_{Diesel}$/km (Cunanan *et al.*, 2021) and 3.4 kWh$_{Diesel}$/km (IEA, 2019a) in 2020. Assuming an increase in efficiency as is observed in literature regarding passenger cars, the specific fuel consumption could potentially decrease to a between 2.5 kWh$_{Diesel}$/km and 2.9 kWh$_{Diesel}$/km. Buses on the other hand present a higher specific fuel consumption compared to truck with values ranging between 3.1 kWh$_{Diesel}$/km and 4.4 kWh$_{Diesel}$/km in 2020 and between 2.5 kWh$_{Diesel}$/km and 3.7 kWh$_{Diesel}$/km.

Considering fossil-based diesel costs of EUR 0.2/kWh (EUR 2/lt), the resulting fuel-related cost of driving will result to be EUR 0.61/km and EUR 0.50/km in 2020 and EUR 0.50/km and EUR 0.58/km in 2050 for ICE trucks. In the case of buses, the values range between EUR 0.63/km and EUR 0.89/km in 2020 and EUR 0.50/km and EUR 0.59/km in 2050.

FT-based diesel, on the other hand shows a decreasing trend, on average, from EUR 0.4/kWh to EUR 0.14/kWh between 2020 and 2050, as reported in Figure 33. The resulting fuel-related cost per km traveled is reported in Table 2, and suggest that if the price of fossil-based diesel remains constant through to 2050, e-fuels will become more competitive.

Table 2. Specific energy consumption of ICE trucks, buses and airplanes along with average specific cost of relative e-fuel and specific cost per kilometer travelled.

	kWh$_{Fuel}$/km		EUR$_{FT-Diesel}$/kWh		EUR/km E-Fuel		EUR/km Fossil fuel	
	2020	2050	2020	2050	2020	2050	2020	2050
ICE Trucks	3.1	2.9	0.4	0.14	1.36	0.4	0.61	0.50
	3.4	2.5			1.22	0.35	0.69	0.58
ICE Buses	3.1	2.5			1.76	0.41	0.63	0.89
	4.4	3.7			1.25	0.35	0.50	0.59
			EUR$_{FT-Kerosene}$/kWh					
Airplanes 80 PAX	15.6		0.31	0.16	4.83	2.56	3.12	
Airplanes 200 PAX	30.1				9.32	4.93	6.02	

The same rationale was applied to air travel. As already stated at the end of Chapter 7.5.4, the specific fuel consumptions were found to be 15.6 kWh_{JETA1}/km and 30.1 kWh_{JETA1}/km, for 80 and 200 passenger capacity aircrafts respectively. With the price of Jet-A1 fuel (kerosene) set to EUR 0.2/kWh_{Kero}, fuel costs of per kilometer flown would be of EUR 3.12/km and EUR 6.02/km, respectively. By utilizing FT-synthesized kerosene on the other hand, the costs could potentially decrease between 2020 and 2050 from EUR 4.83/km to EUR 2.56/km and from EUR 9.32/km and EUR 4.93/km for small and large aircrafts respectively.

7.5.4 Fuel cell electric vehicles

An alternative to the conversion of hydrogen gas into conventional fuels such as gasoline, kerosene and diesel is to use hydrogen directly as the fuel itself. There are two routes to follow to achieve this: hydrogen gas ICEs vehicles and fuel cell electric vehicles. However, this assessment only regards the latter since H2-ICEs have low efficiencies (20% to 35%) and high pollutant emissions (specifically NOx due to high combustion temperatures) which require flue gas treatment and other mitigation strategies. Fuel cell electric vehicles, or FCEV, make use of the fuel cell technology discussed in Chapter 7.1.2 to power on-board electric motors. This typology of drivetrain can be used to drive passenger cars (light duty vehicles), buses, trucks (heavy duty vehicles) and trains. In addition, this technology is foreseen to also play a role in aviation.

Regarding road transport vehicles, FCEV cars can potentially provide a transport service comparable to conventional internal combustion engine vehicles today. Assuming a large-scale deployment of the necessary infrastructure to guarantee reliability of hydrogen as a mobility energy vector (mainly hydrogen refueling stations and hydrogen supply chain), FCEV can ensure long range travel (600km) and short refueling times. Hydrogen is stored directly on board the vehicle in pressurized tanks, which can contain about 6kg_{H2} at 700 bar (with an overall weight of 125 kg and volume of 260 liters) (Viesi, Crema and Testi, 2017). Unit costs of FCEV cars are generally higher (for the same category of vehicle) than ICE vehicles today. However, following the decreasing trend of PEM fuel cells and general cost reduction effect enabled by large scale deployment, costs may become somewhat comparable by 2030. Similarly, efficiencies (reported as kWh_{H2}/km), are destined to decrease following the trends of fuel cell technology improvements, as can be seen in Figure 36.

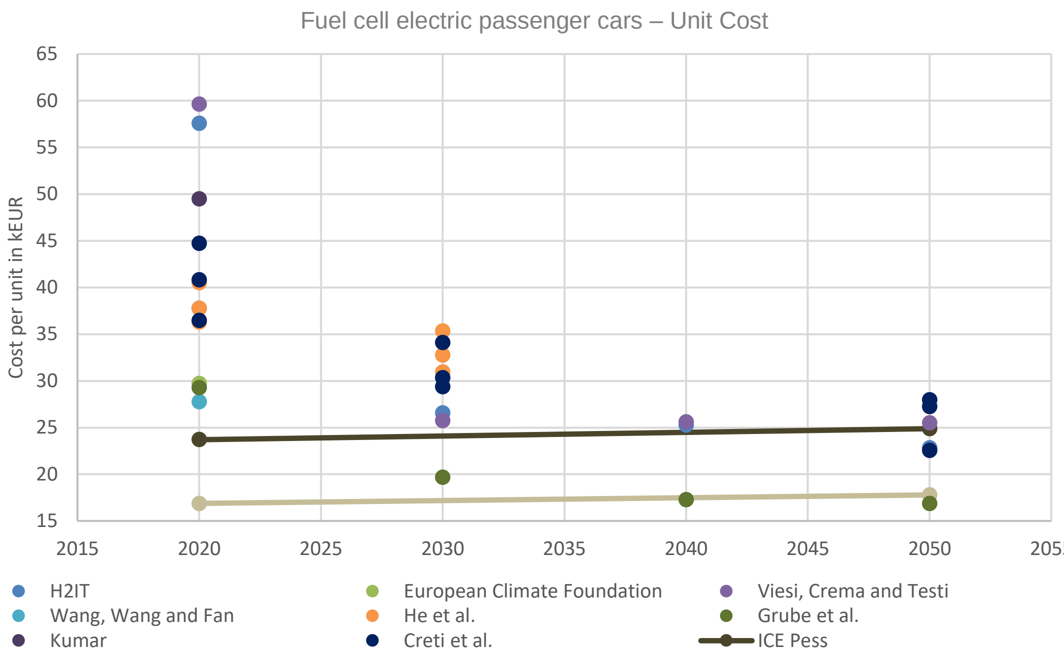

Figure 36. Fuel cell electric passenger cars (light duty vehicles) unit costs decreasing trend in time between 2020 and 2050. Sources: (H2IT, 2019)(European Climate Foundation, 2019) (Viesi, Crema and Testi, 2017)(Wang, Wang and Fan, 2018) (He *et al.*, 2021) (Grube *et al.*, 2021) (Kumar, 2022)(Creti *et al.*, 2015).

A similar decreasing trend can also be observed for the specific hydrogen consumption per unit distance driven. This behavior is mostly justified by the expected increase in the onboard PEMFC increase in efficiency (Figure 37).

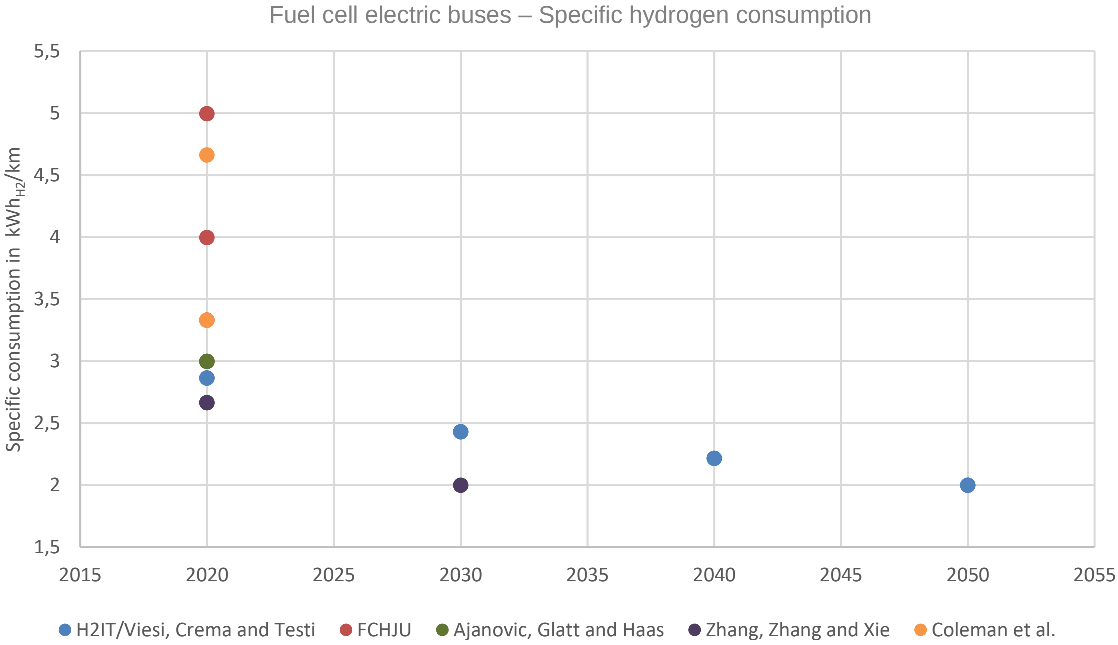

Figure 37. Fuel cell electric passenger cars (light duty vehicles) specific hydrogen consumption decreasing trend in time between 2020 and 2050. Sources: (H2IT, 2019) (Viesi, Crema and Testi, 2017)(Chen and Melaina, 2019) (He *et al.*, 2021) (Ruffini and Wei, 2018)(Creti *et al.*, 2015) (IEA, 2019a).

Long-haul transport trucks are deemed as particularly suitable for fuel cell technology when compared to their battery electric counter parts. For gross weight ratings (total weight of a full loaded truck) greater of 16 tons and delivery routes greater than 300-400 km, fuel cell technology becomes the predominant decarbonized means of transport (H2IT, 2019). According to the ICCT (2022b), the hydrogen capacity of a single truck can be of up to 55 kg_{H2} at 700 bar, which can guarantee up to 660 km of range. Information regarding the unit cost of a single unit is sparse. Today, unit cost range between kEUR 148/unit (Cunanan *et al.*, 2021) and kEUR 450/unit (Kumar, 2022). However, according to the ICCT (2022b), unit costs could decrease (according to the same rationale as illustrated for passenger cars) to about kEUR 205/unit. Regarding the specific consumption of FC powered trucks, value were found to range between 3.76 kWh_{H2}/km (Cunanan *et al.*, 2021) and 2.16 kWh_{H2}/km (IEA, 2019a). Under the assumption that the increase of PEMFC efficiency will also affect specific consumption, values were estimated to drop to a range of between 1.43 kWh_{H2}/km and 1.74 kWh_{H2}/km.

Buses and coaches are being deployed among the public transport fleets in Europe and the United Kingdom. They allow for a comparable service to traditional ICE vehicles and allow for quick refueling times from centralized refueling station usually placed in depots. The hydrogen capacity of the vehicle is similar to that of a fuel cell truck totaling in a t 30-50 kg_{H2}. However, the pressure at which the hydrogen is stored is lower due to less strict spatial constraints, allowing tanks at 350 bar to be place on the roof of the bus/coach (FCHJU, 2017). The unit costs of hydrogen fuel cell buses today are higher than those of their fossil-based ICE counterparts, as can be seen in Figure 38. However, as reported in literature and in accordance with the rationale applied for both passenger cars and trucks, the costs are forecasted to decrease. Today's values range between kEUR 687/unit and kEUR 572/unit (Ajanovic, Glatt and Haas, 2021). The low cost of kEUR 350/unit reported by Zhang, Zhang and Xie (2020) is specific for China and not realistically applicable to Europe, however these cost levels are likely to be reached by 2030 (Figure 38).

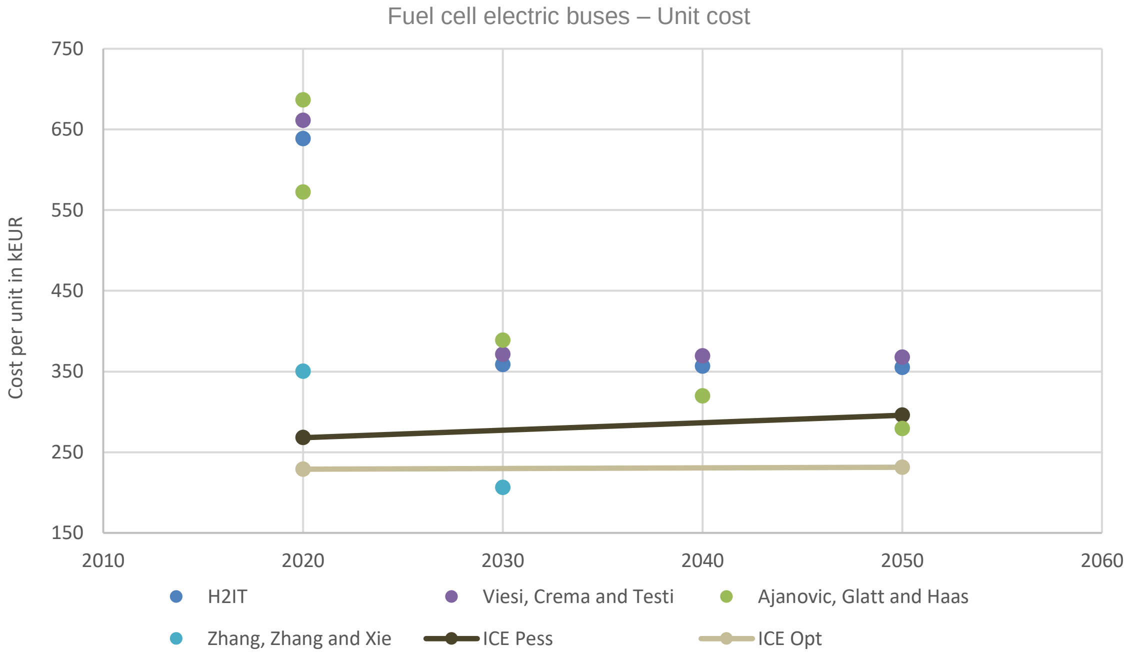

Figure 38. Fuel cell electric buses cars unit costs decreasing trend in time between 2020 and 2050. Sources: (H2IT, 2019) (Viesi, Crema and Testi, 2017) (Ajanovic, Glatt and Haas, 2021)(Zhang, Zhang and Xie, 2020). Notes: all buses considered have comparable lengths of 12m to 13m.

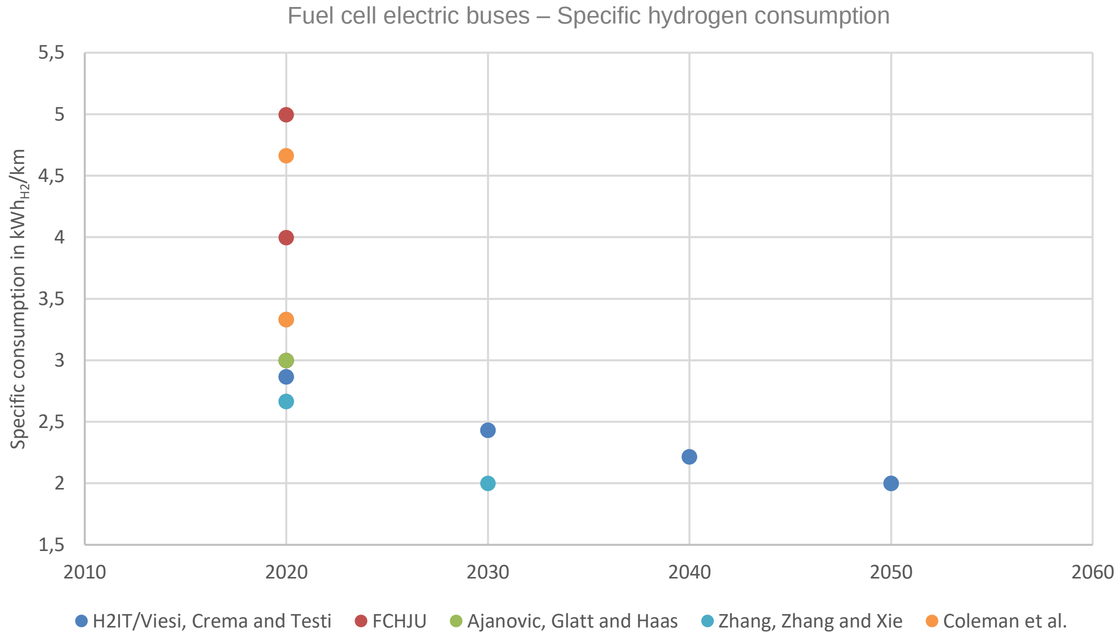

Figure 39. Fuel cell electric buses cars specific hydrogen consumption decreasing trend in time between 2020 and 2050. Sources: (H2IT, 2019) (Viesi, Crema and Testi, 2017)(FCHJU, 2017) (Ajanovic, Glatt and Haas, 2021)(Zhang, Zhang and Xie, 2020)(Coleman *et al.*, 2020). Notes: all buses considered have comparable lengths of 12m to 13m, with the exception the higher values of FCHJU (2017) and Coleman *et al.* (2020) which are relative to a 18m bus.

Regarding the specific consumption of buses (Figure 39), the values found in literature are in general higher than those of trucks, even if only considering 12/13 m buses and excluding 18m buses (represented by the higher values of FCHJU [2017] and Coleman *et al.* [2020]). As for passenger cars and trucks, values are likely to decrease from between 4 kWh$_{H2}$/km (FCHJU, 2017) and 2.66 kWh$_{H2}$/km (Zhang, Zhang and Xie, 2020) to between 2.43 kWh$_{H2}$/km (H2IT, 2019)(Viesi, Crema and Testi, 2017) and 2 kWh$_{H2}$/km (Zhang, Zhang and Xie, 2020) in 2030.

Green hydrogen could also play a role in decarbonizing aviation. Clean Sky 2 and FCHJU (2020) and the ICCT (2022c) both assessed the feasibility of employing hydrogen in two typologies of aircrafts. The first typology is employed for regional travel (maximum ~1,500km) and can hold up to 80 passengers, while the second is characterized by longer journeys (maximum ~6,000km) and capacity of up to 200 passengers. The two reference aircrafts used in their evaluation are the ATR 72-600 (turboprop) and the Airbus A320neo (turbofan), respectively. The latter is especially relevant to the impact of decarbonization of aviation because these types of crafts represent 18% of the global aviation fleet and for 43% of total aviation emissions.

The two studies assess liquefied hydrogen as the means of storing hydrogen onboard the aircrafts due to the high volumetric energy density. The hydrogen is converted into electricity through a fuel cell to power electric motors driving the propeller (ATR 72-600) or into a hybrid configuration of fuel cells (cruising) and hydrogen turbines (take-off) to power the fan (Airbus A320neo). The findings demonstrated that the CAPEX and the OPEX increase, by 30% and 50%, respectively, due to the necessarily longer aircraft needed to accommodate the LH_2 tank, the LH_2 tank itself, and the fuel cells or hydrogen turbines. It was also reported that a decrease in energy demand of -8% and -4% for the ATR 72-600 and the Airbus A320neo, respectively, (due to lower weight and volume of the aircraft) would in any case be belittled by the increase of fuel costs of 42%.

Given the cruise speeds and the relative jet fuel (Jet-A1) consumption, it is possible to determine the energy consumption per kilometer flown. In the case of the regional aircraft (ATR 72-600) the fuel consumption was found to be 650lt/h at a cruising speed of Mach 0.4 (ATR Aircraft, no date), while for the larger aircraft (Airbus A320neo) the fuel consumption is of 2500 liters/h (AviationInfo, 2021) achieving a cruising speed of Mach 0.78 (ICCT, 2022c). The fuel economies were found (through the LHV of Jet-A1 equal to 43.2 MJ/kg) to be 15.6kWh$_{JETA1}$/km and 30.1 kWh$_{JETA1}$/km, respectively. The current price of Jet-A1 fuel (kerosene) EUR 0.2/kWh$_{Kero}$, which would determine fuel costs of per kilometer flown of EUR 3.12/km and EUR 6.02/km. According to the increase of fuel prices of 42% reported by (Clean Sky 2 and FCHJU, 2020) the resulting fuel costs of the hydrogen powered aircrafts amount to EUR 4.43/km and EUR 8.55/km, respectively.

8 Concluding remarks

The presented work provides a description of the constituent elements of a green hydrogen value chain along with a summary of their techno-economic parameters. The underlying research consisted in an extensive review of relevant scientific literature and reports. The values of the techno-economic parameters retrieved from these sources characterize the technologies in terms of investment costs, operation and maintenance costs, efficiencies (and energy demands) and technical lifetimes. Moreover, the evolution in time of said parameters was also accounted for when sufficient data was available. Literature proposes forecasted values based on past trends and by estimating learn-by-doing/research effects on technology costs and efficiencies. This aspect is more accentuated in less mature technologies.

The main output of this work is a robust dataset of techno-economic parameters that summarizes the bibliographical review. To achieve this result, a large number of sources was screened and relevant data points were collected. Most technologies of the hydrogen supply chain benefit from extensive literature coverage, leading to plenty of values per single parameter. In these cases, a statistical approach was taken, which consisted in calculating the 1st and 3rd quartiles of each set. Together with the average of the set, the two quartiles allowed to provide a range of values for each techno-economic parameter.

The intended purpose of the dataset is that of serving as a literature-supported input to the modeling of green hydrogen value chains. In particular, within Work Package 7 of the HyUSPRe project, Task 7.1 assesses the integration of a green hydrogen value chain in the existing European energy system through spatio-temporal optimization modeling, to which techno-economic parameters inputs are essential. The aim is that of determining the relevance of large-scale underground storage in future European hydrogen economies and its implications on the cost of hydrogen for offtakers. In this regard, the activities of the work presented in this report will proceed in the estimation of the cost of hydrogen attributable to the elements assessed in this report. The analysis of the levelized cost of hydrogen production, conversion/reconversion, transport and storage will be carried out to verify the attractiveness for the end-users and, if applicable, to provide insights on the potential improvement on the supply chain.

9 References

Abdi, A., Chiu, J. and Martin, V. (2019) 'State of the art in hydrogen liquefaction', *Proceedings of the ISES Solar World Congress 2019 and IEA SHC*, pp. 1311–1320. doi: 10.18086/swc.2019.23.01.

Agora Energiewende (2021) *No-regret hydrogen. Charting early steps for H_2 infrastructure in Europe*, *Agora Energiewende (White Paper)*. Available at: https://www.agora-energiewende.de/en/publications/no-regret-hydrogen/.

Ajanovic, A., Glatt, A. and Haas, R. (2021) 'Prospects and impediments for hydrogen fuel cell buses', *Energy*, 235, p. 121340. doi: 10.1016/j.energy.2021.121340.

Al-Breiki, M. and Bicer, Y. (2020) 'Comparative cost assessment of sustainable energy carriers produced from natural gas accounting for boil-off gas and social cost of carbon', *Energy Reports*, 6, pp. 1897–1909. doi: 10.1016/j.egyr.2020.07.013.

Al-Khori, K., Bicer, Y. and Koç, M. (2021) 'Comparative techno-economic assessment of integrated PV-SOFC and PV-Battery hybrid system for natural gas processing plants', *Energy*, 222, p. 119923. doi: 10.1016/j.energy.2021.119923.

Amid, A., Mignard, D. and Wilkinson, M. (2016) 'Seasonal storage of hydrogen in a depleted natural gas reservoir', *International Journal of Hydrogen Energy*, 41(12), pp. 5549–5558. doi: 10.1016/j.ijhydene.2016.02.036.

ATR Aircraft (no date) *ATR 72-600 The first choice for operators: Product Brochure*. Available at: https://atrtwk.wpenginepowered.com/wp-content/uploads/2022/06/ATR_Fiche72-600-3.pdf.

AviationInfo (2021) *A320 Fuel Burn Per Hour | Airbus A320 Fuel Consumption*. Available at: https://aviationinfo.net/a320-fuel-burn-per-hour-airbus-a320-fuel-consumption/ (Accessed: 11 January 2023).

Barbose, G. and Satchwell, A. J. (2020) 'Benefits and costs of a utility-ownership business model for residential rooftop solar photovoltaics', *Nature Energy*, 5(10), pp. 750–758. doi: 10.1038/s41560-020-0673-y.

Bartels, J. R. (2008) 'A feasibility study of implementing an Ammonia Economy', *Digital Repository @ Iowa State University*, (December), p. 102. Available at: http://lib.dr.iastate.edu/cgi/viewcontent.cgi?article=2119&context=etd.

Battelle Memorial Institute (2016) *Manufacturing Cost Analysis of PEM Fuel Cell Systems for 5- and 10-kW Backup Power Applications*, *U.S. Department of Energy*. Available at: https://www.energy.gov/sites/prod/files/2016/12/f34/fcto_cost_analysis_pem_fc_5-10kw_backup_power_0.pdf.

Baufumé, S. *et al.* (2013) 'GIS-based scenario calculations for a nationwide German hydrogen pipeline infrastructure', *International Journal of Hydrogen Energy*, 38(10), pp. 3813–3829. doi: 10.1016/j.ijhydene.2012.12.147.

Bazzanella, A. M., Ausfelder, F. and DECHEMA (2017) 'Low carbon energy and feedstock for the European chemical industry', *The European Chemical Industry Council*, p. 168. Available at: https://dechema.de/dechema_media/Downloads/Positionspapiere/Technology_study_Low_carbon_energy_and_feedstock_for_the_European_chemical_industry.pdf.

Bellona (2021) *Hydrogen in steel production: what is happening in Europe – part two*. Available at: https://bellona.org/news/industrial-pollution/2021-05-hydrogen-in-steel-production-what-is-happening-in-europe-part-two (Accessed: 14 December 2022).

Berstad, D., Skaugen, G. and Wilhelmsen, Ø. (2021) 'Dissecting the exergy balance of a hydrogen liquefier: Analysis of a scaled-up claude hydrogen liquefier with mixed refrigerant pre-cooling', *International Journal of Hydrogen Energy*, 46(11), pp. 8014–8029. doi: 10.1016/j.ijhydene.2020.09.188.

Bertuccioli, L. *et al.* (2014) *Study on development of water electrolysis in the EU, Fuel Cells and hydrogen Joint Undertaking*, *Fuel Cells and hydrogen Joint Undertaking*. Available at: https://www.fch.europa.eu/sites/default/files/FCHJUElectrolysisStudy_FullReport (ID 199214).pdf.

BNEF (2020) *Hydrogen Economy Outlook*, *Bloomberg New Energy Finance*. Available at: https://data.bloomberglp.com/professional/sites/24/BNEF-Hydrogen-Economy-Outlook-Key-Messages-30-Mar-2020.pdf.

Böhm, H. *et al.* (2020) 'Projecting cost development for future large-scale power-to-gas implementations by scaling effects', *Applied Energy*, 264(February), p. 114780. doi: 10.1016/j.apenergy.2020.114780.

Böhm, H., Goers, S. and Zauner, A. (2019) 'Estimating future costs of power-to-gas – a component-based approach for technological learning', *International Journal of Hydrogen Energy*, 44(59), pp. 30789–30805. doi: 10.1016/j.ijhydene.2019.09.230.

Bolinger, M. and Bolinger, G. (2022) 'Land Requirements for Utility-Scale PV : An Empirical Update on Power and Energy Density', pp. 1–6. Available at: https://doi.org/10.1109/JPHOTOV.2021.3136805.

Bošnjaković, M., Čikić, A. and Zlatunić, B. (2021) 'Cost-benefit analysis of small-scale rooftop pv systems: The case of dragotin, croatia', *Applied Sciences (Switzerland)*, 11(19). doi: 10.3390/app11199318.

Brändle, G., Schönfisch, M. and Schulte, S. (2020) *Estimating long-term global supply costs for low-carbon hydrogen*. doi: 10.1016/j.apenergy.2021.117481.

Brändle, G., Schönfisch, M. and Schulte, S. (2021) 'Estimating long-term global supply costs for low-carbon hydrogen', *Applied Energy*, 302(July), p. 117481. doi: 10.1016/j.apenergy.2021.117481.

Caglayan, D. G. *et al.* (2020) 'Technical potential of salt caverns for hydrogen storage in Europe', *International Journal of Hydrogen Energy*, 45(11), pp. 6793–6805. doi: 10.1016/j.ijhydene.2019.12.161.

Cavanagh, A. *et al.* (2022a) *HyUSPRE D1.3 Hydrogen storage potential of existing European gas storage sites in depleted gas fields and aquifers*.

Cavanagh, A. *et al.* (2022b) *HyUSPRe Milestone MS4*.

Cesaro, Z. *et al.* (2021) 'Ammonia to power: Forecasting the levelized cost of electricity from green ammonia in large-scale power plants', *Applied Energy*, 282, pp. 1–19. doi: 10.1016/j.apenergy.2020.116009.

Chen, Y. H. *et al.* (2022) 'Design and economic analysis of industrial-scale methanol-to-olefins plants', *Journal of the Taiwan Institute of Chemical Engineers*, 130, p. 103893. doi: 10.1016/j.jtice.2021.05.040.

Chen, Y. and Melaina, M. (2019) 'Model-based techno-economic evaluation of fuel cell vehicles considering technology uncertainties', *Transportation Research Part D: Transport and Environment*, 74(August 2019), pp. 234–244. doi: 10.1016/j.trd.2019.08.002.

Cigolotti, V. and Genovese, M. (2021) *Stationary Fuel Cells: Current and future technologies-Costs, performances, and potential*, *IEA Technology Collaboration Programme: Advanced Fuel Cells*. Available at: https://www.ieafuelcell.com/fileadmin/publications/2021/2021_AFCTCP_Stationary_Application_Performance.pdf.

Clean Sky 2 and FCHJU (2020) *Hydrogen-powered aviation*. doi: 10.2843/766989.

Coleman, D. *et al.* (2020) 'The value chain of green hydrogen for fuel cell buses – A case study for the Rhine-Main area in Germany', *International Journal of Hydrogen Energy*, 45(8), pp. 5122–5133. doi: 10.1016/j.ijhydene.2019.06.163.

Concawe (2019) 'A look into the role of e-fuels in the transport system in Europe (2030-2050)', 28(1), pp. 4–22. Available at: https://www.concawe.eu/wp-content/uploads/E-fuels-article.pdf.

Creti, A. *et al.* (2015) 'A cost benefit analysis of fuel cell electric vehicles'. Available at: https://hal.archives-ouvertes.fr/hal-01116997/document.

Cunanan, C. *et al.* (2021) 'A Review of Heavy-Duty Vehicle Powertrain Technologies: Diesel Engine Vehicles, Battery Electric Vehicles, and Hydrogen Fuel Cell Electric Vehicles', *Clean Technologies*, 3(2), pp. 474–489. doi: 10.3390/cleantechnol3020028.

D'Amore-Domenech, R., Leo, T. J. and Pollet, B. G. (2021) 'Bulk power transmission at sea: Life cycle cost comparison of electricity and hydrogen as energy vectors', *Applied Energy*, 288(May 2020), p.

116625. doi: 10.1016/j.apenergy.2021.116625.

Datta, U., Kalam, A. and Shi, J. (2020) 'The economic prospect of rooftop photovoltaic (PV) system in the commercial buildings in Bangladesh: a case study', *Clean Technologies and Environmental Policy*, 22(10), pp. 2129–2143. doi: 10.1007/s10098-020-01963-3.

Davies, J. *et al.* (2020) *Current status of Chemical Energy Storage Technologies*, *Trends in research, development and deployment in Europe and the rest of the world*. doi: 10.2760/280873.

DENA (2019) *Powerfuels in Industry : Process Heat*. Available at: https://www.powerfuels.org/fileadmin/gap/Publikationen/Factsheets/190612_dena_FS_Process_Heat_web.pdf.

DNV GL (2019a) *Energy Transition Outlook 2019: A global and regional forecast to 2050*, *Energy Transition*. Available at: https://aeeree.org/wp-content/uploads/2019/10/DNV_GL_Energy_transition_Outlook2019_lowres_single.pdf.

DNV GL (2019b) *Hydrogen in the Electricity Value Chain*. Available at: https://www.dnv.com/Publications/hydrogen-in-the-electricity-value-chain-225850#.

DOE (2016) *Hydrpower Vision: A New Chapter for America's Renewable Electricity Source*. Available at: https://www.energy.gov/sites/prod/files/2018/02/f49/Hydropower-Vision-021518.pdf.

DOE (2019) *Current Status of Hydrogen Liquefaction Costs*, *DOE Hydrogen and Fuel Cells Program Record*. Available at: https://www.hydrogen.energy.gov/pdfs/19001_hydrogen_liquefaction_costs.pdf.

Duman, A. C. and Güler, Ö. (2020) 'Economic analysis of grid-connected residential rooftop PV systems in Turkey', *Renewable Energy*, 148(xxxx), pp. 697–711. doi: 10.1016/j.renene.2019.10.157.

Element Energy (2018) *Hydrogen supply chain evidence base*. Available at: https://assets.publishing.service.gov.uk/government/uploads/system/uploads/attachment_data/file/760479/H2_supply_chain_evidence_-_publication_version.pdf.

Element Energy (2019) *Hy4Heat Work Package 6: Conversion of Industrial Heating Equipment to Hydrogen*, *Hy4Heat demonstrating hydrogen for heat*. Available at: https://static1.squarespace.com/static/5b8eae345cfd799896a803f4/t/5e287d78dc5c561cf1609b3d/1579711903964/WP6+Industrial+Heating+Equipment.pdf.

ENTEC (2022) *The role of renewable / storage to scale up the EU deploment of renewable H2*, *Gastronomía ecuatoriana y turismo local.* doi: 10.2833/727785.

ETN Global (2020) *Hydrogen gas turbines*. Available at: https://etn.global/wp-content/uploads/2020/01/ETN-Hydrogen-Gas-Turbines-report.pdf.

European Climate Foundation (2019) 'Fuelling Italy's Future', pp. 1–32. Available at: https://europeanclimate.org/content/uploads/2019/12/fuelling-italys-future-how-the-transition-to-low-carbon-mobility-strengthens-the-economy-summary-report-en.pdf.

European Commission (2014) *Energy Technology Reference Indicator 2014*. doi: 10.2790/057687.

Fasihi, M., Efimova, O. and Breyer, C. (2019) 'Techno-economic assessment of CO 2 direct air capture plants', *Journal of Cleaner Production*, 224, pp. 957–980. doi: 10.1016/j.jclepro.2019.03.086.

FCHJU (2017) 'New Bus Refuelling for European Hydrogen Bus Depots: Guidance document on Large Scale Hydrogen Bus Refuelling', *Fuel Cell and Hydrogen Joint Undertaking*, (1), pp. 1–38. Available at: http://www.fch.europa.eu/sites/default/files/NewBusFuel Press Release 14102016 Final version.pdf#.

Gernaat, D. E. H. J. *et al.* (2020) 'The role of residential rooftop photovoltaic in long-term energy and climate scenarios', *Applied Energy*, 279(August 2019), p. 115705. doi: 10.1016/j.apenergy.2020.115705.

GIE (2021) *GIE Storage Database*. Available at: https://www.gie.eu/transparency/databases/storage-database/ (Accessed: 24 March 2023).

Glenk, G. and Reichelstein, S. (2019) 'Economics of converting renewable power to hydrogen', *Nature Energy*, 4(3), pp. 216–222. doi: 10.1038/s41560-019-0326-1.

Global CCS Institute (2017) *Global Costs of Carbon Capture and Storage*, *Global CCS Institute*. Available at: https://www.globalccsinstitute.com/archive/hub/publications/201688/global-ccs-costupdatev4.pdf.

Gogate, M. R. (2019) ‘Methanol-to-olefins process technology: current status and future prospects’, *Petroleum Science and Technology*, 37(5), pp. 559–565. doi: 10.1080/10916466.2018.1555589.

Gomez-Exposito, A., Arcos-Vargas, A. and Gutierrez-Garcia, F. (2020) ‘On the potential contribution of rooftop PV to a sustainable electricity mix: The case of Spain’, *Renewable and Sustainable Energy Reviews*, 132(July), p. 110074. doi: 10.1016/j.rser.2020.110074.

Groenenberg, R. *et al.* (2020) *Techno-Economic Modelling of Large-Scale Energy Storage Systems*. Available at: https://publications.tno.nl/publication/34637698/2VA30k/TNO-2020-R12004.pdf.

Groß, T. *et al.* (2022) *HyUSPRe D1.2 Report on H2 supply from Renewable Energy Sources, H2 demand centers and H2 transport infrastructure*. Available at: https://www.hyuspre.eu/index.php/downloads/.

Grosse, R. *et al.* (2017) *Long term (2050) projections of techno-economic performance of large-scale heating and cooling in the EU*. doi: 10.2760/24422.

Grube, T. *et al.* (2021) ‘Passenger car cost development through 2050’, *Transportation Research Part D: Transport and Environment*, 101(November), p. 103110. doi: 10.1016/j.trd.2021.103110.

Guidehouse (2021a) *Analysing future demand, supply, and transport of hydrogen*. Available at: https://gasforclimate2050.eu/wp-content/uploads/2021/06/EHB_Analysing-the-future-demand-supply-and-transport-of-hydrogen_June-2021_v3.pdf.

Guidehouse (2021b) *Extending the European Hydrogen Backbone*. Available at: https://gasforclimate2050.eu/wp-content/uploads/2021/06/European-Hydrogen-Backbone_April-2021_V3.pdf.

Guidehouse (2021c) *Picturing the value of underground gas storage to the European hydrogen system*. Available at: https://www.gie.eu/wp-content/uploads/filr/3517/Picturing the value of gas storage to the European hydrogen system_FINAL_140621.pdf.

H2IT (2019) *Piano Nazionale di Sviluppo: Mobilità Idrogeno Italia*. Available at: https://www.h2it.it/wp-content/uploads/2020/03/Piano-Nazionale_Mobilita-Idrogeno_integrale2019.pdf.

Hank, C. *et al.* (2020) ‘Supplementary Information: Energy efficiency and economic assessment of imported energy carriers based on renewable electricity’, *Sustainable Energy & Fuels*, (5). doi: doi.org/10.1039/D0SE00067A.

Hanson, A. G. *et al.* (2022) *Subsurface hydrogen and natural gas storage: state of knowledge and research recommendations report*. Available at: https://www.osti.gov/servlets/purl/1846632/.

He, X. *et al.* (2021) ‘Well-to-wheels emissions, costs, and feedstock potentials for light-duty hydrogen fuel cell vehicles in China in 2017 and 2030’, *Renewable and Sustainable Energy Reviews*, 137(January 2020). doi: 10.1016/j.rser.2020.110477.

Hennig, M. and Haase, M. (2021) ‘Techno-economic analysis of hydrogen enhanced methanol to gasoline process from biomass-derived synthesis gas’, *Fuel Processing Technology*, 216, p. 106776. doi: 10.1016/j.fuproc.2021.106776.

Holst, M. *et al.* (2021) *Cost Forecast for Low Temperature Electrolysis - Technology Driven Bottom-up Prognosis for PEM and Alkaline Water Electrolysis Systems*. Available at: https://www.ise.fraunhofer.de/en/press-media/press-releases/2022/towards-a-gw-industry-fraunhofer-ise-provides-a-deep-in-cost-analysis-for-water-electrolysis-systems.html.

Hydrogen Council (2021) *Hydrogen Insights: A perspective on hydrogen investment, market development and cost competitiveness*. Available at: https://hydrogencouncil.com/wp-content/uploads/2021/02/Hydrogen-Insights-2021.pdf.

Hydrogen Europe (2020) *Strategic Research and Innovation Agenda Final Draft October 2020 Contents*. Available at: https://hydrogeneurope.eu/reports/.

Hystories (2021) *Conceptual design of salt cavern and porous media underground storage site*. Available at: https://hystories.eu/wp-content/uploads/2022/05/Hystories_D7.1-1-Conceptual-design-of-salt-cavern-and-porous-media-underground-storage-site.pdf.

Hystories (2022) *Life Cycle Cost Assessment of an underground storage site*. Available at: https://hystories.eu/wp-content/uploads/2022/05/Hystories_D7.2-1-Life-Cycle-Cost-Assessment-of-an-underground-storage-site.pdf.

HyUnder (2013) *Overview on all known undergound storage technologies for hydrogen*, *HyUnder Deliverable D3.1*. Available at: http://hyunder.eu/wp-content/uploads/2016/01/D3.1_Overview-of-all-known-underground-storage-technologies.pdf.

ICCT (2022a) *Current and future cost of e-kerosene in the United States and Europe*, *Theicct.Org*. Available at: https://theicct.org/wp-content/uploads/2022/02/fuels-us-europe-current-future-cost-ekerosene-us-europe-mar22.pdf.

ICCT (2022b) *Fuel-cell hydrogen long-haul trucks in Europe: a total cost of ownership analysis*. Available at: https://theicct.org/wp-content/uploads/2022/09/eu-hvs-fuels-evs-fuel-cell-hdvs-europe-sep22.pdf.

ICCT (2022c) *Performance Analysis Of Evolutionary Hydrogen-Powered Aircraft*, *The International Council on Clean Transportation*. Available at: https://theicct.org/publication/aviation-global-evo-hydrogen-aircraft-jan22/.

IEA (2010) 'Technology Brief E05 - Biomass for Heat and Power', (May), pp. 1–8. Available at: https://iea-etsap.org/E-TechDS/PDF/E05-BiomassforHP-GS-AD-gct.pdf.

IEA (2015) *Technology Roadmap: Hydrogen and Fuel Cells*. Available at: https://iea.blob.core.windows.net/assets/e669e0b6-148c-4d5c-816b-a7661301fa96/TechnologyRoadmapHydrogenandFuelCells.pdf.

IEA (2019a) *IEA G20 hydrogen report: Assumptions*, *The Future of Hydrogen*. Available at: https://iea.blob.core.windows.net/assets/a02a0c80-77b2-462e-a9d5-1099e0e572ce/IEA-The-Future-of-Hydrogen-Assumptions-Annex.pdf.

IEA (2019b) *The Future of Hydrogen: Seizing today's opportunities*, *IEA Publications*. Available at: https://www.iea.org/reports/the-future-of-hydrogen.

IEA (2019c) *World Energy Outlook 2019*. OECD. doi: 10.1787/caf32f3b-en.

Ikäheimo, J. *et al.* (2018) 'Power-to-ammonia in future North European 100 % renewable power and heat system', *International Journal of Hydrogen Energy*, 43(36), pp. 17295–17308. doi: 10.1016/j.ijhydene.2018.06.121.

International Iron Metallics Association (2019) *DRI production*. Available at: https://www.metallics.org/dri-production.html (Accessed: 3 January 2023).

IRENA (2012) *Renewable Energy Technologies: Cost Analysis Series, Hydropower*, *International Renewable Energy Agency*. Available at: https://www.irena.org/publications/2012/Jun/Renewable-Energy-Cost-Analysis---Hydropower.

IRENA (2019) *Hydrogen: a Renewable Energy Perspective*, *Irena*. Available at: https://irena.org/publications/2019/Sep/Hydrogen-A-renewable-energy-perspective.

IRENA (2020) *Green Hydrogen Cost Reduction: Scaling up Electrolysers to Meet the 1.5 C Climate Goal*, */publications/2020/Dec/Green-hydrogen-cost-reduction*. Available at: /publications/2020/Dec/Green-hydrogen-cost-reduction%0Ahttps://www.irena.org/-/media/Files/IRENA/Agency/Publication/2020/Dec/IRENA_Green_hydrogen_cost_2020.pdf.

IRENA (2022a) *Global Hydrogen Trade to Meet the 1.5°C Climate Goal: Part II – Technology review of hydrogen carriers*. Available at: https://www.irena.org/publications/2022/Apr/Global-hydrogen-trade-Part-II.

IRENA (2022b) *Global hydrogen trade to meet the 1.5 °C climate goal: Part III – Green hydrogen supply cost and potential*.

IRENA (2022c) *Renewable Power Generation Costs in 2021*, *International Renewable Energy Agency*. Available at: https://www.irena.org/-/media/Files/IRENA/Agency/Publication/2018/Jan/IRENA_2017_Power_Costs_2018.pdf.

IRENA (2022d) *Renewable Technology Innovation Indicators : Mapping progress in costs , patents and standards*. Available at: https://www.irena.org/publications/2022/Mar/Renewable-Technology-

Innovation-Indicators.

IRENA (2023) *The changing role of hydropower*. Available at: https://www.irena.org/Publications/2023/Feb/The-changing-role-of-hydropower-Challenges-and-opportunities.

IRENA and Methanol Institute (2021) *Innovation Outlook: Renewable Methanol*. Abu Dhabi. Available at: https://www.irena.org/publications/2021/Jan/Innovation-Outlook-Renewable-Methanol.

Ishimoto, Y. *et al.* (2020) 'Large-scale production and transport of hydrogen from Norway to Europe and Japan: Value chain analysis and comparison of liquid hydrogen and ammonia as energy carriers', *International Journal of Hydrogen Energy*, 45(58), pp. 32865–32883. doi: 10.1016/j.ijhydene.2020.09.017.

ISPT (2017) *Power to Ammonia*, *Institute for Sustainable Process Technology*. Available at: https://www.topsectorenergie.nl/sites/default/files/uploads/Energie en Industrie/Power to Ammonia 2017.pdf.

Jäger-Waldau, A. (2019) *PV Status Report 2019*, *JRC Science for Policy Report*. doi: 10.2760/326629.

Janssen, J. L. L. C. C. *et al.* (2022) 'Country-specific cost projections for renewable hydrogen production through off-grid electricity systems', *Applied Energy*, 309(December 2021), p. 118398. doi: 10.1016/j.apenergy.2021.118398.

Jasper, S. and El-Halwagi, M. M. (2015) 'A techno-economic comparison between two methanol-to-propylene processes', *Processes*, 3(3), pp. 684–698. doi: 10.3390/pr3030684.

Jiang, J. *et al.* (2020) 'Comparative technoeconomic analysis and life cycle assessment of aromatics production from methanol and naphtha', *Journal of Cleaner Production*, 277, p. 123525. doi: 10.1016/j.jclepro.2020.123525.

JRC (2022) *Assessment of Hydrogen Delivery Options*, *European Comission*. doi: 10.2760/869085.

Kim, J. *et al.* (2022) 'Decarbonizing the iron and steel industry: A systematic review of sociotechnical systems, technological innovations, and policy options', *Energy Research and Social Science*, 89(January), p. 102565. doi: 10.1016/j.erss.2022.102565.

Kumar, H. (2022) *Hydrogen Powered Cars and Trucks : Is there a role for them in the electrified U . S . future ?* Available at: https://dspace.mit.edu/bitstream/handle/1721.1/143335/kumar-hemantk-sm-sdm-2022-thesis.pdf?sequence=1&isAllowed=y.

Lanphen, S. (2019) *Hydrogen Import Terminal*. Available at: https://repository.tudelft.nl/islandora/object/uuid%3Ad2429b05-1881-4e42-9bb3-ed604bc15255.

Leeson, D. *et al.* (2017) 'A Techno-economic analysis and systematic review of carbon capture and storage (CCS) applied to the iron and steel, cement, oil refining and pulp and paper industries, as well as other high purity sources', *International Journal of Greenhouse Gas Control*, 61, pp. 71–84. doi: 10.1016/j.ijggc.2017.03.020.

Linde (2019) *Latest Global Trend in Liquid Hydrogen Production - HYPER Closing Seminar*, *Hyper*. Brussels. Available at: https://www.sintef.no/globalassets/project/hyper/presentations-day-1/day1_1430_decker_latest-global-trend-in-liquid-hydrogen-production_linde.pdf.

Lord, A. S., Kobos, P. H. and Borns, D. J. (2014) 'Geologic storage of hydrogen: Scaling up to meet city transportation demands', *International Journal of Hydrogen Energy*, 39(28), pp. 15570–15582. doi: 10.1016/j.ijhydene.2014.07.121.

Mai, Z. *et al.* (2014) *Comparative Analysis between Coal-to-Olefins with CCS and Methanol-to-Olefins*, *Computer Aided Chemical Engineering*. Elsevier. doi: 10.1016/B978-0-444-63455-9.50016-7.

Marocco, P. *et al.* (2021) 'An MILP approach for the optimal design of renewable battery-hydrogen energy systems for off-grid insular communities', *Energy Conversion and Management*, 245, p. 114564. doi: 10.1016/j.enconman.2021.114564.

Michailos, S. *et al.* (2018) *Methanol Work ed Examples for the TEA and LCA Guidelines for CO2 Utilization*. doi: 10.3998/2027.42/145723.

Michalski, J. *et al.* (2017) 'Hydrogen generation by electrolysis and storage in salt caverns: Potentials, economics and systems aspects with regard to the German energy transition', *International Journal of Hydrogen Energy*, 42(19), pp. 13427–13443. doi: 10.1016/j.ijhydene.2017.02.102.

Mokhtara, C. *et al.* (2021) 'Optimal design of grid-connected rooftop PV systems: An overview and a new approach with application to educational buildings in arid climates', *Sustainable Energy Technologies and Assessments*, 47(June), p. 101468. doi: 10.1016/j.seta.2021.101468.

Morgan, E. R. (2013) *Techno-economic feasibility study of ammonia plants powered by offshore wind*, *University of Massachusetts - Amherst, PhD Dissertations*. Available at: https://scholarworks.umass.edu/cgi/viewcontent.cgi?article=1704&context=open_access_dissertations.

Muhammed, N. S. *et al.* (2022) 'A review on underground hydrogen storage: Insight into geological sites, influencing factors and future outlook', *Energy Reports*, 8, pp. 461–499. doi: 10.1016/j.egyr.2021.12.002.

Mukherjee, R. and Singh, S. (2021) 'Evaluating hydrogen rich fuel gas firing', *Petroleum Technology Quarterly*, Q1(Engineers India Limited (EIL)), pp. 59–62. Available at: https://cdn.digitalrefining.com/data/articles/file/1002591-q1-eiGBP-copy.pdf.

Niermann, M. *et al.* (2019) 'Liquid organic hydrogen carriers (LOHCs)-techno-economic analysis of LOHCs in a defined process chain', *Energy and Environmental Science*, 12(1), pp. 290–307. doi: 10.1039/c8ee02700e.

Niziolek, A. M. *et al.* (2016) 'Biomass-Based Production of Benzene, Toluene, and Xylenes via Methanol: Process Synthesis and Deterministic Global Optimization', *Energy and Fuels*, 30(6), pp. 4970–4998. doi: 10.1021/acs.energyfuels.6b00619.

NREL (2021) *Hydropower | Electricity | 2021 | ATB*. Available at: https://atb.nrel.gov/electricity/2021/hydropower#85NLUHRY (Accessed: 18 July 2022).

NREL and PNNL (2015) *Process Design and Economics for the Conversion of Lignocellulosic Biomass to Hydrocarbons via Indirect Liquefaction*, *National Renewable Energy Laboratory: Pacific Northwest National Laboratory*. Available at: https://www.nrel.gov/docs/fy15osti/62402.pdf.

Öberg, S., Odenberger, M. and Johnsson, F. (2022) 'Exploring the competitiveness of hydrogen-fueled gas turbines in future energy systems', *International Journal of Hydrogen Energy*, 47(1), pp. 624–644. doi: 10.1016/j.ijhydene.2021.10.035.

Oh, D. H., Lee, C. H. and Lee, J. C. (2021) 'Performance and Cost Analysis of Natural Gas Combined Cycle Plants with Chemical Looping Combustion', *ACS Omega*, 6(32), pp. 21043–21058. doi: 10.1021/acsomega.1c02695.

Olsson, O. *et al.* (2020) *Deployment of BECCS / U – technologies , supply chain setup & policy options*. Available at: https://www.ieabioenergy.com/wp-content/uploads/2020/06/BECCUS-Webinar-Slide-OO20200616-final.pdf.

Otto, A. *et al.* (2017) 'Power-to-steel: Reducing CO2 through the integration of renewable energy and hydrogen into the German steel industry', *Energies*, 10(4). doi: 10.3390/en10040451.

Peters, R. *et al.* (2022) 'A Techno-Economic Assessment of Fischer–Tropsch Fuels Based on Syngas from Co-Electrolysis', *Processes*, 10(4). doi: 10.3390/pr10040699.

PNNL (2009) *Techno-Economic Analysis for the Conversion of Lignocellulosic Biomass to Gasoline via the Methanol-to-Gasoline (MTG) Process*. doi: 10.1201/b13132-14.

Pregger, T. *et al.* (2019) *Main assumptions for energy pathways*, *Achieving the Paris Climate Agreement Goals: Global and Regional 100% Renewable Energy Scenarios with Non-Energy GHG Pathways for +1.5C and +2C*. doi: 10.1007/978-3-030-05843-2_5.

Proton Ventures (2017) *Opportunities for small scale ammonia production*.

Raab, M., Maier, S. and Dietrich, R. U. (2021) 'Comparative techno-economic assessment of a large-scale hydrogen transport via liquid transport media', *International Journal of Hydrogen Energy*, 46(21), pp. 11956–11968. doi: 10.1016/j.ijhydene.2020.12.213.

Reuß, M. *et al.* (2017) 'Seasonal storage and alternative carriers: A flexible hydrogen supply chain model', *Applied Energy*, 200, pp. 290–302. doi: 10.1016/j.apenergy.2017.05.050.

Reuß, M. E. (2019) *Techno-ökonomische Analyse alternativer Wasserstoffinfrastruktur*, *Energie & Umwelt*. Available at: https://juser.fz-juelich.de/record/864486/files/Energie_Umwelt_467.pdf.

Ruffini, E. and Wei, M. (2018) 'Future costs of fuel cell electric vehicles in California using a learning rate approach', *Energy*, 150(2018), pp. 329–341. doi: 10.1016/j.energy.2018.02.071.

Runge, P. *et al.* (2019) 'Economic comparison of different electric fuels for energy scenarios in 2035', *Applied Energy*, 233–234(October 2018), pp. 1078–1093. doi: 10.1016/j.apenergy.2018.10.023.

Ruokonen, J. *et al.* (2021) 'Modelling and cost estimation for conversion of green methanol to renewable liquid transport fuels via olefin oligomerisation', *Processes*, 9(6). doi: 10.3390/pr9061046.

Sadler, D. *et al.* (2018) *H21 North Of England Report*. Available at: https://www.h21.green/app/uploads/2019/01/H21-NoE-PRINT-PDF-FINAL-1.pdf.

Safari, S. and Ali, H. (2020) 'Electrochemical Modeling and Techno-Economic Analysis of Solid Oxide Fuel Cell for Residential Applications Journal of Renewable', *Journal of Renewable Energy and Environment*, 7(1), pp. 40–50.

Sekkesaeter, Ø. (2019) *Evaluation of Concepts and Systems for Marine Transportation of Hydrogen*. Available at: https://ntnuopen.ntnu.no/ntnu-xmlui/bitstream/handle/11250/2623195/no.ntnu%3Ainspera%3A2525165.pdf?sequence=1&isAllowed=y.

Smolinka, T. *et al.* (2018) 'Studie IndWEDe', pp. 1–201. Available at: https://www.ipa.fraunhofer.de/de/Publikationen/studien/studie-indWEDe.html.

Statista (2021) *Global green hydrogen projects' selling prices 2021*. Available at: https://www.statista.com/statistics/1260117/projected-selling-prices-of-large-scale-hydrogen-green-projects/ (Accessed: 24 January 2022).

Statista (2022a) *Ethylene prices globally 2022*. Available at: https://www.statista.com/statistics/1170573/price-ethylene-forecast-globally/ (Accessed: 4 January 2023).

Statista (2022b) *Global propylene prices 2022*. Available at: https://www.statista.com/statistics/1170576/price-propylene-forecast-globally/ (Accessed: 4 January 2023).

Statista (2022c) *U.S. hydropower plant CAPEX forecast 2050 | Statista*. Available at: https://www.statista.com/statistics/243725/capital-costs-of-a-typical-us-hydrothermal-power-plant/ (Accessed: 18 July 2022).

Stöckl, F., Schill, W. P. and Zerrahn, A. (2021) 'Optimal supply chains and power sector benefits of green hydrogen', *Scientific Reports*, 11(1). doi: 10.1038/s41598-021-92511-6.

Stolzenburg, K. and Mubbala, R. (2013) 'Hydrogen Liquefaction Report', *Hydrogen and Fuel Cells in the Nordic Countries, November 1, 2013*, (278177), p. 33. Available at: https://www.idealhy.eu/uploads/documents/IDEALHY_D3-16_Liquefaction_Report_web.pdf.

Swanson, R. M. *et al.* (2010) 'Techno-economic analysis of biomass-to-liquids production based on gasification', *Fuel*, 89(SUPPL. 1), pp. S11–S19. doi: 10.1016/j.fuel.2010.07.027.

Syah, R. *et al.* (2021) 'The economic evaluation of methanol and propylene production from natural gas at petrochemical industries in Iran', *Sustainability (Switzerland)*, 13(17), pp. 1–23. doi: 10.3390/su13179990.

Szima, S. and Cormos, C. C. (2018) 'Improving methanol synthesis from carbon-free H2 and captured CO2: A techno-economic and environmental evaluation', *Journal of CO2 Utilization*, 24(February), pp. 555–563. doi: 10.1016/j.jcou.2018.02.007.

Tarkowski, R. (2019) 'Underground hydrogen storage: Characteristics and prospects', *Renewable and Sustainable Energy Reviews*, 105(January), pp. 86–94. doi: 10.1016/j.rser.2019.01.051.

Teichmann, D., Arlt, W. and Wasserscheid, P. (2012) 'Liquid Organic Hydrogen Carriers as an efficient vector for the transport and storage of renewable energy', *International Journal of Hydrogen Energy*, 37(23), pp. 18118–18132. doi: 10.1016/j.ijhydene.2012.08.066.

Thiyagarajan, S. R. *et al.* (2022) 'A comprehensive review of the mechanisms and efficiency of underground hydrogen storage', *Journal of Energy Storage*, 51(January), p. 104490. doi: 10.1016/j.est.2022.104490.

TNO (2021) *Technology factsheet: Advanced methanol to olefins process*, *Processes*. doi: 10.3390/pr3030684.

Tremel, A. *et al.* (2015) 'Techno-economic analysis for the synthesis of liquid and gaseous fuels based on hydrogen production via electrolysis', *International Journal of Hydrogen Energy*, 40(35), pp. 11457–11464. doi: 10.1016/j.ijhydene.2015.01.097.

Tsiropoulos, I., Tarvydas, D. and Zucker, A. (2018) *Cost development of low carbon energy technologies - Scenario-based cost trajectories to 2050, 2017 edition*, *JRC Science and Policy Reports*. JRC. doi: 10.2760/23266.

Ueckerdt, F. *et al.* (2021) 'Potential and risks of hydrogen-based e-fuels in climate change mitigation', *Nature Climate Change*, 11(5), pp. 384–393. doi: 10.1038/s41558-021-01032-7.

Vartiainen, E. *et al.* (2021) 'True Cost of Solar Hydrogen', *Solar RRL*, p. 2100487. doi: 10.1002/solr.202100487.

Viesi, D., Crema, L. and Testi, M. (2017) 'The Italian hydrogen mobility scenario implementing the European directive on alternative fuels infrastructure (DAFI 2014/94/EU)', *International Journal of Hydrogen Energy*, 42(44), pp. 27354–27373. doi: 10.1016/j.ijhydene.2017.08.203.

De Vita, A. *et al.* (2018) *Technology pathways in decarbonisation scenarios*. Available at: https://www.researchgate.net/publication/328095638_Technology_pathways_in_decarbonisation_scenarios.

Vogl, V., Åhman, M. and Nilsson, L. J. (2018) 'Assessment of hydrogen direct reduction for fossil-free steelmaking', *Journal of Cleaner Production*, 203, pp. 736–745. doi: 10.1016/j.jclepro.2018.08.279.

Vos, M., Douma, J. and Van den Noort, A. (2020) *Study on the Import of Liquid Renewable Energy: Technology Cost Assessment*. Available at: https://www.gie.eu/wp-content/uploads/filr/2598/DNV-GL_Study-GLE-Technologies-and-costs-analysis-on-imports-of-liquid-renewable-energy.pdf.

de Vries, N. (2019) *Ammonia as marine fuel*. Available at: https://repository.tudelft.nl/islandora/object/uuid%3Abe8cbe0a-28ec-4bd9-8ad0-648de04649b8.

Wang, J., Wang, H. and Fan, Y. (2018) 'Techno-Economic Challenges of Fuel Cell Commercialization', *Engineering*, 4(3), pp. 352–360. doi: 10.1016/j.eng.2018.05.007.

Wang, R. R. *et al.* (2021) 'Hydrogen direct reduction (H-DR) in steel industry—An overview of challenges and opportunities', *Journal of Cleaner Production*, 329(June), p. 129797. doi: 10.1016/j.jclepro.2021.129797.

Welder, L. *et al.* (2018) 'Spatio-temporal optimization of a future energy system for power-to-hydrogen applications in Germany', *Energy*, 158, pp. 1130–1149. doi: 10.1016/j.energy.2018.05.059.

Wijk, A. Van and Wouters, F. (2021) *Hydrogen - The Bridge BEtween Africa and Europe*, *Shaping an Inclusive Energy Transition*. Springer International Publishing. doi: 10.1007/978-3-030-74586-8.

Xiang, D. *et al.* (2015) 'Comparative study of coal, natural gas, and coke-oven gas based methanol to olefins processes in China', *Computers and Chemical Engineering*, 83, pp. 176–185. doi: 10.1016/j.compchemeng.2015.03.007.

Xiao, M. *et al.* (2021) 'Plummeting costs of renewables - Are energy scenarios lagging?', *Energy Strategy Reviews*, 35(March), p. 100636. doi: 10.1016/j.esr.2021.100636.

Yousefi, H. S. (2021) *Design considerations for developing an underground hydrogen storage facility in porous reservoirs*. Available at: https://ris.utwente.nl/ws/portalfiles/portal/269008008/PDEng_Thesis_Seyedhamidreza_Yousefi_public_.pdf.

Zang, G., Sun, P., Elgowainy, A. A., *et al.* (2021) 'Performance and cost analysis of liquid fuel production from H2 and CO2 based on the Fischer-Tropsch process', *Journal of CO2 Utilization*, 46(November 2020), p. 101459. doi: 10.1016/j.jcou.2021.101459.

Zang, G., Sun, P., Elgowainy, A., *et al.* (2021) 'Technoeconomic and Life Cycle Analysis of Synthetic Methanol Production from Hydrogen and Industrial Byproduct CO2', *Environmental Science and Technology*, 55(8), pp. 5248–5257. doi: 10.1021/acs.est.0c08237.

Zauner, A. *et al.* (2022) 'Multidisciplinary Assessment of a Novel Carbon Capture and Utilization Concept including Underground Sun Conversion', *Energies*, 15(3). doi: 10.3390/en15031021.

Zhang, G., Zhang, J. and Xie, T. (2020) 'A solution to renewable hydrogen economy for fuel cell buses – A case study for Zhangjiakou in North China', *International Journal of Hydrogen Energy*, 45(29), pp. 14603–14613. doi: 10.1016/j.ijhydene.2020.03.206.

Zhao, Z., Jiang, J. and Wang, F. (2021) 'An economic analysis of twenty light olefin production pathways', *Journal of Energy Chemistry*, 56, pp. 193–202. doi: 10.1016/j.jechem.2020.04.021.

10 APPENDIX A: Summary of the techno-economic parameters of the green hydrogen supply chain.

10.1 Green hydrogen production

References and assumptions in Appendix 11.1.

Utility-scale PV	Unit	2020			2030			2040			2050		
		Pess.	Avg.	Opt.	Pess.	Avg.	Opt.	Pess.	Avg.	Opt.	Pess.	Avg.	Opt.
Specific invest (per capacity)	EUR/kW_p	2031	1483	989	1303	908	498	884	692	441	740	551	319
Fixed O&M costs	%CAPEX/y	1%	1%	1%	1%	1%	1%	1%	1%	1%	1%	1%	1%
Variable O&M costs	EUR/kWh_{el}	-	-	-	-	-	-	-	-	-	-	-	-
Economic lifetime	y	20	20	20	20	20	20	20	20	20	20	20	20
Technical lifetime	y	25	25	25	25	25	25	25	25	25	25	25	25

Rooftop PV	Unit	2020			2030			2040			2050		
		Pess.	Avg.	Opt.	Pess.	Avg.	Opt.	Pess.	Avg.	Opt.	Pess.	Avg.	Opt.
Specific invest (per capacity)	EUR/kW_p	2647	2068	1260	1805	1400	900	1300	1100	782	989	800	664
Fixed O&M costs	%CAPEX/y	1%	1%	1%	1%	1%	1%	1%	1%	1%	1%	1%	1%
Variable O&M costs	EUR/kWh_{el}	-	-	-	-	-	-	-	-	-	-	-	-
Economic lifetime	y	20	20	20	20	20	20	20	20	20	20	20	20
Technical lifetime	y	25	25	25	25	25	25	25	25	25	25	25	25

Onshore wind	Unit	2020			2030			2040			2050		
		Pess.	Avg.	Opt.	Pess.	Avg.	Opt.	Pess.	Avg.	Opt.	Pess.	Avg.	Opt.
Specific invest (per capacity)	EUR/kW_{el}	1853	1590	1349	1604	1285	938	1556	1227	938	1199	1026	938
Fixed O&M costs	%CAPEX/y	3%	3%	3%	3%	3%	3%	3%	3%	3%	3%	3%	3%
Variable O&M costs	EUR/kWh_{el}	-	-	-	-	-	-	-	-	-	-	-	-
Economic lifetime	y	20	20	20	20	20	20	20	20	20	20	20	20
Technical lifetime	y	25	25	25	25	25	25	25	25	25	25	25	25

Offshore Wind	Unit	2020 Pess.	2020 Avg.	2020 Opt.	2030 Pess.	2030 Avg.	2030 Opt.	2040 Pess.	2040 Avg.	2040 Opt.	2050 Pess.	2050 Avg.	2050 Opt.
Specific invest (per capacity)	EUR/kW$_{el}$	4203	3560	2890	3201	2590	1921	2799	2233	1596	2429	1896	1369
Fixed O&M costs	%CAPEX/y	2%	2%	2%	2%	2%	2%	2%	2%	2%	2%	2%	2%
Variable O&M costs	EUR/kWh$_{el}$	-	-	-	-	-	-	-	-	-	-	-	-
Economic lifetime	y	20	20	20	20	20	20	20	20	20	20	20	20
Technical lifetime	y	25	25	25	25	25	25	25	25	25	25	25	25

Run of River	Unit	2020 Pess.	2020 Avg.	2020 Opt.	2030 Pess.	2030 Avg.	2030 Opt.	2040 Pess.	2040 Avg.	2040 Opt.	2050 Pess.	2050 Avg.	2050 Opt.
Specific invest (per capacity)	EUR/kW$_{el}$	7620	6323	3748	6930	5750	3409	6769	5684	3325	6651	5498	3369
Fixed O&M costs	%CAPEX/y	2%	2%	1%	2%	2%	1%	2%	2%	1%	2%	2%	1%
Variable O&M costs	EUR/kWh$_{el}$	0.006	0.006	0.006	0.006	0.006	0.006	0.006	0.006	0.006	0.006	0.006	0.006
Technical lifetime	y	40	50	60	40	50	60	40	50	60	40	50	60

Bioenergy	Unit	2020 Pess.	2020 Avg.	2020 Opt.	2030 Pess.	2030 Avg.	2030 Opt.	2040 Pess.	2040 Avg.	2040 Opt.	2050 Pess.	2050 Avg.	2050 Opt.
Specific invest (per capacity)	EUR/kW$_{el}$	5627	4361	3245	5235	3993	3045	5190	3682	2750	5176	3912	2668
Fixed O&M costs	%CAPEX/y	3%	2%	1%	2%	2%	1%	2%	2%	1%	2%	1%	1%
Variable O&M costs	EUR/kWh$_{el}$	0.048	0.022	0.002	0.048	0.022	0.002	0.048	0.022	0.002	0.048	0.022	0.002
Technical lifetime	y	30	27	25	30	27	25	30	27	25	30	27	25

PEM-Electrolyzer	Unit	2020 Pess.	2020 Avg.	2020 Opt.	2030 Pess.	2030 Avg.	2030 Opt.	2040 Pess.	2040 Avg.	2040 Opt.	2050 Pess.	2050 Avg.	2050 Opt.
Specific invest (per capacity)	EUR/kW$_{el}$	1663	1317	1008	1069	856	555	555	468	386	559	448	234
Fixed O&M costs	%CAPEX/y	2.0%	2.0%	2.0%	2.0%	2.0%	2.0%	1.8%	1.8%	1.8%	1.6%	1.6%	1.6%
Variable O&M costs	EUR/kWh$_{el}$	0.158	0.100	0.045	0.067	0.046	0.026	0.046	0.030	0.015	0.024	0.014	0.005
Efficiency	%HHV	71%	72%	74%	74%	78%	80%	76%	81%	84%	79%	83%	87%
Technical lifetime	y	20	25	30	20	25	30	20	25	30	20	25	30

Co-funded by the European Union

Alkaline Electrolyzer	Unit	2020 Pess.	2020 Avg.	2020 Opt.	2030 Pess.	2030 Avg.	2030 Opt.	2040 Pess.	2040 Avg.	2040 Opt.	2050 Pess.	2050 Avg.	2050 Opt.
Specific invest (per capacity)	EUR/kW_{el}	1121	867	602	843	638	437	733	450	161	670	428	148
Fixed O&M costs	%CAPEX/y	3%	3%	3%	3%	3%	3%	3%	3%	3%	3%	3%	3%
Variable O&M costs	EUR/kWh_{el}	0.063	0.041	0.020	0.028	0.020	0.013	0.024	0.016	0.009	0.019	0.012	0.005
Efficiency	%HHV	73%	76%	80%	78%	80%	83%	78%	80%	83%	80%	84%	87%
Technical lifetime	y	28	28	28	29	29	29	30	30	30	33	33	33

10.2 Hydrogen conversion and reconversion

References and assumptions in Appendix 11.2.

Ammonia synthesis (Haber-Bosch)	Unit	2020 Pess.	2020 Avg.	2020 Opt.	2030 Pess.	2030 Avg.	2030 Opt.	2040 Pess.	2040 Avg.	2040 Opt.	2050 Pess.	2050 Avg.	2050 Opt.
Specific invest (per capacity)	EUR/kW_{H2}	1018	676	334	868	601	334	776	555	334	515	424	334
Fixed O&M costs	%CAPEX/y	2.5%	2.0%	1.5%	2.5%	2.0%	1.5%	2.5%	2.0%	1.5%	2.5%	2.0%	1.5%
Variable O&M costs	EUR/kWh_{H2}	0.00290	0.00154	0.00057	0.00248	0.00137	0.00057	0.00221	0.00127	0.00057	0.00147	0.00097	0.00057
Efficiency	%	74%	78%	83%	74%	78%	83%	74%	78%	83%	74%	78%	83%
Economic lifetime	y	-	-	-	-	-	-	-	-	-	-	-	-
Technical lifetime	y	25	25	25	25	25	25	25	25	25	25	25	25

Ammonia Cracking	Unit	2020 Pess.	2020 Avg.	2020 Opt.	2030 Pess.	2030 Avg.	2030 Opt.	2040 Pess.	2040 Avg.	2040 Opt.	2050 Pess.	2050 Avg.	2050 Opt.
Specific invest (per capacity)	EUR/kW_{H2}	610	465	264	524	402	243	439	339	221	354	277	199
Fixed O&M costs	%CAPEX/y	3.0%	2.5%	2.0%	3.0%	2.5%	2.0%	3.0%	2.5%	2.0%	3.0%	2.5%	2.0%
Variable O&M costs	EUR/kWh_{H2}	0.00209	0.00133	0.00060	0.00180	0.00115	0.00055	0.00150	0.00097	0.00050	0.00121	0.00079	0.00045
Efficiency	%	81%	85%	88%	81%	85%	88%	81%	85%	88%	81%	85%	88%
Economic lifetime	y	-	-	-	-	-	-	-	-	-	-	-	-
Technical lifetime	y	20	20	20	20	20	20	20	20	20	20	20	20

LOHC Hydrogenation	Unit	2020 Pess.	2020 Avg.	2020 Opt.	2030 Pess.	2030 Avg.	2030 Opt.	2040 Pess.	2040 Avg.	2040 Opt.	2050 Pess.	2050 Avg.	2050 Opt.
Specific invest (per capacity)	EUR/kW_{H2}	311	201	91	246	163	80	160	113	65	160	113	65
Fixed O&M costs	%CAPEX/y	3.0%	2.5%	2.0%	3.0%	2.5%	2.0%	3.0%	2.5%	2.0%	3.0%	2.5%	2.0%
Variable O&M costs	EUR/kWh_{H2}	0.00107	0.00057	0.00021	0.00084	0.00047	0.00018	0.00055	0.00032	0.00015	0.00055	0.00032	0.00015
Efficiency	%	96%	97%	99%	96%	97%	99%	96%	97%	99%	96%	97%	99%
Economic lifetime	y	-	-	-	-	-	-	-	-	-	-	-	-
Technical lifetime	y	20	20	20	20	20	20	20	20	20	20	20	20

LOHC Dehydrogenation	Unit	2020 Pess.	2020 Avg.	2020 Opt.	2030 Pess.	2030 Avg.	2030 Opt.	2040 Pess.	2040 Avg.	2040 Opt.	2050 Pess.	2050 Avg.	2050 Opt.
Specific invest (per capacity)	EUR/kW_{H2}	1370	945	190	774	633	184	465	322	178	243	170	97
Fixed O&M costs	%CAPEX/y	4.0%	3.4%	2.5%	4.0%	3.4%	2.5%	4.0%	3.4%	2.5%	4.0%	3.4%	2.5%
Variable O&M costs	EUR/kWh_{H2}	0.00625	0.00364	0.00054	0.00353	0.00244	0.00052	0.00212	0.00124	0.00051	0.00111	0.00065	0.00028
Efficiency	%	73%	74%	76%	74%	75%	76%	74%	75%	76%	75%	76%	76%
Economic lifetime	y	-	-	-	-	-	-	-	-	-	-	-	-
Technical lifetime	y	15	15	15	15	15	15	15	15	15	15	15	15

Hydrogen liquefaction	Unit	2020 Pess.	2020 Avg.	2020 Opt.	2030 Pess.	2030 Avg.	2030 Opt.	2040 Pess.	2040 Avg.	2040 Opt.	2050 Pess.	2050 Avg.	2050 Opt.
Specific invest (per capacity)	EUR/kW_{H2}	2415	1939	1316	2054	1662	1270	1705	1477	1250	1111	1053	996
Fixed O&M costs	%CAPEX/y	4.0%	3.0%	2.0%	4.0%	3.0%	2.0%	4.0%	3.0%	2.0%	4.0%	3.0%	2.0%
Variable O&M costs	EUR/kWh_{H2}	0.01103	0.00664	0.00300	0.00938	0.00569	0.00290	0.00778	0.00506	0.00285	0.00507	0.00361	0.00227
Efficiency	%	77%	79%	83%	81%	83%	85%	83%	84%	85%	85%	85%	86%
Economic lifetime	y	-	-	-	-	-	-	-	-	-	-	-	-
Technical lifetime	y	30	30	30	30	30	30	30	30	30	30	30	30

Liquid hydrogen regasification	Unit	2020 Pess.	2020 Avg.	2020 Opt.	2030 Pess.	2030 Avg.	2030 Opt.	2040 Pess.	2040 Avg.	2040 Opt.	2050 Pess.	2050 Avg.	2050 Opt.
Specific invest (per capacity)	EUR/kW$_{H2}$	315	188	73	274	167	69	232	146	65	191	125	60
Fixed O&M costs	%CAPEX/y	4.0%	3.0%	2.0%	4.0%	3.0%	2.0%	4.0%	3.0%	2.0%	4.0%	3.0%	2.0%
Variable O&M costs	EUR/kWh$_{H2}$	0.00144	0.00064	0.00017	0.00125	0.00057	0.00016	0.00106	0.00050	0.00015	0.00087	0.00043	0.00014
Efficiency	%	98%	99%	100%	98%	99%	100%	99%	99%	100%	99%	99%	100%
Economic lifetime	y	-	-	-	-	-	-	-	-	-	-	-	-
Technical lifetime	y	20	30	20	20	30	20	20	30	20	20	30	20

Methanol synthesis	Unit	2020 Pess.	2020 Avg.	2020 Opt.	2030 Pess.	2030 Avg.	2030 Opt.	2040 Pess.	2040 Avg.	2040 Opt.	2050 Pess.	2050 Avg.	2050 Opt.
Specific invest (per capacity)	EUR/kW$_{H2}$	930	637	360	831	596	360	733	547	360	634	497	360
Fixed O&M costs	%CAPEX/y	6.0%	5.0%	4.0%	6.0%	5.0%	4.0%	6.0%	5.0%	4.0%	6.0%	5.0%	4.0%
Variable O&M costs	EUR/kWh$_{H2}$	0.10757	0.01740	0.00628	0.07968	0.01574	0.00633	0.05179	0.01407	0.00639	0.02391	0.01241	0.00645
Efficiency	%	84%	86%	88%	84%	86%	88%	84%	86%	88%	84%	86%	88%
Economic lifetime	y	-	-	-	-	-	-	-	-	-	-	-	-
Technical lifetime	y	18	20	22	18	20	22	18	20	22	18	20	22

Methanol cracking	Unit	2020 Pess.	2020 Avg.	2020 Opt.	2030 Pess.	2030 Avg.	2030 Opt.	2040 Pess.	2040 Avg.	2040 Opt.	2050 Pess.	2050 Avg.	2050 Opt.
Specific invest (per capacity)	EUR/kW$_{H2}$	374	285	196	374	285	196	374	285	196	374	285	196
Fixed O&M costs	%CAPEX/y	4.0%	3.4%	2.5%	4.0%	3.4%	2.5%	4.0%	3.4%	2.5%	4.0%	3.4%	2.5%
Variable O&M costs	EUR/kWh$_{H2}$	0.00625	0.00364	0.00054	0.00353	0.00244	0.00052	0.00212	0.00124	0.00051	0.00111	0.00065	0.00028
Efficiency	%	80%	78%	76%	80%	78%	76%	80%	78%	76%	80%	78%	76%
Economic lifetime	y	-	-	-	-	-	-	-	-	-	-	-	-
Technical lifetime	y	15	15	15	15	15	15	15	15	15	15	15	15

10.3 Transport of hydrogen and its derivatives

References and assumptions in Appendix 11.3.

New pipelines (onshore)	Unit	2020 Pess.	2020 Avg.	2020 Opt.	2030 Pess.	2030 Avg.	2030 Opt.	2040 Pess.	2040 Avg.	2040 Opt.	2050 Pess.	2050 Avg.	2050 Opt.
Specific invest (per length and diameter)	kEUR/ (km x cm)	40	32	23	40	32	23	40	32	23	40	32	23
Fixed O&M costs	%CAPEX/y	3.0%	2.5%	2.0%	3.0%	2.5%	2.0%	3.0%	2.5%	2.0%	3.0%	2.5%	2.0%
Variable O&M costs	EUR/kWh	-	-	-	-	-	-	-	-	-	-	-	-
Losses	$\%LHV_{H2}/km$	4.4E-05	1.5E-05	4.8E-06	4.4E-05	1.5E-05	4.8E-06	4.4E-05	1.5E-05	4.8E-06	4.4E-05	1.5E-05	4.8E-06
Economic lifetime	y	-	-	-	-	-	-	-	-	-	-	-	-
Technical lifetime	y	40	50	60	40	50	60	40	50	60	40	50	60

Reassigned / Repurposed Pipelines (Onshore)	Unit	2020 Pess.	2020 Avg.	2020 Opt.	2030 Pess.	2030 Avg.	2030 Opt.	2040 Pess.	2040 Avg.	2040 Opt.	2050 Pess.	2050 Avg.	2050 Opt.
Specific invest (per length and diameter)	kEUR/ (km x cm)	9	7	6	9	7	6	9	7	6	9	7	6
Fixed O&M costs	%CAPEX/y	3.0%	2.5%	2.0%	3.0%	2.5%	2.0%	3.0%	2.5%	2.0%	3.0%	2.5%	2.0%
Variable O&M costs	EUR/kWh	-	-	-	-	-	-	-	-	-	-	-	-
Losses	$\%LHV_{H2}/km$	4.4E-05	1.5E-05	4.8E-06	4.4E-05	1.5E-05	4.8E-06	4.4E-05	1.5E-05	4.8E-06	4.4E-05	1.5E-05	4.8E-06
Economic lifetime	y	-	-	-	-	-	-	-	-	-	-	-	-
Technical lifetime	y	30	40	50	30	40	50	30	40	50	30	40	50

New pipelines (offshore)	Unit	2020 Pess.	2020 Avg.	2020 Opt.	2030 Pess.	2030 Avg.	2030 Opt.	2040 Pess.	2040 Avg.	2040 Opt.	2050 Pess.	2050 Avg.	2050 Opt.
Specific invest (per length and diameter)	kEUR/ (km x cm)	77	62	45	77	62	45	77	62	45	77	62	45
Fixed O&M costs	%CAPEX/y	3.0%	2.5%	2.0%	3.0%	2.5%	2.0%	3.0%	2.5%	2.0%	3.0%	2.5%	2.0%
Variable O&M costs	EUR/kWh	-	-	-	-	-	-	-	-	-	-	-	-
Losses	$\%LHV_{H2}/km$	4.4E-05	1.5E-05	4.8E-06	4.4E-05	1.5E-05	4.8E-06	4.4E-05	1.5E-05	4.8E-06	4.4E-05	1.5E-05	4.8E-06
Economic lifetime	y	-	-	-	-	-	-	-	-	-	-	-	-
Technical lifetime	y	40	50	60	40	50	60	40	50	60	40	50	60

Reassigned / Repurposed Pipelines (Offshore)	Unit	2020			2030			2040			2050		
		Pess.	Avg.	Opt.	Pess.	Avg.	Opt.	Pess.	Avg.	Opt.	Pess.	Avg.	Opt.
Specific invest (per length and diameter)	kEUR/ (km x cm)	18	14	11	18	14	11	18	14	11	18	14	11
Fixed O&M costs	%CAPEX/y	3.0%	2.5%	2.0%	3.0%	2.5%	2.0%	3.0%	2.5%	2.0%	3.0%	2.5%	2.0%
Variable O&M costs	EUR/kWh	-	-	-	-	-	-	-	-	-	-	-	-
Losses	%LHV_{H2}/km	4.4E-05	1.5E-05	4.8E-06	4.4E-05	1.5E-05	4.8E-06	4.4E-05	1.5E-05	4.8E-06	4.4E-05	1.5E-05	4.8E-06
Economic lifetime	y	-	-	-	-	-	-	-	-	-	-	-	-
Technical lifetime	y	30	40	50	30	40	50	30	40	50	30	40	50

Ammonia shipping	Unit	2020			2030			2040			2050		
		Pess.	Avg.	Opt.	Pess.	Avg.	Opt.	Pess.	Avg.	Opt.	Pess.	Avg.	Opt.
Specific invest (per capacity)	EUR/kWh_{H2}	0.34	0.29	0.19	0.32	0.25	0.17	0.30	0.23	0.15	0.30	0.23	0.15
Fixed O&M costs	%CAPEX/y	3.5%	3.0%	2.5%	3.5%	3.0%	2.5%	3.5%	3.0%	2.5%	3.5%	3.0%	2.5%
Variable O&M costs	EUR/ (km x kWh)	8.5E-07	3.9E-07	1.4E-07	8.5E-07	3.9E-07	1.4E-07	8.5E-07	3.9E-07	1.4E-07	8.5E-07	3.9E-07	1.4E-07
Losses	%/km	0	0	0	0	0	0	0	0	0	0	0	0
Economic lifetime	y	-	-	-	-	-	-	-	-	-	-	-	-
Technical lifetime	y	30	30	30	30	30	30	30	30	30	30	30	30

LOHC (including methanol) shipping	Unit	2020			2030			2040			2050		
		Pess.	Avg.	Opt.	Pess.	Avg.	Opt.	Pess.	Avg.	Opt.	Pess.	Avg.	Opt.
Specific invest (per capacity)	EUR/kWh_{H2}	0.65	0.50	0.39	0.59	0.48	0.37	0.54	0.45	0.36	0.54	0.45	0.36
Fixed O&M costs	%CAPEX/y	5.0%	4.5%	4.0%	5.0%	4.5%	4.0%	5.0%	4.5%	4.0%	5.0%	4.5%	4.0%
Variable O&M costs	EUR/ (km x kWh)	8.5E-07	3.9E-07	1.4E-07	8.5E-07	3.9E-07	1.4E-07	8.5E-07	3.9E-07	1.4E-07	8.5E-07	3.9E-07	1.4E-07
Losses	%/km	0	0	0	0	0	0	0	0	0	0	0	0
Economic lifetime	y	-	-	-	-	-	-	-	-	-	-	-	-
Technical lifetime	y	30	30	30	30	30	30	30	30	30	30	30	30

Liquid hydrogen shipping	Unit	2020 Pess.	2020 Avg.	2020 Opt.	2030 Pess.	2030 Avg.	2030 Opt.	2040 Pess.	2040 Avg.	2040 Opt.	2050 Pess.	2050 Avg.	2050 Opt.
Specific invest (per capacity)	EUR/kWh_{H2}	3.92	2.38	1.05	2.71	1.88	1.05	1.50	1.28	1.05	1.50	1.28	1.05
Fixed O&M costs	%CAPEX/y	4.0%	3.5%	3.0%	4.0%	3.5%	3.0%	4.0%	3.5%	3.0%	4.0%	3.5%	3.0%
Variable O&M costs	EUR/ (km x kWh)	8.5E-07	3.9E-07	1.4E-07	8.5E-07	3.9E-07	1.4E-07	8.5E-07	3.9E-07	1.4E-07	8.5E-07	3.9E-07	1.4E-07
Losses	%/km	3.8E-06	3.1E-06	2.4E-06	3.8E-06	3.1E-06	2.4E-06	3.8E-06	3.1E-06	2.4E-06	3.8E-06	3.1E-06	2.4E-06
Economic lifetime	y	-	-	-	-	-	-	-	-	-	-	-	-
Technical lifetime	y	30	30	30	30	30	30	30	30	30	30	30	30

10.4 Storage of hydrogen and its derivatives

References and assumptions in Appendix 11.4.

Above-ground pressurized hydrogen storage	Unit	2020 Pess.	2020 Avg.	2020 Opt.	2030 Pess.	2030 Avg.	2030 Opt.	2040 Pess.	2040 Avg.	2040 Opt.	2050 Pess.	2050 Avg.	2050 Opt.
Specific invest (per storage capacity)	$EUR/kWh_{Sto.Cap.H2}$	58	22	13	58	22	13	58	22	13	58	22	13
Fixed O&M costs (per storage capacity invest)	$\%CAPEX_{Sto.Cap.H2}/y$	3	2	1	3	2	1	3	2	1	3	2	1
Specific Invest (per charge/discharge capacity)	EUR/kW_{H2}	146.00	146.00	146.00	146.00	146.00	146.00	146.00	146.00	146.00	146.00	146.00	146.00
Fixed O&M costs (per charge/discharge capacity invest)	$\%CAPEX_{Charge/Disch.}/y$	1.00	1.00	1.00	1.00	1.00	1.00	1.00	1.00	1.00	1.00	1.00	1.00
Variable O&M cost for charge	$EUR/MWh_{H2charged}$	1.20	1.20	1.20	1.20	1.20	1.20	1.20	1.20	1.20	1.20	1.20	1.20
Variable O&M cost for discharge	$EUR/MWh_{H2discharged}$	0	0	0	0	0	0	0	0	0	0	0	0
Self-discharge (losses)	%	0.75%	0.50%	0.25%	0.75%	0.50%	0.25%	0.75%	0.50%	0.25%	0.75%	0.50%	0.25%
Charge efficiency (losses while injection)	%	100%	100%	100%	100%	100%	100%	100%	100%	100%	100%	100%	100%
Discharge efficiency (losses while withdrawal)	%	100%	100%	100%	100%	100%	100%	100%	100%	100%	100%	100%	100%
Technical lifetime	y	28	30	30	28	30	30	28	30	30	28	30	30

Pipe systems	Unit	2020			2030			2040			2050		
		Pess.	Avg.	Opt.	Pess.	Avg.	Opt.	Pess.	Avg.	Opt.	Pess.	Avg.	Opt.
Specific invest (per storage capacity)	$EUR/kWh_{Sto.Cap.H2}$	10	10	9	10	10	9	10	10	9	10	10	9
Fixed O&M costs (per storage capacity invest)	$\%CAPEX_{Sto.Cap.H2}/y$	19%	19%	19%	19%	19%	19%	19%	19%	19%	19%	19%	19%
Variable O&M (per cycled quantity)	$EUR/MWh_{H2stored}$	-	-	-	-	-	-	-	-	-	-	-	-
Charge rate/Injection rate	GWh_{H2}/day	1.5	1.5	1.5	1.5	1.5	1.5	1.5	1.5	1.5	1.5	1.5	1.5
Discharge rate/Withdrawal rate	GWh_{H2}/day	5.76	4.34	2.92	5.76	4.34	2.92	5.76	4.34	2.92	5.76	4.34	2.92
Self-discharge (losses)	%	-	-	-	-	-	-	-	-	-	-	-	-
Charge efficiency (losses while injection)	%	-	-	-	-	-	-	-	-	-	-	-	-
Discharge efficiency (losses while withdrawal)	%	-	-	-	-	-	-	-	-	-	-	-	-
Technical lifetime	y	30	30	30	30	30	30	30	30	30	30	30	30

Ammonia tanks	Unit	2020			2030			2040			2050		
		Pess.	Avg.	Opt.	Pess.	Avg.	Opt.	Pess.	Avg.	Opt.	Pess.	Avg.	Opt.
Specific invest (per storage capacity)	$EUR/kWh_{Sto.Cap.H2}$	0.19	0.17	0.16	0.19	0.17	0.16	0.19	0.17	0.16	0.19	0.17	0.16
Fixed O&M costs (per storage capacity invest)	$\%CAPEX_{Sto.Cap.H2}/y$	2%	2%	2%	2%	2%	2%	2%	2%	2%	2%	2%	2%
Variable O&M (per cycled quantity)	$EUR/MWh_{H2stored}$	-	-	-	-	-	-	-	-	-	-	-	-
Self-discharge (losses)	%	14.6%	14.6%	14.6%	14.6%	14.6%	14.6%	14.6%	14.6%	14.6%	14.6%	14.6%	14.6%
Charge efficiency (losses while injection)	%	-	-	-	-	-	-	-	-	-	-	-	-
Discharge efficiency (losses while withdrawal)	%	-	-	-	-	-	-	-	-	-	-	-	-
Technical lifetime	y	30	30	30	30	30	30	30	30	30	30	30	30

LOHC tanks	Unit	2020			2030			2040			2050		
		Pess.	Avg.	Opt.	Pess.	Avg.	Opt.	Pess.	Avg.	Opt.	Pess.	Avg.	Opt.
Specific invest (per storage capacity)	EUR/kWh $_{Sto.Cap.H2}$	0.24	0.21	0.19	0.24	0.21	0.19	0.24	0.21	0.19	0.24	0.21	0.19
Fixed O&M costs (per storage capacity invest)	%CAPEX $_{Sto.Cap.H2}$/y	16.8%	13.5%	10.3%	16.8%	13.5%	10.3%	16.8%	13.5%	10.3%	16.8%	13.5%	10.3%
Variable O&M (per cycled quantity)	EUR/MWh $_{H2stored}$	-	-	-	-	-	-	-	-	-	-	-	-
Self-discharge (losses)	%	0%	0%	0%	0%	0%	0%	0%	0%	0%	0%	0%	0%
Charge efficiency (losses while injection)	%	-	-	-	-	-	-	-	-	-	-	-	-
Discharge efficiency (losses while withdrawal)	%	-	-	-	-	-	-	-	-	-	-	-	-
Technical lifetime	y	30	30	30	30	30	30	30	30	30	30	30	30

Liquid hydrogen tanks	Unit	2020			2030			2040			2050		
		Pess.	Avg.	Opt.	Pess.	Avg.	Opt.	Pess.	Avg.	Opt.	Pess.	Avg.	Opt.
Specific invest (per storage capacity)	EUR/kWh $_{Sto.Cap.H2}$	5.24	4.62	2.70	5.24	4.62	2.70	5.24	4.62	2.70	5.24	4.62	2.70
Fixed O&M costs (per storage capacity invest)	%CAPEX $_{Sto.Cap.H2}$/y	1.999%	1.998%	0.999%	1.999%	1.998%	0.999%	1.999%	1.998%	0.999%	1.999%	1.998%	0.999%
Variable O&M (per cycled quantity)	EUR/MWh $_{H2stored}$	-	-	-	-	-	-	-	-	-	-	-	-
Self-discharge (losses while storing, e.g. boil-off)	% /year	13.4%	9.3%	5.1%	13.4%	9.3%	5.1%	13.4%	9.3%	5.1%	13.4%	9.3%	5.1%
Charge efficiency (losses while injection)	%	-	-	-	-	-	-	-	-	-	-	-	-
Discharge efficiency (losses while withdrawal)	%	-	-	-	-	-	-	-	-	-	-	-	-
Technical lifetime	y	23	25	28	23	25	28	23	25	28	23	25	28

Methanol tanks	Unit	2020			2030			2040			2050		
		Pess.	Avg.	Opt.	Pess.	Avg.	Opt.	Pess.	Avg.	Opt.	Pess.	Avg.	Opt.
Specific invest (per storage capacity)	$EUR/kWh_{Sto.Cap.H2}$	0.11	0.11	0.11	0.11	0.11	0.11	0.11	0.11	0.11	0.11	0.11	0.11
Fixed O&M costs (per storage capacity invest)	$\%CAPEX_{Sto.Cap.H2}/y$	0.2%	0.2%	0.2%	0.2%	0.2%	0.2%	0.2%	0.2%	0.2%	0.2%	0.2%	0.2%
Variable O&M (per cycled quantity)	$EUR/MWh_{H2stored}$	-	-	-	-	-	-	-	-	-	-	-	-
Charge rate/Injection rate	GWh_{H2}/day	-	-	-	-	-	-	-	-	-	-	-	-
Discharge rate/Withdrawal rate	GWh_{H2}/day	-	-	-	-	-	-	-	-	-	-	-	-
Self-discharge (losses)	%	-	-	-	-	-	-	-	-	-	-	-	-
Charge efficiency (losses while injection)	%	-	-	-	-	-	-	-	-	-	-	-	-
Discharge efficiency (losses while withdrawal)	%	-	-	-	-	-	-	-	-	-	-	-	-
Technical lifetime	y	30	30	30	30	30	30	30	30	30	30	30	30

New Salt caverns	Unit	2020 Pess.	2020 Avg.	2020 Opt.	2030 Pess.	2030 Avg.	2030 Opt.	2040 Pess.	2040 Avg.	2040 Opt.	2050 Pess.	2050 Avg.	2050 Opt.
Specific invest for **subsurface** components (per storage capacity)	$EUR/kWh_{Sto.Cap.H2}$	0.49	0.30	0.25	0.49	0.30	0.25	0.49	0.30	0.25	0.49	0.30	0.25
Fixed O&M costs for **subsurface** components (per storage capacity invest)	$\%CAPEX_{Sto.Cap.H2}/y$	4.0%	4.0%	2.2%	4.0%	4.0%	2.2%	4.0%	4.0%	2.2%	4.0%	4.0%	2.2%
Specific invest for **surface** components (per capacity)	EUR/kW_{H2}	327	205	183	327	205	183	327	205	183	327	205	183
Fixed O&M costs for **surface** components (per capacity invest)	$\%CAPEX_{Capacity}/y$	4%	4%	4%	4%	4%	4%	4%	4%	4%	4%	4%	4%
Specific invest for cushion gas (per storage capacity)	$EUR/kWh_{Sto.Cap.H2}$	0.13	0.10	0.04	0.13	0.10	0.04	0.13	0.10	0.04	0.13	0.10	0.04
Overall CAPEX (per storage capacity)	$EUR/kWh_{Sto.Cap.H2}$	1.32	0.92	0.68	1.32	0.92	0.68	1.32	0.92	0.68	1.32	0.92	0.68
Overall OPEX	$\%CAPEX_{Overall}/y$	4.8%	4.0%	3.8%	4.8%	4.0%	3.8%	4.8%	4.0%	3.8%	4.8%	4.0%	3.8%
Overall variable O&M cost	$EUR/MWh_{H2stored}$	0.60	0.53	0.53	0.60	0.53	0.53	0.60	0.53	0.53	0.60	0.53	0.53
Variable O&M cost for charge	$EUR/MWh_{H2charged}$	1.59	1.59	1.59	1.59	1.59	1.59	1.59	1.59	1.59	1.59	1.59	1.59
Variable O&M cost for discharge	$EUR/MWh_{H2discharged}$	0.66	0.66	0.66	0.66	0.66	0.66	0.66	0.66	0.66	0.66	0.66	0.66
Charge rate/Injection rate	GWh_{H2}/day	10.4	20.7	31.0	10.4	20.7	31.0	10.4	20.7	31.0	10.4	20.7	31.0
Discharge rate/Withdrawal rate	GWh_{H2}/day	10.4	35.9	62.1	10.4	35.9	62.1	10.4	35.9	62.1	10.4	35.9	62.1
Self-discharge (losses)	%	0.84%	0.84%	0.52%	0.84%	0.84%	0.52%	0.84%	0.84%	0.52%	0.84%	0.84%	0.52%
Charge efficiency (losses while injection)	%	100%	100%	100%	100%	100%	100%	100%	100%	100%	100%	100%	100%
Discharge efficiency (losses while withdrawal)	%	98.00%	98.75%	99.63%	98.00%	98.75%	99.63%	98.00%	98.75%	99.63%	98.00%	98.75%	99.63%
Energy use for charge (e.g. compression)	$kWh_{use}/kWh_{H2charged}$	0.089	0.031	0.026	0.089	0.031	0.026	0.089	0.031	0.026	0.089	0.031	0.026

New Salt caverns	Unit	2020			2030			2040			2050		
		Pess.	Avg.	Opt.	Pess.	Avg.	Opt.	Pess.	Avg.	Opt.	Pess.	Avg.	Opt.
Energy use for discharge (e.g. gas cleaning)	$kWh_{use}/kWh_{H2discharged}$	0.009	0.008	0.005	0.009	0.008	0.005	0.009	0.008	0.005	0.009	0.008	0.005
Technical lifetime for **subsurface** components	y	30	30	35	30	30	35	30	30	35	30	30	35
Technical lifetime for **surface** components	y	30	30	30	30	30	30	30	30	30	30	30	30
ABEX **Subsurface**	$\%CAPEX_{Subsurface}$	20%	20%	20%	20%	20%	20%	20%	20%	20%	20%	20%	20%
ABEX **Surface**	$\%CAPEX_{Surface}$	20%	20%	20%	20%	20%	20%	20%	20%	20%	20%	20%	20%

Pore Storage	Unit	2020			2030			2040			2050		
		Pess.	Avg.	Opt.	Pess.	Avg.	Opt.	Pess.	Avg.	Opt.	Pess.	Avg.	Opt.
Specific invest for **subsurface** components (per storage capacity)	$EUR/kWh_{Sto.Cap.H2}$	0.28	0.15	0.09	0.28	0.15	0.09	0.28	0.15	0.09	0.28	0.15	0.09
Fixed O&M costs for **subsurface** components (per storage capacity invest)	$\%CAPEX_{Sto.Cap.H2}/y$	2.38%	1.75%	1.13%	2.38%	1.75%	1.13%	2.38%	1.75%	1.13%	2.38%	1.75%	1.13%
Specific invest for **surface** components (per capacity)	EUR/kW_{H2}	430	343	257	430	343	257	430	343	257	430	343	257
Fixed O&M costs for **surface** components (per capacity invest)	$\%CAPEX_{Capacity}/y$	3.7%	3.7%	3.7%	3.7%	3.7%	3.7%	3.7%	3.7%	3.7%	3.7%	3.7%	3.7%
Specific invest for cushion gas (per storage capacity)	$EUR/kWh_{Sto.Cap.H2}$	0.25	0.17	0.11	0.25	0.17	0.11	0.25	0.17	0.11	0.25	0.17	0.11
Overall CAPEX (per storage capacity)	$EUR/kWh_{Sto.Cap.H2}$	0.57	0.47	0.31	0.57	0.47	0.31	0.57	0.47	0.31	0.57	0.47	0.31
Overall OPEX	$\%CAPEX_{Overall}/y$	3.1%	2.2%	1.3%	3.1%	2.2%	1.3%	3.1%	2.2%	1.3%	3.1%	2.2%	1.3%
Overall variable O&M cost	$EUR/MWh_{H2stored}$	-	-	-	-	-	-	-	-	-	-	-	-

Pore Storage	Unit	2020			2030			2040			2050		
		Pess.	Avg.	Opt.	Pess.	Avg.	Opt.	Pess.	Avg.	Opt.	Pess.	Avg.	Opt.
Variable O&M cost for charge	$EUR/MWh_{H2charged}$	1.14	1.14	1.14	1.14	1.14	1.14	1.14	1.14	1.14	1.14	1.14	1.14
Variable O&M cost for discharge	$EUR/MWh_{H2discharged}$	2.69	2.69	2.69	2.69	2.69	2.69	2.69	2.69	2.69	2.69	2.69	2.69
Charge rate/Injection rate	GWh_{H2}/day	13.98	39.44	68.40	13.98	39.44	68.40	13.98	39.44	68.40	13.98	39.44	68.40
Discharge rate/Withdrawal rate	GWh_{H2}/day	26.87	61.10	105.00	26.87	61.10	105.00	26.87	61.10	105.00	26.87	61.10	105.00
Self-discharge (losses)	%	3.2%	2.7%	2.1%	3.2%	2.7%	2.1%	3.2%	2.7%	2.1%	3.2%	2.7%	2.1%
Charge efficiency (losses while injection)	%	100%	100%	100%	100%	100%	100%	100%	100%	100%	100%	100%	100%
Discharge efficiency (losses while withdrawal)	%	98.8%	99.0%	99.3%	98.8%	99.0%	99.3%	98.8%	99.0%	99.3%	98.8%	99.0%	99.3%
Energy use for charge (e.g. compression)	$kWh_{use}/kWh_{H2charged}$	0.019	0.019	0.019	0.019	0.019	0.019	0.019	0.019	0.019	0.019	0.019	0.019
Energy use for discharge (e.g. gas cleaning)	$kWh_{use}/kWh_{H2discharged}$	0.045	0.045	0.045	0.045	0.045	0.045	0.045	0.045	0.045	0.045	0.045	0.045
Technical lifetime for **subsurface** components	y	30	30	40	30	30	40	30	30	40	30	30	40
Technical lifetime for **surface** components	y	30	30	30	30	30	30	30	30	30	30	30	30
ABEX **Subsurface**	$\%CAPEX_{Subsurface}$	20%	20%	20%	20%	20%	20%	20%	20%	20%	20%	20%	20%
ABEX **Surface**	$\%CAPEX_{Surface}$	20%	20%	20%	20%	20%	20%	20%	20%	20%	20%	20%	20%

10.5 Hydrogen final use

References and assumptions in Appendix 11.5.

H2-based CCGT	Unit	2020 Pess.	2020 Avg.	2020 Opt.	2030 Pess.	2030 Avg.	2030 Opt.	2040 Pess.	2040 Avg.	2040 Opt.	2050 Pess.	2050 Avg.	2050 Opt.
Specific invest (per capacity)	EUR/kW_{el}	1165	1118	1072	1165	1118	1072	1165	1118	1072	1165	1118	1072
Fixed O&M costs	%CAPEX/y	1.9%	1.6%	1.4%	1.9%	1.6%	1.4%	1.9%	1.6%	1.4%	1.9%	1.6%	1.4%
Variable O&M costs	EUR/kWh_{el}	0.006	0.003	0.001	0.006	0.003	0.001	0.006	0.003	0.001	0.006	0.003	0.001
Efficiency	%	58%	60%	62%	58%	60%	62%	58%	60%	62%	58%	60%	62%
Technical lifetime	y	28	30	32	28	30	32	28	30	32	28	30	32

H2-based GT	Unit	2020 Pess.	2020 Avg.	2020 Opt.	2030 Pess.	2030 Avg.	2030 Opt.	2040 Pess.	2040 Avg.	2040 Opt.	2050 Pess.	2050 Avg.	2050 Opt.
Specific invest (per capacity)	EUR/kW_{el}	583	559	536	583	559	536	583	559	536	583	559	536
Fixed O&M costs	%CAPEX/y	3.4%	2.5%	1.7%	3.4%	2.5%	1.7%	3.4%	2.5%	1.7%	3.4%	2.5%	1.7%
Variable O&M costs	EUR/kWh_{el}	0.015	0.010	0.002	0.015	0.010	0.002	0.015	0.010	0.002	0.015	0.010	0.002
Efficiency	%	27%	30%	32%	27%	30%	32%	27%	30%	32%	27%	30%	32%
Technical lifetime	y	28	30	32	28	30	32	28	30	32	28	30	32

Stationary fuel cell (PEM)	Unit	2020 Pess.	2020 Avg.	2020 Opt.	2030 Pess.	2030 Avg.	2030 Opt.	2040 Pess.	2040 Avg.	2040 Opt.	2050 Pess.	2050 Avg.	2050 Opt.
Specific invest (per capacity)	EUR/kW_{el}	5255	4394	2858	3000	2257	999	1713	1159	349	722	429	195
Fixed O&M costs	%CAPEX/y	6%	5%	4%	6%	5%	4%	6%	5%	4%	6%	5%	4%
Variable O&M costs	EUR/kWh_{el}	0.111	0.083	0.056	0.044	0.033	0.022	0.029	0.016	0.010	0.013	0.010	0.006
Efficiency	%	35.0%	38.9%	41.5%	53.0%	55.0%	58.0%	55.2%	59.0%	62.6%	56.3%	61.8%	65.4%
Technical lifetime	y	5	7	10	5	7	10	5	7	10	5	7	10

Industrial hydrogen Boilers	Unit	2020			2030			2040			2050		
		Pess.	Avg.	Opt.	Pess.	Avg.	Opt.	Pess.	Avg.	Opt.	Pess.	Avg.	Opt.
Specific invest (per capacity)	EUR/kW_{th}	255	232	188	255	232	188	255	232	188	255	232	188
Fixed O&M costs	%CAPEX/year	3.5%	3.0%	2.5%	3.5%	3.0%	2.5%	3.5%	3.0%	2.5%	3.5%	3.0%	2.5%
Variable O&M costs	EUR/kWh_{th}	0.0006	0.0004	0.0002	0.0006	0.0004	0.0002	0.0006	0.0004	0.0002	0.0006	0.0004	0.0002
Efficiency	%	93.0%	93.5%	94.0%	93.0%	93.5%	94.0%	93.0%	93.5%	94.0%	93.0%	93.5%	94.0%
Technical lifetime	y	25.0	27.5	30.0	25.0	30.0	35.0	25.0	30.0	35.0	25.0	32.5	40.0

Steel production - DRI	Unit	2020			2030			2040			2050		
		Pess.	Avg.	Opt.	Pess.	Avg.	Opt.	Pess.	Avg.	Opt.	Pess.	Avg.	Opt.
Specific invest (per capacity)	EUR/kW	4200	3373	2545	4045	3250	2455	3926	3155	2384	3857	3100	2343
Fixed O&M costs	%CAPEX/year	16%	15%	14%	17%	16%	15%	19%	18%	17%	21%	20%	19%
Variable O&M costs	EUR/kWh	-	-	-	-	-	-	-	-	-	-	-	-
Efficiency	kg_{H2}/ton_{Steel}	58	58	58	58	58	58	58	58	58	58	58	58
Technical lifetime	y	20	22.5	25	20	22.5	25	20	22.5	25	20	22.5	25

Methanol to olefins	Unit	2020			2030			2040			2050		
		Pess.	Avg.	Opt.	Pess.	Avg.	Opt.	Pess.	Avg.	Opt.	Pess.	Avg.	Opt.
Specific invest (per capacity)	EUR/kW_{MeOH}	405	332	239	405	332	239	405	332	239	405	332	239
Fixed O&M costs	%CAPEX/y	7%	6%	5%	7%	6%	5%	7%	6%	5%	7%	6%	5%
Variable O&M costs	EUR/kWh_{MeOh}	0.0050	0.0025	0.0013	0.0000	0.0025	0.0013	0.0000	0.0025	0.0013	0.0000	0.0025	0.0013
Efficiency	%	70%	75%	80%	70%	75%	80%	70%	75%	80%	70%	75%	80%
Technical lifetime	y	20	20	20	20	20	20	20	20	20	20	20	20

Methanol to aromatics	Unit	2020			2030			2040			2050		
		Pess.	Avg.	Opt.	Pess.	Avg.	Opt.	Pess.	Avg.	Opt.	Pess.	Avg.	Opt.
Specific invest (per capacity)	EUR/kW_{MeOH}	296	236	139	296	236	139	296	236	139	296	236	139
Fixed O&M costs	%CAPEX/y	9%	7%	5%	9%	7%	5%	9%	7%	5%	9%	7%	5%
Variable O&M costs	EUR/kWh_{MeOh}	0.0050	0.0025	0.0013	0.0050	0.0025	0.0013	0.0000	0.0025	0.0013	0.0000	0.0025	0.0013
Efficiency	%	23%	28%	33%	23%	28%	33%	23%	28%	33%	23%	28%	33%
Technical lifetime	y	20	20	20	20	20	20	20	20	20	20	20	20

Internal combustion engine cars	Unit	2020			2030			2040			2050		
		Pess.	Avg.	Opt.	Pess.	Avg.	Opt.	Pess.	Avg.	Opt.	Pess.	Avg.	Opt.
Specific invest (per capacity)	EUR/unit	23699	20907	16878	24087	21235	17176	24481	21568	17479	24882	21906	17788
Fixed O&M costs	%CAPEX/y	15%	13%	10%	15%	13%	10%	15%	13%	10%	15%	13%	10%
Efficiency	kWh/km	0.85	0.74	0.60	0.72	0.65	0.55	0.71	0.63	0.52	0.71	0.61	0.49
Methanol to gasoline fuel cost	EUR/km	0.36	0.21	0.06	0.17	0.11	0.05	0.15	0.10	0.05	0.14	0.09	0.04
Fischer-Tropsch fuel cost	EUR/km	0.53	0.31	0.10	0.15	0.11	0.06	0.14	0.10	0.05	0.14	0.09	0.04
Technical lifetime	y	12	12	12	12	12	12	12	12	12	12	12	12

Internal combustion engine trucks	Unit	2020			2030			2040			2050		
		Pess.	Avg.	Opt.	Pess.	Avg.	Opt.	Pess.	Avg.	Opt.	Pess.	Avg.	Opt.
Specific invest (per capacity)	EUR/unit	146060	137742	129710	148451	139902	132000	150881	142096	134330	153351	144324	136701
Fixed O&M costs	%CAPEX/y	15%	13%	10%	15%	13%	10%	15%	13%	10%	15%	13%	10%
Efficiency	kWh/km	3.44	3.26	3.07	2.90	2.85	2.81	2.89	2.77	2.65	2.88	2.68	2.49
Methanol to gasoline fuel cost	EUR/km	1.47	0.88	0.30	0.68	0.48	0.27	0.62	0.43	0.24	0.56	0.38	0.20
Fischer-Tropsch fuel cost	EUR/km	2.14	1.32	0.50	0.61	0.46	0.31	0.58	0.42	0.25	0.58	0.39	0.19
Technical lifetime	y	15	15	15	15	15	15	15	15	15	15	15	15

Internal combustion engine buses	Unit	2020			2030			2040			2050		
		Pess.	Avg.	Opt.	Pess.	Avg.	Opt.	Pess.	Avg.	Opt.	Pess.	Avg.	Opt.
Specific invest (per capacity)	EUR/unit	267950	250000	228972	283040	261764	228972	289430	265951	228972	295821	270933	231357
Fixed O&M costs	%CAPEX/y	15%	13%	10%	15%	13%	10%	15%	13%	10%	15%	13%	10%
Efficiency	kWh/km	4.43	3.61	3.14	3.89	3.27	2.99	3.78	3.11	2.75	3.68	2.96	2.52
Methanol to gasoline fuel cost	EUR/km	1.89	1.10	0.30	0.91	0.60	0.29	0.81	0.53	0.25	0.71	0.46	0.20
Fischer-Tropsch fuel cost	EUR/km	2.76	1.64	0.51	0.82	0.57	0.33	0.76	0.51	0.26	0.74	0.47	0.20
Technical lifetime	y	12	12	12	12	12	12	12	12	12	12	12	12

FCEV cars	Unit	2020			2030			2040			2050		
		Pess.	Avg.	Opt.	Pess.	Avg.	Opt.	Pess.	Avg.	Opt.	Pess.	Avg.	Opt.
Specific invest (per capacity)	EUR/unit	47111	41554	36377	32319	29196	25942	25527	23225	19149	25000	23000	19000
Fixed O&M costs	EUR/unit	8%	7%	6%	8%	7%	6%	8%	7%	6%	8%	7%	6%
Variable O&M costs	EUR/km	0.09	0.08	0.07	0.09	0.08	0.07	0.09	0.08	0.07	0.09	0.08	0.07
Efficiency	kWh/km	0.38	0.33	0.28	0.27	0.25	0.22	0.24	0.23	0.21	0.22	0.21	0.20
Technical lifetime	y	10	12	15	10	12	15	10	12	15	10	12	15

FCEV trucks	Unit	2020			2030			2040			2050		
		Pess.	Avg.	Opt.	Pess.	Avg.	Opt.	Pess.	Avg.	Opt.	Pess.	Avg.	Opt.
Specific invest (per capacity)	EUR/unit	376887	337597	293495	258555	237196	209303	204214	188688	154501	199999	186858	153295
Fixed O&M costs	EUR/unit	8%	7%	6%	8%	7%	6%	8%	7%	6%	8%	7%	6%
Variable O&M costs	EUR/km	0.185	0.1455	0.106	0.185	0.1455	0.106	0.185	0.1455	0.106	0.185	0.1455	0.106
Efficiency	kWh/km	2.94	2.48	2.01	2.06	1.87	1.55	1.82	1.71	1.51	1.74	1.60	1.43
Technical lifetime	y	13	15	17	13	15	17	13	15	17	13	15	17

FCEV buses	Unit	2020			2030			2040			2050		
		Pess.	Avg.	Opt.	Pess.	Avg.	Opt.	Pess.	Avg.	Opt.	Pess.	Avg.	Opt.
Specific invest (per capacity)	EUR/unit	673950	581827	461417	384381	352190	320000	369385	348546	319606	367569	333841	279059
Fixed O&M costs	EUR/unit	8%	7%	6%	8%	7%	6%	8%	7%	6%	8%	7%	6%
Variable O&M costs	EUR/km	0.28	0.2616	0.22	0.28	0.2616	0.22	0.28	0.2616	0.22	0.28	0.2616	0.22
Efficiency	kWh/km	3.83	3.36	2.86	2.69	2.54	2.21	2.38	2.31	2.16	2.26	2.17	2.04
Technical lifetime	y	10	12	15	10	12	15	10	12	15	10	12	15

11 APPENDIX B: Data references and main assumptions for techno-economic dataset.

The following appendix provides the references and underlying assumptions for the values proposed throughout the chapters of this report and dataset presented in the previous appendix. Most technologies of the hydrogen value chain benefit from comprehensive literature coverage. Therefore, when multiple values were found per technology parameter, the statistical approach presented in Chapter 2 was applied. This approach provides that the 1st and 3rd quartiles, as well as the average, were calculated to determine the Optimistic and Pessimistic and Average scenarios. This procedure was carried out for all items of this technology and for all time horizons.

11.1 Green hydrogen production

Utility-scale PV

References	***Assumptions***
(IRENA, 2019) (IEA, 2019c) (Pregger *et al.*, 2019) (DNV GL, 2019a) (Brändle, Schönfisch and Schulte, 2021)(Brändle, Schönfisch and Schulte, 2020)(Janssen *et al.*, 2022)(Xiao *et al.*, 2021)(IRENA, 2022b)(IRENA, 2022d)(Wiser, Bolinger and Seel, 2020)(Gernaat *et al.*, 2020)(Jäger-Waldau, 2019).	Statistical approach as reported in Chapter 2 applied to CAPEX, fixed OPEX and technical lifetime.

Rooftop PV

References	***Assumptions***
(Datta, Kalam and Shi, 2020)(Gernaat *et al.*, 2020)(Barbose and Satchwell, 2020)(Gomez-Exposito, Arcos-Vargas and Gutierrez-Garcia, 2020)(Duman and Güler, 2020)(Mokhtara *et al.*, 2021)(Bošnjaković, Čikić and Zlatunić, 2021) (Jäger-Waldau, 2019).	Statistical approach as reported in Chapter 2 applied to CAPEX, fixed OPEX and technical lifetime.

Wind onshore

References	***Assumptions***
(IRENA, 2019)(IEA, 2019c)(Pregger *et al.*, 2019)(DNV GL, 2019a)(Brändle, Schönfisch and Schulte, 2021)(Brändle, Schönfisch and Schulte, 2020) (Janssen *et al.*, 2022) (Xiao *et al.*, 2021)(IRENA, 2022b)(IRENA, 2022d).	Statistical approach as reported in Chapter 2 applied to CAPEX, fixed OPEX and technical lifetime.

Wind offshore

References	***Assumptions***
(IRENA, 2019)(IEA, 2019c)(Pregger *et al.*, 2019)(DNV GL, 2019a)(Brändle, Schönfisch and Schulte, 2021)(Brändle, Schönfisch and Schulte, 2020) (Janssen *et al.*, 2022) (Xiao *et al.*, 2021)(IRENA, 2022b)(IRENA, 2022d).	Statistical approach as reported in Chapter 2 applied to CAPEX, fixed OPEX and technical lifetime.

Run-of-river hydropower plants

References	***Assumptions***
(IRENA, 2012)(IRENA, 2022c)(DOE, 2016)(NREL, 2021)(Statista, 2022c)(European Commission, 2014)(IRENA & ETSAP, 2015)(IEA, 2021)(Tsiropoulos, Tarvydas and Zucker, 2018).	Statistical approach as reported in Chapter 2 applied to CAPEX. Fixed OPEX and technical lifetime from (Tsiropoulos, Tarvydas and Zucker, 2018) and (IEA, 2021).

Biomass generated power

References	***Assumptions***
(Grosse *et al.*, 2017)(De Vita *et al.*, 2018)(IEA, 2010)	Statistical approach as reported in Chapter 2 applied to CAPEX, fixed OPEX, variable OPEX and technical lifetime. The approach was applied including different bioenergy generation methods such (see Chapter 3.1.4).

PEM-WEL

References	***Assumptions***
(Brändle, Schönfisch and Schulte, 2021)(Brändle, Schönfisch and Schulte, 2020)(IEA, 2019b) (Böhm, Goers and Zauner, 2019)(Hydrogen Europe, 2020)(Glenk and Reichelstein, 2019)(Smolinka *et al.*, 2018)(Bertuccioli *et al.*, 2014)(Holst *et al.*, 2021)(Böhm *et al.*, 2020)(Zauner *et al.*, 2022)	Statistical approach as reported in Chapter 2 applied to CAPEX, fixed OPEX, efficiency and technical lifetime. Variable OPEX calculated from stack replacement needs (IEA, 2019b) and stack CAPEX share of 50% (IRENA, 2020) (See Chapter 3.2).

A-WEL

References	***Assumptions***
(IEA, 2019b) (Janssen *et al.*, 2022)(Vartiainen *et al.*, 2021) (Böhm, Goers and Zauner, 2019) (Hydrogen Europe, 2020)(IRENA, 2020) (Glenk and Reichelstein, 2019) (Smolinka *et al.*, 2018)(Bertuccioli *et al.*, 2014)(Holst *et al.*, 2021)(Böhm *et al.*, 2020)	Statistical approach as reported in Chapter 2 applied to CAPEX, fixed OPEX, efficiency and technical lifetime. Variable OPEX calculated from stack replacement needs (IEA, 2019b) and stack CAPEX share of 50% (IRENA, 2020) (See Chapter 3.2).

11.2 Hydrogen conversion and reconversion

Ammonia synthesis

References	***Assumptions***
(IEA, 2019a)(BNEF, 2019)(Sadler *et al.*, 2018)(Vos, Douma and Van den Noort, 2020) (Ikäheimo *et al.*, 2018)(Cesaro *et al.*, 2021)(Bartels, 2008)(Tremel *et al.*, 2015)(Ishimoto *et al.*, 2020)(Morgan, 2013)(Palys and Daoutidis, 2020)(Proton Ventures, 2017)(Sekkesaeter, 2019)(Hank *et al.*, 2020)(Guidehouse, 2021a)(IRENA, 2022a).	Statistical approach as reported in Chapter 2 applied to CAPEX, fixed OPEX, variable OPEX, efficiency (calculated from energy consumption, see Figure 9) and technical lifetime. This procedure was carried out for all items of this technology but for only 2020 values. Future forecast of CAPEX for Optimistic scenario is set to remain mostly constant through to 2050, while Pessimistic is assumed to decrease based on economies of scale (IRENA, 2022a).

Ammonia cracking

References	***Assumptions***
(IEA, 2019a)(BNEF, 2019)(Sadler *et al.*, 2018)(Vos, Douma and Van den Noort, 2020)(Ishimoto *et al.*, 2020)(ISPT, 2017) (Sekkesaeter, 2019)(de Vries, 2019) (Cesaro *et al.*, 2021)(Guidehouse, 2021a)(Lanphen, 2019) (IRENA, 2022a).	Statistical approach as reported in Chapter 2 applied to CAPEX, fixed OPEX, variable OPEX, efficiency (calculated from energy consumption, see Figure 11) and technical lifetime. This procedure was carried out for all items of this technology but for only 2020 values. Future forecast of CAPEX for Optimistic scenario is set to remain mostly constant through to 2050, while Pessimistic is assumed to decrease based on economies of scale (IRENA, 2022a).

Liquid organic hydrogen carriers (LOHC) hydrogenation

References	***Assumptions***
(Reuß *et al.*, 2017)(IEA, 2019a)(Niermann *et al.*, 2019) (BNEF, 2019)(Vos, Douma and Van den Noort, 2020)(Runge *et al.*, 2019)(Teichmann, Arlt and Wasserscheid, 2012)(Stöckl, Schill and Zerrahn, 2021)(Sekkesaeter, 2019) (Hank *et al.*, 2020)(Raab, Maier and Dietrich, 2021)(Guidehouse, 2021a)(IRENA, 2022a).	Statistical approach as reported in Chapter 2 applied to CAPEX, fixed OPEX, variable OPEX, efficiency (calculated from energy consumption, see Figure 13) and technical lifetime. This procedure was carried out for all items of this technology but for only 2020 values. Future forecast of CAPEX for Optimistic scenario is set to remain mostly constant through to 2050, while Pessimistic is assumed to decrease based on economies of scale (IRENA, 2022a). Future forecast of Efficiency for Optimistic scenario is set to remain mostly constant through to 2050, while Pessimistic is assumed to increase based on improvement in technology performance (IRENA, 2022a).

LOHC Dehydrogenation

References	***Assumptions***
(Reuß *et al.*, 2017)(IEA, 2019a)(Niermann *et al.*, 2019) (BNEF, 2019)(Vos, Douma and Van den Noort, 2020)(Runge *et al.*, 2019)(Sekkesaeter, 2019)(Hank *et al.*, 2020)(Raab, Maier and Dietrich, 2021)(Guidehouse, 2021a)(Lanphen, 2019)(IRENA, 2022a).	Statistical approach as reported in Chapter 2 applied to CAPEX, fixed OPEX, variable OPEX, efficiency (calculated from energy consumption, see Figure 15) and technical lifetime. This procedure was carried out for all items of this technology but for only 2020 values. Future forecast of CAPEX for Optimistic scenario is set to remain mostly constant through to 2050, while Pessimistic is assumed to decrease based on economies of scale (IRENA, 2022a). Future forecast of Efficiency for Optimistic scenario is set to remain mostly constant through to 2050, while Pessimistic is assumed to increase based on improvement in technology performance (IRENA, 2022a).

Hydrogen liquefaction

References	***Assumptions***
(Reuß *et al.*, 2017)(DOE, 2019)(IEA, 2019a)(Sadler *et al.*, 2018)(Wijayanta *et al.*, 2019)(Linde, 2019)(BNEF, 2019)(Hydrogen Europe, 2020)(Stolzenburg and Mubbala, 2013)(Vos, Douma and Van den Noort, 2020)(Teichmann, Arlt and Wasserscheid, 2012)(D'Amore-Domenech, Leo and Pollet, 2021)(Stöckl, Schill and Zerrahn, 2021)(IEA, 2015)(Sekkesaeter, 2019)(Berstad, Skaugen and Wilhelmsen, 2021)(Hank *et al.*, 2020)(Raab, Maier and Dietrich, 2021)(Guidehouse, 2021a)(Brändle, Schönfisch and Schulte, 2021)(Brändle, Schönfisch and Schulte, 2020)(IRENA, 2022a).	Statistical approach as reported in Chapter 2 applied to CAPEX, fixed OPEX, variable OPEX, efficiency (calculated from energy consumption, see Figure 17) and technical lifetime. This procedure was carried out for all items of this technology but for only 2020 values. Future forecast of CAPEX for Optimistic scenario is set to remain mostly constant through to 2050, while Pessimistic is assumed to decrease based on economies of scale (IRENA, 2022a). Future forecast of Efficiency for Optimistic scenario is set to remain mostly constant through to 2050, while Pessimistic is assumed to increase based on improvement in technology performance (IRENA, 2022a).

Liquid hydrogen regasification

References	***Assumptions***
(Reuß *et al.*, 2017)(IEA, 2019a)(Sadler *et al.*, 2018)(Wijayanta *et al.*, 2019) (Vos, Douma and Van den Noort, 2020)(Element Energy, 2018)(Sekkesaeter, 2019) (Raab, Maier and Dietrich, 2021)(Guidehouse, 2021a)(Lanphen, 2019) (IRENA, 2022a).	Statistical approach as reported in Chapter 2 applied to CAPEX, fixed OPEX, variable OPEX, efficiency (calculated from energy consumption, see Figure 19) and technical lifetime. This procedure was carried out for all items of this technology but for only 2020 values. Future forecast of CAPEX for Optimistic scenario is set to remain mostly constant through to 2050, while Pessimistic is assumed to decrease based on economies of scale (IRENA, 2022a). Future forecast of Efficiency for Optimistic scenario is set to remain mostly constant through to 2050, while Pessimistic is assumed to increase based on improvement in technology performance (IRENA, 2022a).

Methanol synthesis

References	***Assumptions***
(Runge *et al.*, 2019)(JRC, 2016)(Hank *et al.*, 2018)(Hank *et al.*, 2020)(Szima and Cormos, 2018)(JRC, 2022)	Statistical approach as reported in Chapter 2 applied to CAPEX, fixed OPEX, variable OPEX, efficiency (calculated from energy consumption, see Figure 21) and technical lifetime. This procedure was carried out for all items of this technology but for only 2020 values. Future forecast of CAPEX for Optimistic scenario is set to remain mostly constant through to 2050, while Pessimistic is assumed to decrease based on economies of scale (IRENA, 2022a)

Methanol cracking

References	***Assumptions***
(JRC, 2022).	Lack of great amount of data. Mostly considered (JRC, 2022).

11.3 Transport of hydrogen and its derivatives

New onshore pipelines

References	***Assumptions***
(Saadi, Lewis and McFarland, 2018)(Krewitt and Schmid, 2005)(Reuß *et al.*, 2017)(Baufumé *et al.*, 2013)(Element Energy, 2018)(Guidehouse, 2021b)(Reddi *et al.*, 2016)(Krieg, 2012)(Reuß, 2019)(Guidehouse, 2021a) (Brändle, Schönfisch and Schulte, 2021)(Brändle, Schönfisch and Schulte, 2020)(DNV GL, 2019b)	Statistical approach as reported in Chapter 2 applied to CAPEX, fixed OPEX and technical lifetime. This procedure was carried out for only 2020 values. Future forecasts are maintained constant. Losses are calculated as energy needed for repressurization with respect to the LHV of the transported hydrogen.

Repurposed onshore pipelines

References	***Assumptions***
(Guidehouse, 2021b)(Guidehouse, 2021a).	Statistical approach as reported in Chapter 2 applied to CAPEX, fixed OPEX and technical lifetime. This procedure was carried out for only 2020 values. Future forecasts are maintained constant. Losses are calculated as energy needed for repressurization with respect to the LHV of the transported hydrogen.

New offshore pipelines

References	***Assumptions***
(Niermann *et al.*, 2021)(Hydrogen Council, 2021) (D'Amore-Domenech, Leo and Pollet, 2021)(Miao, Giordano and Chan, 2021)(Statista, 2021).	CAPEX determined through the estimated increase in price compared to the onshore pipeline. The same rationale as the onshore pipeline is applied to determine the losses.

Repurposed offshore pipelines

References	***Assumptions***
(Niermann *et al.*, 2021)(Hydrogen Council, 2021) (D'Amore-Domenech, Leo and Pollet, 2021)(Miao, Giordano and Chan, 2021)(Statista, 2021).	CAPEX determined through the estimated increase in price compared to the onshore pipeline. The same rationale as the onshore pipeline is applied to determine the losses.

Ammonia shipping

References	***Assumptions***
(IEA, 2019a)(Sadler *et al.*, 2018)(Ishimoto *et al.*, 2020)(Vos, Douma and Van den Noort, 2020)(Sekkesaeter, 2019)(Hank *et al.*, 2020)(Al-	Statistical approach as reported in Chapter 2 applied to CAPEX, fixed OPEX and variable OPEX (which is considered as the cost of fuel oil consumption for navigation). This procedure was carried out for only 2020 values. Future forecast

Breiki and Bicer, 2020)(Guidehouse, 2021a)(Lanphen, 2019)(IRENA, 2022a).	of CAPEX for Optimistic scenario is set to remain mostly constant through to 2050.

LOHC shipping

References	***Assumptions***
(IEA, 2019a)(Niermann *et al.*, 2019) (Vos, Douma and Van den Noort, 2020)(Teichmann, Arlt and Wasserscheid, 2012)(Sekkesaeter, 2019)(Hank *et al.*, 2020)(Guidehouse, 2021a) (Lanphen, 2019)(IRENA, 2022a).	Statistical approach as reported in Chapter 2 applied to CAPEX, fixed OPEX and variable OPEX (which is considered as the cost of fuel oil consumption for navigation). This procedure was carried out for only 2020 values. Future forecast of CAPEX for Optimistic scenario is set to remain mostly constant through to 2050.

Liquefied hydrogen shipping

References	***Assumptions***
(IEA, 2019a)(Wijayanta *et al.*, 2019) (Vos, Douma and Van den Noort, 2020) (Ishimoto *et al.*, 2020) (Teichmann, Arlt and Wasserscheid, 2012)(Sekkesaeter, 2019)(Hank *et al.*, 2020)(Raab, Maier and Dietrich, 2021)(Guidehouse, 2021a) (Lanphen, 2019)(IRENA, 2022a).	Statistical approach as reported in Chapter 2 applied to CAPEX, fixed OPEX and variable OPEX (which is considered as the cost of fuel oil consumption for navigation). This procedure was carried out for only 2020 values. Future forecast of CAPEX for Optimistic scenario is set to remain mostly constant through to 2050, while Pessimistic is assumed to decrease based on economies of scale (IRENA, 2022a).

11.4 Storage of hydrogen and its derivatives

General assumption: Statistical approach as reported in Chapter 2 when sufficient data points where available. This procedure was carried out for most elements of the technology for 2020 and the trend was set constant in time through to 2050.

Above ground pressurized hydrogen tanks

Parameter	***References***
Specific Invest per volume	(Hystories, 2022a)(Navigant, 2019) (ENTEC, 2022) (Agora Energiewende, 2021)(DNV GL, 2019b) (Element Energy, 2018) (JRC, 2022).
OPEX fix (per volume)	(Hystories, 2022a) (ENTEC, 2022) (Agora Energiewende, 2021)(DNV GL, 2019b) (Element Energy, 2018).
Specific Invest in/out	(Hystories, 2022a).
OPEX fix (per in/out)	(Hystories, 2022a).
Variable cost for charge	(Hystories, 2022a).
Variable cost for discharge	(Hystories, 2022a).
Self-discharge (losses)	(Hystories, 2022a)(IEA, 2019b).
Charge efficiency (losses while injection)	(Hystories, 2022a).
Discharge efficiency (losses while withdrawal)	(Hystories, 2022a).
Technical lifetime	(Hystories, 2022a) (ENTEC, 2022) (Agora Energiewende, 2021).

Pipe systems

Parameter	***References***
Specific Invest per storage capacity	(HyUnder, 2013)(Welder *et al.*, 2018).
Charge rate / injection rate	(Welder *et al.*, 2018).
Discharge rate / withdrawal rate	(HyUnder, 2013)(Welder *et al.*, 2018).
Technical lifetime	(Welder *et al.*, 2018).

Ammonia tanks

Parameter	***References***
Specific Invest per storage capacity	(Guidehouse, 2021a) (ENTEC, 2022) (JRC, 2022).
OPEX fix (per storage capacity)	(Guidehouse, 2021a) (ENTEC, 2022).
Self-discharge (losses)	(JRC, 2022).
Technical lifetime	(ENTEC, 2022).

LOHC tanks

Parameter	***References***
Specific Invest per storage capacity	(Guidehouse, 2021a) (ENTEC, 2022).
OPEX fix (per storage capacity)	(Guidehouse, 2021a) (ENTEC, 2022).
Technical lifetime	(ENTEC, 2022).

Methanol tanks

Parameter	***References***
Specific Invest per storage capacity	(ENTEC, 2022).
OPEX fix (per storage capacity)	(ENTEC, 2022).
Technical lifetime	(ENTEC, 2022).

Liquefied hydrogen tanks

Parameter	***References***
Specific Invest per storage capacity	(Guidehouse, 2021a)(ENTEC, 2022)(DNV GL, 2019b)(JRC, 2022).
OPEX fix (per storage capacity)	(Guidehouse, 2021a) (ENTEC, 2022)(DNV GL, 2019b).
Self-discharge (losses)	(IEA, 2019b) (JRC, 2022).
Technical lifetime	(ENTEC, 2022) (JRC, 2022).

Pore storage

Parameter	***References***
Specific Invest for subsurface components	(Hystories, 2022b)(ENTEC, 2022) (HyUnder, 2013) (Lord, Kobos and Borns, 2014).
OPEX fix for subsurface components	(Hystories, 2022b)(ENTEC, 2022).
Specific Invest for surface components	(Hystories, 2022b) (Lord, Kobos and Borns, 2014).

OPEX fix for surface components	(Hystories, 2022b).
Specific Invest for cushion gas	(Hystories, 2022b) (HyUnder, 2013) (Lord, Kobos and Borns, 2014).
Overall CAPEX	(Guidehouse, 2021c)(DNV GL, 2019b)(European Commission, 2021) (Lord, Kobos and Borns, 2014).
Overall OPEX	(DNV GL, 2019b)(European Commission, 2021).
Variable cost for charge	(Hystories, 2022b).
Variable cost for discharge	(Hystories, 2022b).
Charge rate / injection rate	(Hystories, 2022b)(HyUnder, 2013)(Amid, Mignard and Wilkinson, 2016) (Lord, Kobos and Borns, 2014).
Discharge rate / withdrawal rate	(Hystories, 2022b)(HyUnder, 2013)(Amid, Mignard and Wilkinson, 2016) (Lord, Kobos and Borns, 2014).
Self-discharge (losses)	(Hystories, 2022b) (Amid, Mignard and Wilkinson, 2016).
Charge efficiency (losses while injection)	(Hystories, 2022b) (DNV GL, 2019b).
Discharge efficiency (losses while withdrawal)	(Hystories, 2022b) (DNV GL, 2019b).
Energy use for charge (e.g. compression)	(Hystories, 2022b).
Energy use for discharge (e.g. gas cleaning)	(Hystories, 2022b).
Technical lifetime for subsurface components	(Hystories, 2022b) (ENTEC, 2022) (Lord, Kobos and Borns, 2014).
Technical lifetime for surface components	(Hystories, 2022b) (Lord, Kobos and Borns, 2014).
ABEX Subsurface	(Hystories, 2022b).
ABEX Surface	(Hystories, 2022b).

New salt caverns

Parameter	***References***
Specific Invest for subsurface components	(Hystories, 2022b)(ENTEC, 2022)(HyUnder, 2013) (Michalski *et al.*, 2017)(Tarkowski and Czapowski, 2018)(Lord, Kobos and Borns, 2014).
OPEX fix for subsurface components	(Hystories, 2022b) (ENTEC, 2022)(Michalski *et al.*, 2017).
Specific Invest for surface components	(Hystories, 2022b) (Michalski *et al.*, 2017) (Lord, Kobos and Borns, 2014).
OPEX fix for surface components	(Hystories, 2022b) (Michalski *et al.*, 2017).
Specific Invest for cushion gas	(Hystories, 2022b)(HyUnder, 2013) (Tarkowski and Czapowski, 2018) (Lord, Kobos and Borns, 2014).
Overall CAPEX	(Guidehouse, 2021c)(Agora Energiewende, 2021)(DNV GL, 2019b)(European Commission, 2021)(Element Energy, 2018)(JRC, 2022)(Wijk and Wouters, 2021)(Welder *et al.*, 2018) (Tarkowski and Czapowski, 2018)(Lord, Kobos and Borns, 2014).
Overall OPEX	(Agora Energiewende, 2021) (DNV GL, 2019b)(European Commission, 2021)(Element Energy, 2018).
Overall variable cost	(Element Energy, 2018).
Variable cost for charge	(Hystories, 2022b).
Variable cost for discharge	(Hystories, 2022b).
Charge rate / Injection rate	(Hystories, 2022b) (HyUnder, 2013) (Welder *et al.*, 2018) (Lord, Kobos and Borns, 2014).
Discharge rate / Withdrawal rate	(Hystories, 2022b) (HyUnder, 2013) (Welder *et al.*, 2018) (Lord, Kobos and Borns, 2014).
Self-discharge (losses)	(Hystories, 2022b) (Element Energy, 2018) (Lord, Kobos and Borns, 2014).
Charge efficiency (losses while injection)	(Hystories, 2022b) (DNV GL, 2019b)(IEA, 2019b).
Discharge efficiency (losses while withdrawal)	(Hystories, 2022b) (DNV GL, 2019b)(IEA, 2019b)(Valle-Falcones *et al.*, 2022).
Energy use for charge (e.g. compression)	(Hystories, 2022b) (JRC, 2022) (Tarkowski and Czapowski, 2018).
Energy use for discharge (e.g. gas cleaning)	(Hystories, 2022b) (JRC, 2022) (Tarkowski and Czapowski, 2018).
Technical lifetime for subsurface components	(Hystories, 2022b)(ENTEC, 2022) (Agora Energiewende, 2021) (JRC, 2022) (Welder *et al.*, 2018) (Michalski *et al.*, 2017) (Lord, Kobos and Borns, 2014).
Technical lifetime for surface components	(Hystories, 2022b) (Agora Energiewende, 2021) (Welder *et al.*, 2018) (Michalski *et al.*, 2017) (Lord, Kobos and Borns, 2014).
ABEX Subsurface	(Hystories, 2022b).
ABEX Surface	(Hystories, 2022b).

11.5 Hydrogen final use

Open Circuit Gas turbines (OCGT)

References	***Assumptions***
(Öberg, Odenberger and Johnsson, 2022)(DNV GL, 2019b)(European Commission, 2014).	Values for CAPEX are set for 2020 by applying the price markup suggested by (Öberg, Odenberger and Johnsson, 2022) to the turbine prices proposed in (European Commission, 2014).

Combined Cycle Gas turbines (CCGT)

References	***Assumptions***
(Hernandez and Gençer, 2021) (Öberg, Odenberger and Johnsson, 2022)(Sadler *et al.*, 2018) DNV GL, 2019b)(Grosse *et al.*, 2017)(Oh, Lee and Lee, 2021).	Values for CAPEX are set for 2020 by applying the price markup suggested by (Öberg, Odenberger and Johnsson, 2022) to the turbine prices proposed in (European Commission, 2014).

Stationary PEM Fuel Cells

References	***Assumptions***
(Hydrogen Europe, 2020)(Battelle Memorial Institute, 2016)(Marocco *et al.*, 2021) (Cigolotti and Genovese, 2021).	Statistical approach as reported in Chapter 2 applied to CAPEX, fixed OPEX, variable OPEX and lifetime This procedure was carried out also for efficiency of this technology for the 2020 and 2030 time horizons. The trend was extended to 2040 and 2050 assuming a similar trend in decrease of CAPEX and increase of efficiency as encountered in PEM Electrolyzers.

Industrial heat generation – water boilers

References	***Assumptions***
(Element Energy, 2019) (Grosse *et al.*, 2017)	Reported data for industrial water boilers. Indirect heating is deemed as more likely to employ hydrogen while direct heating (e.g. kilns) may encounter more issues with product quality. The CAPEX data was determined by applying price markup suggested by (Element Energy, 2019) to the data on conventional boilers found in (Grosse *et al.*, 2017).

Steel production

References	***Assumptions***
(IEA, 2019a)(Vogl, Åhman and Nilsson, 2018)(Otto *et al.*, 2017)	CAPEX values extrapolated from (IEA, 2019a).

Methanol-to-olefins

References	***Assumptions***
(Xiang *et al.*, 2015)(Zhao, Jiang and Wang, 2021)(Jasper and El-Halwagi, 2015)(Mai *et al.*, 2014)(Chen *et al.*, 2022)(Syah *et al.*, 2021)(Haro *et al.*, 2011)(Nguyen *et al.*, 2020)(TNO, 2021).	Statistical approach as reported in Chapter 2 applied to CAPEX, fixed OPEX, variable OPEX and efficiency (which was calculated as shown in Figure 29). This procedure was carried out for 2020 and the trend was set constant in time through to 2050. Technical lifetime was taken from (Haro *et al.*, 2011).

Methanol-to-aromatics

References	***Assumptions***
(Yang *et al.*, 2022)(Niziolek *et al.*, 2016)(Ward *et al.*, 2016)(Jiang *et al.*, 2020)(Bazzanella, Ausfelder and DECHEMA, 2017).	Statistical approach as reported in Chapter 2 applied to CAPEX and fixed OPEX. This procedure was carried out for CAPEX of the technology for 2020 and the trend was set constant in time through to 2050. Variable OPEX and Technical lifetime were assumed equal to those of the methanol to olefin process. Efficiency calculated as shown in Figure 31 from (Jiang *et al.*, 2020) and (Bazzanella, Ausfelder and DECHEMA, 2017).

Methanol-to-gasoline

References	***Assumptions***
(Ruokonen *et al.*, 2021) .	Product cost of the e-fuel found in (Ruokonen *et al.*, 2021) for all time scenarios. The optimistic and pessimistic scenarios were generated based on different methanol prices discussed in Chapter 7.4 when discussing their impact on the production cost of olefins and aromatics. Similarly, the decreasing trends in time reflect those of future renewable methanol prices.

Fischer-Tropsch Kerosene

References	***Assumptions***
(Zang, Sun, A. A. Elgowainy, *et al.*, 2021)(Peters *et al.*, 2022)(Concawe, 2019)(ICCT, 2022a)	Statistical approach as reported in Chapter 2 applied to product cost of the e-fuel for all time scenarios. Decreasing trend reported as found in literature

Fischer-Tropsch Diesel

References	***Assumptions***
(Zang, Sun, A. A. Elgowainy, *et al.*, 2021)(Peters *et al.*, 2022)(Swanson *et al.*, 2010) (Concawe, 2019) (ICCT, 2022a).	Statistical approach as reported in Chapter 2 applied to product cost of the e-fuel for all time scenarios. Decreasing trend reported as found in literature.

Internal combustion engine vehicles - Cars

References	***Assumptions***
(H2IT, 2019) (European Climate Foundation, 2019)(Viesi, Crema and Testi, 2017)(Wang, Wang and Fan, 2018)(Chen and Melaina, 2019)(He *et al.*, 2021)(Grube *et al.*, 2021)(Ruffini and Wei, 2018)(Kumar, 2022)(Creti *et al.*, 2015)(IEA, 2019a).	Statistical approach as reported in Chapter 2 applied to CAPEX, fixed OPEX and technical lifetime. Fuel cost calculated through efficiencies and e-fuel costs of the previous sections.

Internal combustion engine vehicles – Trucks

References	***Assumptions***
(Cunanan *et al.*, 2021) (Kumar, 2022)(ICCT, 2022b) (IEA, 2019a).	Statistical approach as reported in Chapter 2 applied to CAPEX, fixed OPEX and technical lifetime. This procedure was carried out for CAPEX and efficiency of this technology and for the 2020 and 2030. The trends were then extended to 2040 and 2050 following a similar trend of the ICE cars. Technical lifetime calculated from (Kumar, 2022). Fuel cost calculated through efficiencies and e-fuel costs of the previous sections.

Internal combustion engine vehicles – Buses

References	***Assumptions***
(H2IT, 2019) (Viesi, Crema and Testi, 2017) (Ajanovic, Glatt and Haas, 2021).	Statistical approach as reported in Chapter 2 applied to CAPEX. Efficiency values taken from (Viesi, Crema and Testi, 2017). Fixed OPEX values assumed to be equal to those of ICE trucks. Fuel cost calculated through efficiencies and e-fuel costs of the previous sections.

Fuel cell electric vehicles - Cars

References	***Assumptions***
(H2IT, 2019)(European Climate Foundation, 2019)(Viesi, Crema and Testi, 2017)(Wang, Wang and Fan, 2018)(Chen and Melaina, 2019)(He *et al.*, 2021)(Grube *et al.*, 2021)(Ruffini and Wei, 2018)(Kumar, 2022)(Creti *et al.*, 2015)(IEA, 2019a).	Statistical approach as reported in Chapter 2 applied to CAPEX, fixed OPEX, efficiency and technical lifetime. Variable costs taken from (IEA, 2019a) and (Kumar, 2022).

Fuel cell electric vehicles – Trucks

References	***Assumptions***
(H2IT, 2019)(Cunanan *et al.*, 2021) (Kumar, 2022)(ICCT, 2022b) (IEA, 2019a).	Statistical approach as reported in Chapter 2 applied to CAPEX, variable OPEX, efficiency and technical lifetime. This procedure was carried out for CAPEX and efficiency of this technology and for the 2020 and 2030. The trends were then extended to 2040 and 2050 following a similar trend of the FC cars. Fixed OPEX taken from (Kumar, 2022).

Fuel cell electric vehicles – Buses

References	***Assumptions***
(H2IT, 2019) (Viesi, Crema and Testi, 2017)(FCHJU, 2017b)(Ajanovic, Glatt and Haas, 2021)(Zhang, Zhang and Xie, 2020)(Coleman *et al.*, 2020).	Statistical approach as reported in Chapter 2 applied to CAPEX and efficiency. Fixed OPEX values assumed to be equal to those of ICE trucks. Variable OPEX taken from (Ajanovic, Glatt and Haas, 2021). Technical lifetime taken from (Viesi, Crema and Testi, 2017).